ABSTRACT

Title of Dissertation: THE REGULATION OF THE INTESTINAL COPPER EXPORTER IS COORDINATED WITH SYSTEMIC COPPER HOMEOSTASIS

Haarin Chun, Doctor of Philosophy, 2017

Dissertation Directed By: Assistant Professor, Dr. Byung-Eun Kim, Department of Animal and Avian Sciences

Copper (Cu) plays key catalytic and regulatory roles in biochemical reactions essential for normal growth, development, and health. Defects in Cu metabolism cause Menkes and Wilson's disease, myeloneuropathy, and cardiovascular disease and are associated with other pathophysiological states. Consequently, it is critical to understand the mechanisms by which organisms control the acquisition, distribution, and utilization of Cu. While it is well established that the enterocyte is a key regulatory point for Cu absorption into the body, how the intestine responds to systemic Cu requirements is poorly understood. Here, we demonstrate that fine-tuned Cu homeostasis is required for normal growth and development in *C. elegans*. Moreover, we show that CUA-1, the ATP7A/B homolog in worms, localizes to lysosome-like organelles (gut granules) in the intestine under Cu-overload conditions for Cu detoxification, while Cu-deficiency results in a redistribution of CUA-1 to basolateral membranes for Cu efflux to peripheral tissues. Defects in gut granule

biogenesis exhibit result in abnormal Cu sequestration and increased susceptibility to toxic Cu levels. Our studies establish that CUA-1 is a key intestinal Cu exporter, and that its trafficking is regulated in response to systemic Cu status in worms. In addition, while the Cu transporter ATP7A plays a major role in both intestinal Cu mobilization to the periphery and prevention of Cu over-accumulation, it is unclear how regulation of ATP7A contributes to Cu homeostasis in response to systemic Cu fluctuation in mammals. Here we show, using Cu-deficient mouse models, that steady-state levels of ATP7A are lower in peripheral tissues (including the heart, spleen, and liver) under Cu deficiency and that subcutaneous administration of Cu to these animals restore normal ATP7A levels in these tissues. Importantly, ATP7A in the intestine is regulated in the opposite manner - low systemic Cu increases ATP7A while subcutaneous Cu administration decreases ATP7A suggesting that intestine-specific non-autonomous regulation of ATP7A abundance may serve as a key homeostatic control for Cu export into the circulation. Altogether, our results implicate CUA-1/ATP7A Cu exporter in the intestine as a key modulator for organismal Cu homeostasis in metazoans.

THE REGULATION OF THE INTESTINAL COPPER EXPORTER IS COORDINATED WITH SYSTEMIC COPPER HOMEOSTASIS

by

Haarin Chun

Dissertation submitted to the Faculty of the Graduate School of the
University of Maryland, College Park, in partial fulfillment
of the requirements for the degree of
Doctor of Philosophy
2017

Advisory Committee:
Dr. Byung-Eun Kim, Chair
Dr. Tom Porter
Dr. Antony Jose
Dr. Bhanu Telugu
Dr. Leslie Pick, Dean's Representative

Acknowledgements

The work presented here could not have been possible without the continued support and encouragement from my advisor, my committee, my colleagues, my friends, and my family. First and foremost, I would like to thank to my advisor, Dr. Byung-Eun Kim, for his guidance and support. When I interviewed with Dr. Kim to apply to graduate school, he said he had a dream about me and will support my successful graduate study. He has always encouraged me even when I met with disappointing results, challenged me to pursue better achievements in my presentation skills and critical thinking, and trained me in a professional way to study for molecular and cellular biology and genetics; he indeed kept his promise during my graduate years. One simply could not wish for better or friendlier mentor.

I would also like to express my gratitude to all my committee members, Dr. Leslie Pick, Dr. Tom Porter, Dr. Antony Jose, and Dr. Bhanu Telugu, and my previous committee members, Dr. Brian Bequette and Dr. Liquing Yu, for all their efforts and valuable time putting into scientific discussions. I appreciate their thoughtful suggestions and comments that have sparked me to do better science.

A special thank you to my colleagues in the Kim lab and the Animal Sciences department. Thank you to Alex, my first bench neighbor, who helped me adapt to a new life at the University of Maryland. Thank you to Sai for being wonderful fellow graduate student and helping in many ways. Thank you to Anuj for the scientific support and kindness. I must thank Tammy, Xiaojing, Simon, and Tamika who were always willing to help and proofread my writings. Thank you to Jianbing, Jason, Nicole, Kate, Rini, and Ian for being wonderful friends. I also thank my best friend,

Hyunsu, whom I enjoyed sharing scientific discussion with by having dinner and our favorite McFlurry in the past five years. Thank you to Dr. Iqbal Hamza for your guidance and support in making a better scientific story.

Thank you to my previous advisor, Dr. Hang-Cheol Shin at Soongsil University, who contributed his valuable time to my master study and to write a wonderful recommendation letter for pursuing my dream at the University of Maryland. Thank you to my previous supervisor, Dr. Nam Doo Kim, who supported me in learning computer-aided drug design using molecular modeling when I was working in a company in South Korea.

Lastly, I would like to thank my family members, my parents (Seongdeok and Insun), my younger brother (Haram), parents-in-law (Kwonhyung and Wonsoon), and sister-in-law (Jae Eun) for their constant love and support. I am so grateful to have them in my life. Above all, I would like to thank my wife, Ju Young, for her love, patience, and support. Your prayer for me was what sustained me thus far.

Table of Contents

List of Tables

Chapter 1

List of Figures

Chapter 1

Chapter 3

Chapter 4

List of Abbreviations

ANOVA	Analysis of variance
Ag	Silver
ATP	Adenosine triphosphate
BCS	Bathocuproinedisulfonic acid
BLOC-1	Biogenesis of Lysosome-related Organelles Complex-1
BW	Body weight
CCO	Cytochrome c oxidase
CCS	Copper chaperone for superoxide dismutase
CHX	Cycloheximide
Cu	Copper
$CuCl_2$	Copper(II) chloride
DAPI	4',6-diamidino-2-phenylindole
DMEM	Dulbecco's Modified Eagle Medium
DMSO	Dimethyl sulfoxide
EDTA	Ethylenediaminetetraacetic acid
Fe	Iron
GFP	Green fluorescent protein
HA	Hemagglutinin
HBSS	Hanks' balanced salt solution
HEK293	Human embryonic kidney cells 293
HUVEC	Human umbilical vein endothelial cell

ICP-MS	Inductively coupled plasma-mass spectrometry
IECs	Intestinal epithelial cells
IEC-6	Rat intestinal epithelial cells
MEF	Mouse embryonic fibroblast
MRE	Metal responsive elements
MT	Metallothionein
MTF-1	Metal-responsive transcription factor-1
NGM	Nematode growth medium
PBS	Phosphate-buffered saline
PCR	Polymerase chain reaction
P12	Postnatal day 12
RT-PCR	Reverse transcription quantitative PCR
SDS-PAGE	Sodium dodecyl sulfate polyacrylamide gel electrophoresis
Se	Selenium
SOD1	Cu, Zn superoxide dismutase
SQ	Subcutaneously
TEER	Trans epithelial electrical resistance
TGN	trans-Golgi network
WGA	Wheat germ agglutinin
WT	Wild-type
Zn	Zinc

Chapter 1: Introduction

Copper (Cu) has been harnessed throughout much of human civilization as a conductor of heat and electricity, as a building material and a constituent of various metal alloys, and as an antimicrobial agent over 10,000 years. However, the acquisition and metabolism of Cu and the diseases associated with Cu imbalance in human health have only recently been relatively studied. Cu is an indispensable trace element that is essential for a vast array of cellular processes in organisms from bacteria to humans. Cu serves as a redox-reactive, catalytic co-factor in the enzymatic reactions that drive oxidative phosphorylation, iron acquisition, protection from oxidative stress, neuropeptide maturation, blood clotting, and angiogenesis, among many other critical physiological functions (Table 1.1) (1-3). However, the ability of Cu to undergo reversible redox changes also makes this element deleterious to the organism when present in excess. Buildup of Cu in cells and tissues - particularly those that are highly oxygenated - can facilitate the production of reactive hydroxyl radicals leading to lipid peroxidation in membranes, oxidation of proteins, and structural damage to nucleic acids (4,5). Because of its dichotomous potential as an essential co-factor and toxic ions, cells have evolved sophisticated homeostatic mechanisms for the regulation of Cu acquisition and distribution (6,7). Organs communicate to ensure that intestinally derived micronutrients are distributed appropriately throughout the body, balancing cellular requirements against toxicity (8,9); all organismal Cu must pass through the intestine prior to distribution to other tissues. Therefore, organ-specific regulation of Cu metabolism must take place

Table 1.1. List of selected Cu binding and Cu homeostasis proteins. Adopted and modified from (2).

Protein	Function
Amyloid precursor protein (APP)	Protein involved in neuronal development and potentially Cu metabolism; cleavage leads to generation of Aβ Peptide that aggregates in senile plaque associated with Alzheimer's disease.
Atox1	Metallochaperone that delivers Cu to ATP7A and ATP7B Cu(I) transporters
ATP7A	Cu(1)-transporting P-type ATPase expressed in all tissues
ATP7B	Cu(1)-transporting P-type ATPase expressed primarily in the liver
Carbon monoxide dehydrogenase to acetyl-CoA synthase	Moorella thermoacetica bifunctional enzyme; reduces CO_2 to CO with subsequent
CCS	Metallochaperone that delivers Cu to Cu/Zn SOD
Ceruloplasmin (Cp)	Serum ferroxidase that functions in Fe(III) loading onto transferrin
Coagulation factors V and VIII	Homologous pro-coagulants present on the surface of platelets, where they nucleate the assembly of multiprotein proteolytic complexes involved in blood coagulation
COMMD1	Proteins involved in ATP7A/B trafficking
CopZ	Archaeoglobus fulgidus [2Fe-2S] and Zn(II)- containing Cu chaperone
Cox17	Metallochaperone that transfers Cu to Sco1 and Cox11 for cytochrome oxidase Cu loading in mitochondria
Ctr1	High-Affinity Cu(I) transporter involved in cellular Cu uptake
Ctr2	Protein regulates biogenesis of a cleaved form of mammalian Ctr1
Cu/Zn SOD (SOD1)	Antioxidant enzyme, catalyzes the disproportionation of superoxide to hydrogen peroxide and dioxygen
Cytochrome c oxidase (CCO)	Terminal enzyme in the mitochondrial respiratory chain, catalyzes the reduction of dioxygen to water
Dopamine β-hydroxylase (DBH)	Oxygenase, converts dopamine to norepinephrine
Ethylene receptor (ETR1)	Member of a plant receptor family that uses a Cu cofactor for ethylene binding and signaling

Hemocyanin	Oxygen transport protein found in the hemolymph of many invertebrates such as arthropods and molluscs
Hephaestin	Transmembrane multi-Cu ferroxidase; involved in iron efflux from enterocytes and macrophages
Glucose oxidase	Pentose phosphate pathway oxidoreductase that catalyzes the oxidation of D-glucose into D-glucono-1, 5-lactone and hydrogen peroxide
Laccase	Phenol oxidase involved in melanin production
Lysyl oxidase	Catalyzes formation of aldehydes from lysine in collagen and elastin precursors for connective tissue maturation
Metallohthionein (MT)	Cysteine-rich small-molecular-weight metal-binding and detoxification protein
Peptidylglycine-α-amidating mono-oxygenase (PAM)	Catalyzes conversion of pptidylglycine substrates into α-amidated products; neuropeptide maturation
Prion protein (PrP)	Protein whose fuction is unclear but binds Cu via the N-terminal octapeptide repeats
Steap proteins/Fre1/Fre2	Family of metalloreductases involved in Fe(III) and Cu(II) reduction
Tyrosinase	Monophenol mono-oxygenase; melanin synthesis
XIAP	Inhibitor of apoptosis through binding and catalytic inhibition of several caspases

among tissue types to ensure that Cu import and export from the intestine are coordinated with extra-intestinal tissue Cu requirements. Here, will review current knowledge of how Cu is imported, delivered, stored, and excreted at cellular levels and how Cu is acquired from the dietary sources and distributed to the peripheral tissues in mammals.

Delivery of Cu into cells and subcellular compartments

Cu import into cells

Cellular Cu uptake into eukaryotic cells is accomplished via Ctr1, a high affinity Cu importer that is structurally and functionally conserved from yeast to humans (Figure 1.1) (10-12). The Ctr1 polypeptide is composed of three major domains: a methionine-rich N-terminus, a metal binding motif (MX_3M) in the second transmembrane domain, and a cytoplasmic cysteine-histidine cluster in the C-terminus. Structural and functional studies demonstrated that while the N-terminus motifs are thought to bind and facilitate Cu transfer to the channel, the metal binding motif on the second transmembrane domain is required for Cu uptake selectively via formation of Cu-S linkages (13,14). Genetic and structural studies indicate that Ctr1 is present in the membrane as a homotrimer with a minimal membrane-spanning pore 9 Å, which is likely where Cu ions traverse the membrane (14-16). Mammalian Ctr1-mediated Cu uptake is specific for reduced Cu(I); however, the mechanism by which it is reduced prior to import is unknown (17). As candidates for this reducing activity, duodenal matalloreductase DcytB and Steap protein family (steap2, steap3, and

steap4), both of which are localized to the plasma membrane and intracellular membrane, are reported to possess cupric reductase activity in cultured cells (18-20). Further *in vivo* studies were needed to confirm this hypothesis. The essentiality of Ctr1 has been demonstrated by embryonic lethality in mice systemically deleted for Ctr1 (21,22).

The regulation of Ctr1 activity is mainly controlled at the level of subcellular localization and abundance change. While the intracellular localization of Ctr1 is variable in different cells, it is predominantly localized to the plasma membrane in Cu-limiting conditions. However, its localization shifts to the intracellular vesicular membrane compartment as a result of Ctr1 endocytosis in response to increased Cu levels (23-25). Elevated exogenous Cu also induces degradation of glycosylated full-lengths of Ctr1, presumably to prevent the excessive accumulation of toxic levels of Cu (25).

While there is evidence for endosomal Cu stores in mammals, it has not been clearly established how stored Cu in vesicular compartments is mobilized to the cytoplasm. A protein structurally related to the mammalian Ctr1, called Ctr2, functions in the generation of a truncated form of Ctr1 lacking a large portion of the N-terminus histidine- and methionine-rich metal-binding ectodomain (26,27). While Ctr2 does not function as a direct Cu importer, it does stimulate the cleavage of the Ctr1 Cu-binding ectodomain, in a mechanism involving a direct, rate limiting reaction by the cathepsin L/B endolysosomal proteases (26,28). The truncated form of Ctr1 (tCtr1) produced by the cleavage of the Ctr1 ectodomain has decreased cellular Cu import activity as compared with the full-length form of Ctr1 (13).

Figure 1.1. A current model for Cu metabolism in mammalian cells. A summary of the proteins involved in Cu acquisition, mobilization, stores, and export are shown in the figure. Each protein and its function are reviewed in the text.

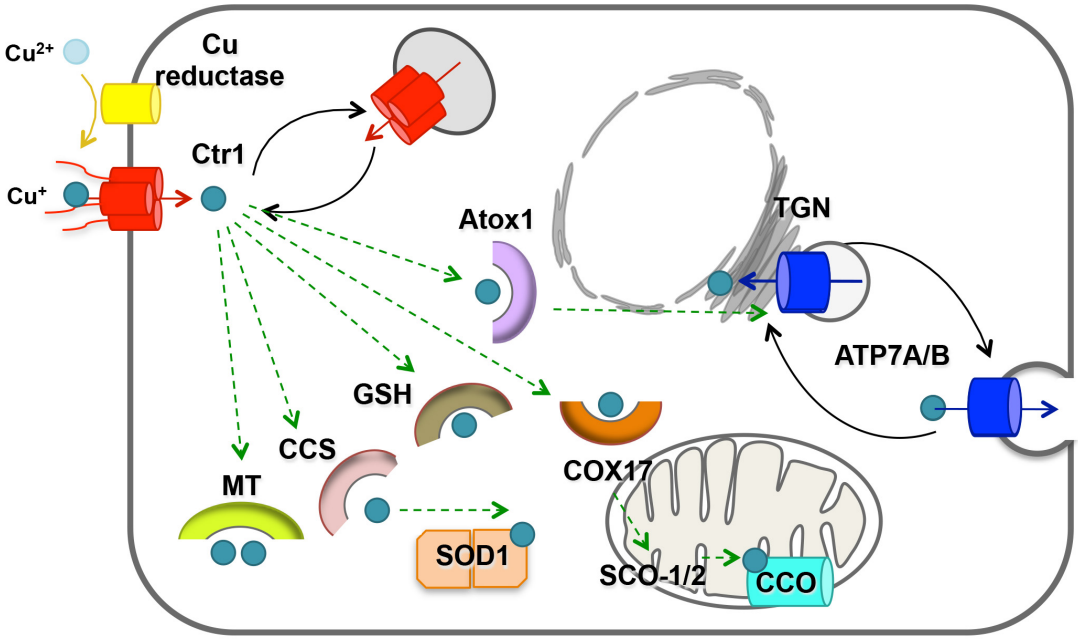
Cu2+
Cu
reductase
Ctr1
Cu+
Atox1
TGN
ATP7A/B
GSH
CCS
COX17
MT
SOD1
SCO-1/2
CCO

Interestingly, mouse embryonic fibroblasts (MEFs) lacking Ctr1 retain some Cu accumulation activity with low affinity for Cu(I), suggesting that alternative mechanism exist for Cu uptake. Cu-chloride complexes by an anion exchanger and divalent metal transporter 1 (DMT1) have been proposed as Cu entry pathways (29,30). However, accumulated evidence strongly suggests that intestinal DMT1 is not required for the intestinal transport of dietary Cu in mouse experiments, and genetic ablation will confirm the *in vivo* role of anion exchanger for Cu uptake (31).

Cu chaperones and ligands in the cytoplasm

Intracellular delivery of imported exogenous Cu ions to its target proteins and subcellular compartment requires fine-tuned control to sense cellular Cu levels, relay Cu ions, and prevent cytotoxicity from free intracellular Cu. Here, we will discuss the function and regulation of several Cu chaperones and other ligands including metallothionein (MT) and glutathione (GSH).

Two cytosolic Cu chaperones, Cu chaperone for superoxide dismutase (CCS) and Atox1 deliver Cu to Cu, Zn superoxide dismutase (SOD1) and the ATP7A/B Cu exporter localized to the membrane of the secretory pathway, respectively (7). Both CCS and SOD1 are located in the cytoplasm, where active SOD1 functions as an antioxidant to protect cells from superoxide (O_2^-) radicals produced as a by-product of oxygen metabolism. While both proteins share similar protein structure, CCS does not have catalytic activity but instead delivers Cu to SOD1 by direct docking. CCS protein levels are post-translationally regulated in response to cellular bioavailable Cu. During times of elevated intracellular Cu, Cu-bound CCS is ubiquitinated by X-

linked inhibitor of apoptosis (XIAP) E3 ubiquitin ligase or other E3 ligases and targeted for proteasomal degradation, resulting in low steady-state levels of CCS protein (32-35). While CCS levels do not influence SOD1 protein abundance, the enzymatic activity of SOD1 is dependent on both CCS and Cu levels (34,36). Deletion of CCS in mice is not lethal, but significantly lowers SOD1 activity, and reduces fertility in female mice (37).

The Atox1 Cu chaperone transfers Cu to the metal binding sites in the cytosolic N-terminus of the Cu(I)-transporting ATPases, ATP7A and ATP7B. Loss of the gene encoding Atox1 in mice results in severe growth impairment (perinatal lethal) and reduced Cu transport across the placenta and systemic delivery (38). In addition, Atox1 has been suggested to act as a transcription factor, stimulating the expression of the genes encoding SOD3 and other proteins involved in cell proliferation under Cu overload conditions (39).

MTs are small cysteine-rich proteins (~30% of amino acid residues) that bind up to 12 Cu(I) ions through their thiol group. MTs are capable of binding to some physiological metals, such as Cu, Zn, and Se, and thus their gene expression is dependent on availability of such dietary metals. How are MTs expression regulated in response to Cu levels? Under elevated Cu conditions, accumulated Cu in the nucleus induces the binding of metal transcription factor 1 (MTF1) to metal responsive elements (MREs) in the promoter of MT genes, resulting in rapid induction of MT gene transcription (40). Given that ablation of MT1 and MT2 in mice results in elevated susceptibility to toxic metals including Cu, MTs are required for the protection against metal toxicity (41,42). In addition, MTs are known to act in

Cu storage under Cu deficiency. Consistent with this notion, MEFs lacking MT exhibited decreased cell viability under Cu-limiting conditions (43).

GSH is a tripeptide (glutamate, cysteine, and glycine) that is capable of preventing damage to important cellular components caused by reactive oxygen species, and Cu is also one of the known binding ligands with lower affinity than MT. In Cu deficient rats, experimental removal of hepatic GSH levels lead to reduced Cu in the blood and bile but elevated hepatic Cu levels, suggesting that GSH may function in delivering Cu stores (44). In support of this, reduced GSH levels also inhibit ATP7A/B Cu exporters resulting in hyperaccumulation of Cu (45). It is possible that GSH may acts as a Cu chaperone in an Atox1-independent manner in loading Cu onto ATP7A/B.

Cu delivery to mitochondria

The oxidative phosphorylation system in mitochondria generates the huge amounts of cellular ATP used as energy currency. Five multi-subunit protein complexes (complexes I to V) in the mitochondrial inner membrane comprise the mitochondrial respiratory chain (46). Cytochrome c oxidase (CCO), termed complex IV, is the terminal enzyme of the oxidative phosphorylation and oxidizes cytochrome c and transfers electrons to molecular oxygen, Cox1 and Cox2 as a reaction of Cu–electron-coupled transfer. Cox1 contains two heme moieties (a and a3) and the Cu_B site, the Cu_A site is positioned in the intermembrane space domain of Cox2 (47). During the assembly of CCO, Cu insertion into Cox1 and Cox2 is mediated by concerted action of some Cu-binding proteins including Cox17, Cox1, Sco1, Sco2,

and COA6. COX17 is crucial for Cu delivery to both Cox1 and Cox2 from cytosol to IMS. The transfer of Cu ions from Cox17 to the Cu_B site in Cox1 is facilitated by Cox11 (48). In the case of Cu transfer from Cox17 to the Cu_A site in Cox2, two related essential mitochondrial proteins, Sco1 and Sco2, are involved. While Sco1 solely participates in delivering Cu to Cox2, more importantly, COA6 is required for Sco2 for the relay of Cu to Cox2 (48,49). Mice lacking any of these genes involved in Cu transfer to CCO are known to show lethality *in utero* (7,49). While these proteins play a crucial role in the biogenesis of CCO and insertion of Cu into Cu_A and Cu_B sites, it is not known how Cu traverses mitochondria membranes.

Cu delivery to secretory compartments and export out of cells

Many Cu-dependent enzymes must receive Cu ions in the trans-Golgi network (TGN) for their structural integrity and enzymatic activity. The two mammalian P-type Cu(I)-transporting ATPases, ATP7A and ATP7B, function in loading Cu onto newly synthesized Cu-dependent enzymes by delivering Cu into the lumen of the secretory compartment or exporting excess Cu from cells. Cellular Cu ions are transferred from Atox1 to six cysteine-rich cytoplasmic metal binding motif (GMTCXXC) repeats in the N-terminus of the ATP7A/B (50). Under basal conditions, the two efflux pumps are predominantly located in the TGN. However, under high Cu conditions, ATP7A is trafficked to vesicles and the plasma membrane to promote Cu export, whereas ATP7B to cytoplasmic vesicles. In polarized epithelial cells, both proteins show opposite direction in Cu-stimulated trafficking: ATP7A moves to basolateral membranes, whereas ATP7B relocalizes to apical membranes.

The di-leucine in the C-terminus and nine amino acids (^{37}FAFDNVGYE^{45}) in the N-terminus are known to serve basolateral and apical membrane targeting signals in ATP7A and ATP7B, respectively (51-54). While both Cu pumps retain the similar conserved core structure and Cu transport function, these Cu exporters are not thought to have biologically redundant functions (7). Mutations in the gene encoding ATP7A are responsible for Menkes Disease, characterized by cerebral and cerebellar neurodegeneration, connective tissue disorders, coarse hair, and lethality typically by 2 or 3 years. Physiologically, Menkes disease phenotypes are coupled to the inability to pump Cu across basolateral membrane of intestinal epithelial cells to the periphery, or across the blood brain barrier, resulting in hyperaccumulation of intestinal Cu and severe Cu deficiency in the periphery (50,55,56). Impaired ATP7B function in Wilson disease results in an excessive buildup of Cu in the liver and neurons (50,55).

Cu homeostasis at the organismal level in mammals

Mammals have distinct anatomical and physiological tissues and organs, demanding different requirement for Cu ions; therefore, organ-specific and systemic Cu homeostasis is required to regulate toxic but essential Cu atoms. Here we briefly review the role and molecular function of a few organs in Cu homeostasis (Figure 1.2).

Figure 1.2. Current model for intestinal Cu absorption and peripheral distribution. The Ctr1 high-affinity Cu transporter is shown at the apical membrane of IECs. Cu is pumped into the secretory compartment for loading onto Cu-dependent enzymes, or out across the basolateral membrane by the Cu-transporting P-type ATPase ATP7A. In the bloodstream, Cu is transported via the portal vein to the liver. Hepatic Cu is transported to the peripheral tissues via the systemic circulation, and excess Cu is excreted in the bile. Image was adopted and modified from (*10*).

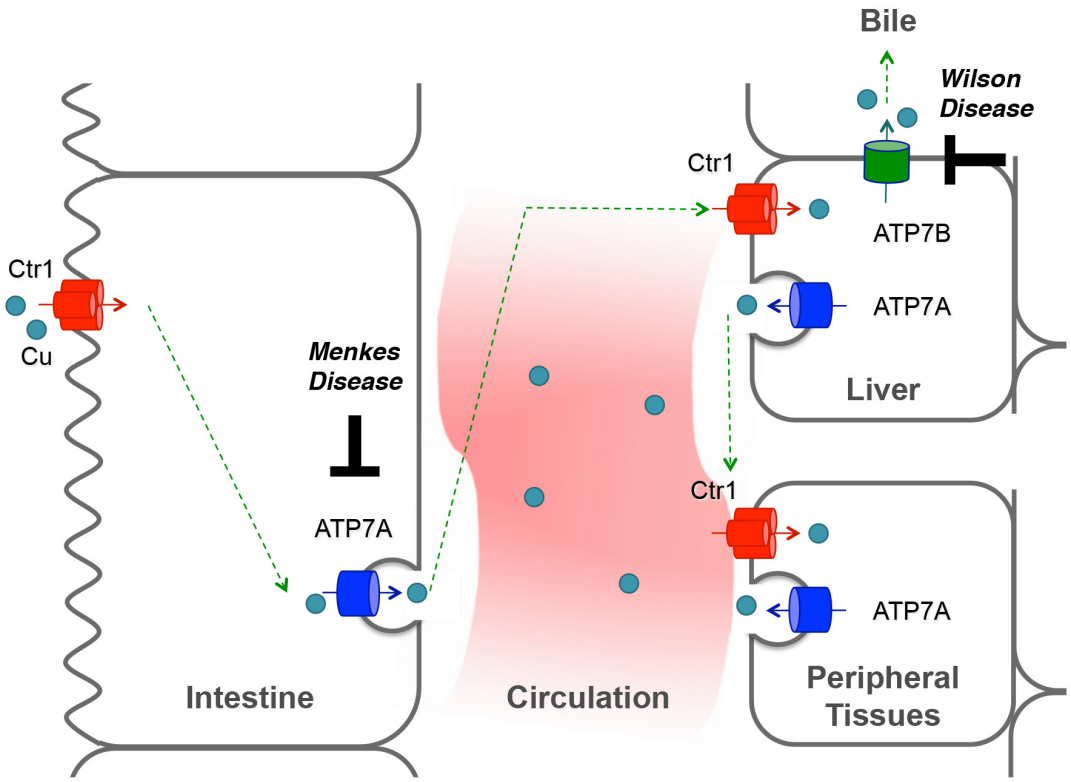
Bile
Wilson Disease
Ctr1
ATP7B
ATP7A
Liver
Ctr1
Cu
Menkes Disease
ATP7A
Intestine
Circulation
Ctr1
ATP7A
Peripheral Tissues

Intestinal Cu uptake and export to portal circulation

Dietary Cu(II) is reduced and subsequently taken up by Ctr1 localized on the apical membrane of intestinal epithelial cells (IECs) of the intestine (57). Imported Cu ions bind to Cu chaperones and ligands, as discussed above, and is routed for intracellular targets including mitochondria and SOD1, incorporated into Cu-dependent proteins in the TGN, and mobilized across the basolateral membrane into peripheral circulation by ATP7A. Several factors such as sex, age, and the amount of dietary Cu are known to affect Cu uptake from dietary sources in the lumen of the intestine (7). Biotin labeling of Ctr1 in intact mouse intestine showed that Ctr1 is localized to both the apical membrane and intracellular vesicles of IECs under Cu adequate diet, whereas the majority of Ctr1 is found on the apical membrane in response to a Cu deficient diet, indicating that Ctr1 localization is regulated for optimal dietary Cu uptake (23). While no significant differences in ATP7A/B expressions were observed between pups and weaned rodents, suckling pups exhibited higher expression of Ctr1 at the apical membrane and elevated Cu levels in IECs than older mice, suggesting the age-specific differences in Cu demands (58).

The critical importance of intestinal Ctr1 for dietary Cu uptake was proven by intestine-specific Ctr1 knockout mice, characterized by severe whole-body Cu deficiency, poor viability, and cardiac hypertrophy (15). However, some non-bioavailable Cu was still accumulated in the IECs, suggesting that Ctr1-independnent Cu uptake from lumen of the intestine to IECs.

Hepatic Cu uptake, storage, and export

Once Cu is transferred to portal circulation from IECs, the liver takes up Cu via hepatic Ctr1 at the basolateral membrane of hepatocytes and distributes it to peripheral tissues. Also, as a major storage organ for Cu and other trace metals, the liver stores Cu and excretes excess Cu to the bile (58,59). While mice carrying a liver-specific ablation of Ctr1 displayed some reduced levels of hepatic Cu, activities of Cu-dependent proteins, and Cu excretion via the bile, no significant differences in Cu levels of the other peripheral tissues were observed, suggesting that a Ctr1-independent mechanism that uptakes Cu and distributes it to circulation may exist (60). Like the age-dependent Ctr1 localization change in IECs, ATP7A abundances and Cu stores in the liver decline progressively during development from birth to adults (61). While it is not known if change of Cu levels in the liver is solely correlated with hepatic ATP7A expression, these data suggest that higher demands for Cu in peripheral tissues in young mice are supplied by hepatic Cu stores, presumably through ATP7A.

Ceruloplasmin (Cp), Cu-dependent ferroxidase, is also known as the Cu deliverer to blood. Hepatic Cu is incorporated to apo-Cp by ATP7B and exocytosed to blood, and 70~95% of total circulating Cu is bound to Cp. However, deletion of the Cp gene in mice resulted in a normal range of Cu levels in blood and peripheral tissues, indicating that Cp may not crucial for exporting Cu to circulation (62,63). Hepatic ATP7B is responsible for metallation of Cu dependent enzymes in the TGN and mobilization of excess Cu to the bile; therefore, hepatic symptoms of Wilson

disease derived from ATP7B mutation can be explained by blockage of biliary Cu excretion (59,64).

Cu metabolism in the heart

Cardiac hypertrophy, a pathological enlargement of cardiomyocytes in the heart, is one of the major symptoms of Cu deficiency in mammals due to the requirement for Cu for CCO in mitochondrial oxidative phosphorylation and SOD1 activity (65). Cardiac Ctr1 localizes to the intercalated discs in cardiomyocytes and supplies Cu for the constant contraction of myocytes (58). Cardiac-specific Ctr1 knockout mice exhibited severe Cu depletion in the heart, cardiomyopathy, and perinatal lethality (61). Interestingly, ATP7A protein levels in both the liver and the intestine were drastically elevated in these knockout mice concomitant with decreased hepatic Cu levels and increased Cu in circulation. These data strongly suggest that inter-organ signaling of Cu status may exist to supply more Cu to Cu-demanding organs such as the heart from the major Cu storage and uptake organs (liver and intestine) by increasing expression of ATP7A Cu efflux pumps.

Cu homeostasis in *C. elegans*

Our understanding of the mechanisms that regulate Cu metabolism has been advanced through the use of several model organisms. *Saccharomyces cerevisiae* have been instrumental in uncovering the complex pathways orchestrating cellular Cu uptake and trafficking pathways (7,66-69). *Drosophila* has been important

in the identification of mechanisms involved in metal-responsive transcription regulation (70-72). More recently, the optically transparent roundworm *Caenorhabditis elegans* (*C. elegans*) has emerged as a highly amenable model of micronutrient metabolism (73-75). Surprisingly, the *C. elegans* model system has been relatively unexploited for questions related to Cu homeostasis, despite the fact that these worms have a defined and highly versatile intestinal capacity for nutrient absorption (76-78). While *C. elegans* has been widely used in the study of the metabolism of metals including Fe, heme, and Zn (74,79-83), Cu-related studies have only been performed for chemosensation of Cu, Cu relay to SOD1, and checking tissue-wide expression of genes encoding the ortholog of Atox1 and ATP7A/B in worms (84,85).

Previous studies have used yeast to demonstrate that *cua-1* has a Cu efflux function, as the gene encoding worm CUA-1 was able to rescue a yeast strain lacking *CCC2* gene, which encodes a functional counterpart (86). Worms harboring *cua-1* transcriptional reporters have been used to detect tissue-wide expression of *cua-1*, indicating that several tissues such as intestine and hypodermis express *cua-1*. An essential role of *cua-1* for Cu transport in *C. elegans* has been suggested, as ablation of *cua-1* results in embryonic lethality (85,87), however how CUA-1 in the intestine responds to systemic Cu status is not understood, and its intracellular location and Cu responsiveness also have not been determined. While worms also have orthologs of most proteins involved in Cu homeostasis in mammals, CCS was not found using a BLAST search. Interestingly, worms utilized Cu-GSH complexes to deliver Cu to SOD1 as a CCS-independent mechanism (88,89).

Figure 1.3. Homologs of genes encoding proteins involved in Cu metabolism in *C. elegans*. A summary of the proteins involved in Cu acquisition, mobilization, stores, and export in worms are shown in the figure. Proteins listed in black boxes are conserved worm proteins. "X" means there are no homologs, and "?" indicates that homologs are not firmly determined in worms.

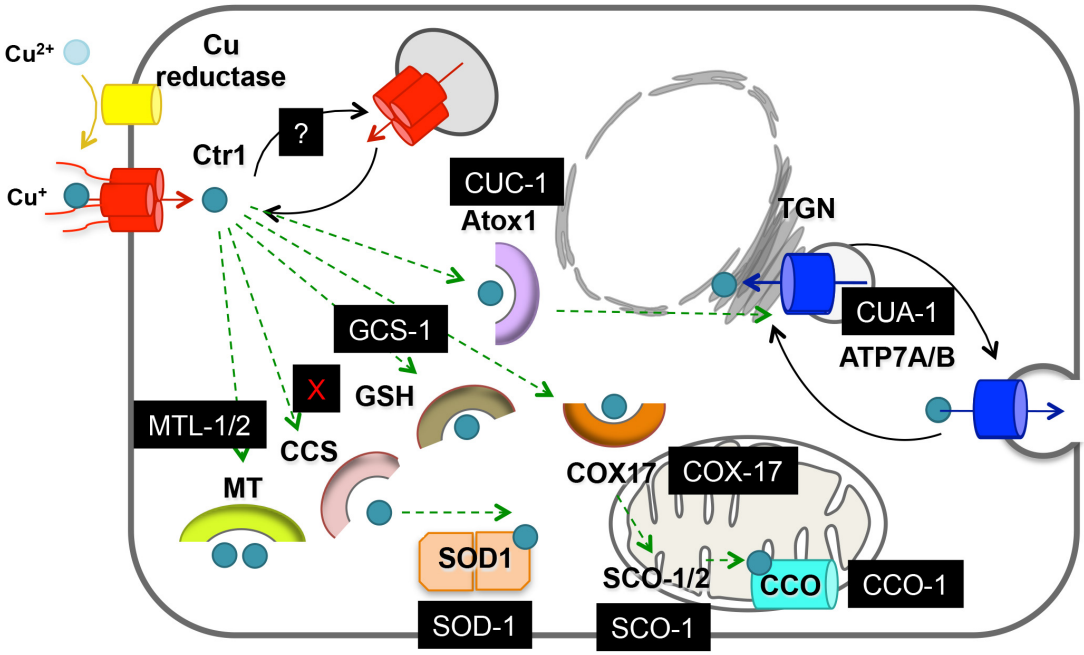
Cu2+
Cu reductase
?
Ctr1
Cu+
CUC-1
Atox1
TGN
CUA-1
ATP7A/B
GCS-1
X
GSH
MTL-1/2
CCS
MT
COX17
COX-17
SOD1
SCO-1/2
CCO
CCO-1
SOD-1
SCO-1

Chapter 2: Materials and Methods

Worm Methods

Worm Culture and Strains

C. elegans were cultivated at 20°C on nematode growth medium (NGM) plates seeded with *Escherichia coli* OP50 or HT115(DE3) as a food source. Strain information (including the Bristol N2 strain, transgenic strains, and deletion strains used in this study) is detailed in Supplemental Table. Several worm strains were obtained from the Caenorhabditis Genetics Center (CGC), which is funded by National Institutes of Health (NIH) Office of Research Infrastructure Programs (P40 OD010440). Presence of the *cua-1(ok904)* allele was confirmed by sequencing of the *cua-1* locus. Genotyping primers for the *cua-1(ok904)* allele can be found in Appendix II. Genotypes of transgenic animals and mutant worms were confirmed by DNA sequencing or PCR. $CuCl_2$ was used as the source for Cu supplementation in NGM dishes and media in all experiments.

Worm Analysis Using COPAS Biosort or Microscopy

Gravid hermaphrodites were bleached to release their eggs, which were allowed to hatch and arrest at L1 stage in M9 buffer overnight. The resultant age-synchronized L1 larvae were cultured on NGM plates for approximately 2.5 days. Worms from each condition (~200 worms) were analyzed for time of flight (length), extinction (width), and GFP fluorescence using a COPAS Biosort FP-250 (Union

Biometrica). To visualize live worms, animals were paralyzed in M9 buffer containing 10 mM sodium azide (NaN_3) and mounted on agarose pads. GFP, mCherry, Cu probe CF4, autofluorescence, and LysoTracker fluorescence in worms were imaged using an SP5 X confocal microscope (Leica).

Inductively-Coupled Plasma Mass Spectrometry (ICP-MS)

Metal contents of worms and MEFs were measured using inductively coupled plasma mass spectrometry (ICP-MS) as previously described (15). Values were normalized to wet weight of worms or cells. For sample preparation, synchronized L1 worms were grown on 10 cm NGM plates seeded with OP50 or HT115 RNAi bacteria and supplemented with the indicated amounts of Cu or BCS. Worm or cell pellets were collected and washed extensively with M9 buffer or PBS, respectively, transferred to acid-washed tubes, and frozen at -80°C. At least three independent biological replicates were analyzed.

Reverse transcription quantitative PCR (RT-qPCR)

Synchronized larvae were grown to the L4/young adult stage on NGM plates seeded with OP50 bacteria and supplemented with indicated concentrations of Cu or BCS. Then, the worms were extensively washed with M9 buffer and collected for RNA isolation. Briefly, worms were resuspended in TRIzol (Invitrogen) reagent followed by lysis using a FastPrep-24 (MP Biomedicals) homogenizer in Lysing Matrix Tubes (MP Biomedicals). Total RNA was isolated using TRIzol, treated with DNAse I (Ambion), and cDNA was produced using SuperScript VILO Master Mix

(Invitrogen). RT-qPCR was performed on an Agilent Mx3005P qPCR System thermocycler (Agilent Genomics) using SYBR Green JumpStart Taq ReadyMix (Sigma). Expression levels of *cua-1* were compared to an internal GAPDH (*gpd-2*) control, and the fold changes were determined using the $2^{(-\Delta\Delta Ct)}$ method (90). The primers used for PCR are listed in Appendix II.

Plasmid Construction and Transgenic Strain Generation

To generate *C. elegans* expression plasmids, gene-specific gateway *attB* primers were used to amplify DNA sequences such as promoters, ORFs, and 3' UTRs. Purified DNA fragments were recombined into donor vectors first, and then into expression plasmids using Gateway recombination reactions (Invitrogen). For mammalian cell expression plasmids, the GFP-tagged ORF of CUA-1 was digested with *NheI* and *BamHI*, and ligated into the pEGFP-C1 vector (Clontech). Transgenic animals were produced by introducing transcriptional or translational reporters into *unc-119* worms using the PDS-1000 particle delivery system (Bio-Rad) for bombardment transformation (82,83).

RNA Interference (RNAi)

RNAi bacteria strains against *cua-1* (Y76A2A.2) and *pgp-2* (C34G6.4) were obtained from the Ahringer feeding library (91) and *cuc-1* (ZK652.11) was obtained from the ORFeome-based RNAi library (92). Bacteria transformed with the empty L4440 vector were used as a negative RNAi control. Synchronized L1 animals were grown on RNAi plates (NGM dishes containing 2 mM IPTG, 12 μg/mL tetracycline,

and 50 μg/mL carbenicillin) that were seeded with HT115(DE3) bacteria expressing dsRNA for each gene.

Cell culture and Immunoblotting

Atp7a$^{+/+}$ and *Atp7a*$^{-/-}$ MEFs were cultured in Dulbecco's Modified Eagle Medium (DMEM; Lonza) supplemented with 10% (v/v) heat-inactivated fetal bovine serum (FBS; Atlanta biologicals) and 100 units/ml penicillin/streptomycin (Lonza). The plasmid expressing CUA-1.1::GFP was transfected to *Atp7a*$^{-/-}$ MEFs using PolyJet (SignaGen). All cells were cultured under 5% CO_2 at 37°C. Cells at ~70% confluence were collected and washed three times with ice-cold PBS (pH 7.4). Cell pellets were suspended in about 5 times their volume in ice-cold cell lysis buffer (PBS pH 7.4, 1% triton X-100, 0.1% sodium dodecyl sulfate, 1 mM EDTA) containing Halt protease inhibitor cocktail (Thermo Scientific), briefly vortexed, and incubated for 1 h. Early stage adult worms grown from synchronized larvae were collected and washed with M9 buffer. Worms were resuspended in the same lysis buffer followed by disruption using a FastPrep-24 (MP Biomedicals) homogenizer in the presence of glass beads. The same lysis buffer was used for disruption of MEFs on ice for 30 min. Cell suspensions and worm lysates were centrifuged at 16,000 × g at 4°C for 15 min. After centrifugation, the clarified lysates were used for immunoblotting, and protein concentrations were measured using the BCA Protein Assay Kit (Thermo Scientific). Samples (100 μg/lane) were fractionated on a 4-20% gradient gel (BioRad). The anti-ATP7A antibody (a gift from Dr. Stephen G. Kaler, NIH, Bethesda), anti-GFP (Covance), and anti-tubulin antibody (Sigma) were used at

a 1:1,000 dilution. The anti-CCS antibody (Santa Cruz Biotechnology) and anti-GAPDH antibody (Sigma) were used at 1:4000 dilution and 1:10,000 dilution, respectively. Horseradish peroxidase-conjugated anti-rabbit or anti-mouse IgG (Rockland Immunochemicals) was used as the secondary antibody for immunoblotting (1:5,000 dilution). Immunoblots were detected using SuperSignal West Pico Chemiluminescent Substrate reagents (Thermo Fisher Scientific) using a chemidocumentation imaging system (Bio-Rad).

Staining with the Cu Probe CF4 and LysoTracker

The Cu Fluor-4 (CF4) sensor combines a piperidine-substituted rhodol with a trifluoromethyl-substituted bottom ring bearing a thioether receptor, along with a matched control Cu Fluor-4 (Control CF4) dye that lacks the Cu-responsive receptor to help distinguish between Cu-dependent and dye-dependent responses (93,94). Replacement of the thioether-rich receptor arms for Cu(I)-recognition in CF4 by isostructural octyl groups in control CF4 provides a mimic of the size, shape, and hydrophobicity of thioethers but do not bind Cu, offering a matched pair of probes to disentangle Cu-dependent fluorescence responses from potential dye-dependent ones. We used the Rhodol based-CF4 probe and control CF4 probe (both final concentration, 25 μM) for staining Cu(I) in intact worms and 2 μM LysoTracker Red DND-99 (Invitrogen) for detecting gut granules. Both chemicals were prepared in M9 buffer and dispensed onto NGM plates (74). L3 stage worms were cultured on these dishes for 12-16 h in the dark. Post-incubation, stained worms were transferred to seeded NGM plates containing Cu concentrations equivalent to treatment conditions.

After 2h incubation, worms were collected and washed three times with M9 buffer, and imaged via confocal microscopy.

Cu-Microinjection Experiments

To deliver Cu directly to the basolateral side of the intestine and peripheral tissues, $CuCl_2$ solution was microinjected into the pseudocoelom in the posterior region of young adult worms that had been grown in 50 μM BCS treated NGM dishes. Histidine or $CuCl_2$ with histidine (1:2 molar ratio) diluted in M9 buffer was injected to worms using an Eppendorf Femtojet microinjector attached to a Leica inverted microscope under specified settings (pi= 30 psi, pc=4.5 psi, ti= 4 sec). Worms were recovered on seeded plates for 6 h and then mounted on 2% agarose pads for imaging.

Mammalian Methods

Antibodies

The anti-ATP7A antibody (generous gift from Drs. Stephen G. Kaler, National Institutes of Health (NIH), Bethesda, MD and Michael J. Petris, University of Missouri, Columbia, MO), anti-ATP7B antibody (generous gift from Dr. Svetlana Lutsenko, Johns Hopkins University, Baltimore, MD) anti-Ctr1 antibody (15), anti-β-tubulin antibody (Cell Signaling Technology), anti-β-actin antibody (Sigma), anti-COX-IV subunit IV antibody (Invitrogen), and anti-Na^+/K^+-ATPase (Thermo Scientific) antibody were each used at a 1:1,000 dilution. The anti-CCS antibody

(Santa Cruz Biotechnology) and anti-GAPDH antibody (Sigma) were used at a 1:400 dilution and 1:10,000 dilution, respectively. Horseradish peroxidase-conjugated anti-rabbit or -mouse IgG (Rockland Immunochemicals) was used as the secondary antibody for immunoblotting at a 1:5,000 dilution. Immunoblots were detected using SuperSignal West Pico or Femto Chemiluminescent Substrate reagents (Thermo Fisher Scientific) using a chemidocumentation imaging system (Bio-Rad). The anti-Na^+/K^+- ATPase antibody was purchased from the Developmental Studies Hybridoma Bank (DSHB) for immunofluorescence experiments. Alexa Fluor 488 anti-rabbit IgG, Alexa Fluor 568 anti-mouse IgG, Alexa Fluor 647 WGA-conjugate, and ProLong Gold Antifade mounting reagent with DAPI were obtained from Life Technologies.

Cell Culture

Rat intestinal epithelial cells (IEC-6) and HUVEC cells were obtained from the American Type Culture Collection (ATCC) and cultured according to the distributor's recommendations. Wild-type ($Ctr1^{+/+}$) and $Ctr1^{-/-}$ MEFs were cultured in Dulbecco's Modified Eagle Medium (DMEM; Lonza) supplemented with 10% (v/v) heat-inactivated fetal bovine serum (FBS; Atlanta Biologicals), 1× MEM non-essential amino acids (Lonza), 50 μg/mL uridine, 100 U/mL penicillin/streptomycin (Lonza), and 55 μM 2-mercaptoethanol. All cells were cultured under 5% CO_2 at 37°C. Cells at ~60% confluence were collected and washed three times with ice-cold PBS (pH 7.4). $CuCl_2$ (Alfa Aesar) and bathocuproinedisulfonic acid Cu chelator (BCS; Acros) were used for Cu level-responsive ATP7A expression change experiments with various cell lines. For proteasomal degradation inhibition

experiments, IEC-6 cells were treated with 50 μg/mL cycloheximide (CHX; Sigma), 20 μM MG-132 (Sigma), and 100 nM bortezomib (ApexBio). Cell pellets were suspended in ice-cold cell lysis buffer (PBS pH 7.4, 1% Triton X-100, 0.1% sodium dodecyl sulfate (SDS), 1 mM EDTA) containing Halt protease inhibitor cocktail (Thermo Scientific), briefly vortexed, and incubated for 1 h. Cell suspensions were centrifuged at 16,000 x*g* at 4°C for 15 min to remove insoluble material, and supernatants were collected. Protein concentrations were measured using the BCA Protein Assay Kit (Thermo Scientific). The indicated amount of protein extract was fractionated by SDS-gel electrophoresis on 4-20% gradient gels (Bio-Rad) and immunoblotted.

IEC-6 cells were grown on 24-mm polyester membrane transwells with 0.4-μm pores (Corning) until confluent. When cultures reach to 90% confluence, the growth medium was exchanged every day. Formation of tight junctions was monitored by the measurement of transepithelial electrical resistance (TEER) using an EVOM2 meter and STX2 electrodes (World Precision Instruments). Cells were judged to be ready for Cu uptake experiments when the TEER value was ~400 Ω× cm^2. After incubating cells with 200 μM BCS for 24 h, both compartments were filled with fresh culture medium containing BCS, $CuCl_2$, or 10 mM EDTA for 12 h. Cells were rinsed with ice-cold PBS (pH 7.4), scraped in the same lysis buffer to harvest, and analyzed by immunoblotting.

Primary hepatocytes were isolated from mice at P12 according to the procedure previously described in detail (95). Briefly, an incision was made on the right atrium with scissors to ensure a route for overflow, then perfusion was performed with calcium-free Hanks' balanced salt solution (HBSS; Lonza) supplemented with 0.5 mM EDTA (Sigma) at 37°C at a rate of 3.5 mL/min, followed by HBSS supplemented with 0.3 mg/mL collagenase (Sigma) and 5 mM $CaCl_2$ under the same conditions at a rate of 5 mL/min. The total-collected liver cell suspension was then filtered through a 100-μm nylon mesh and centrifuged at 50 x*g* for 5 min. Next, the pellet was resuspended and incubated in DMEM with 10% FBS, 0.1 μM insulin (Sigma), and 100 U/mL penicillin/streptomycin. After 3 h of incubation at 37°C in an atmosphere of 5% CO_2, the medium was changed to M199 supplemented with 0.1 μM dexamethasone, 0.1 μM 3,3',5-triiodo-L-thyronine, 0.1 μM insulin, and 100 U/mL penicillin/streptomycin and incubated for further analysis.

Animal and Tissue Preparations

For the Cu administration experiment, pups at P7 (C57BL/6J, Jackson Laboratory) were SQ administered 50 μL of saline containing 10 μg $CuCl_2$ with 19.12 μg L-histidine/g of mouse BW or 50 μL of saline alone for 3 consecutive days and sacrificed at P10. The intestinal Ctr1 knockout mice ($Ctr1^{int/int}$) and control mice ($Ctr1^{flox/flox}$ and $Ctr1^{flox/+}$) were generated as described previously (15). $Ctr1^{flox/flox}$ and $Ctr1^{int/int}$ mice pups were administered with same amount of Cu-histidine or saline alone given subcutaneously at P10 and dissected two days later (P12). To generate dietary Cu-deficient mice, dietary treatment of dams began on embryonic day 16 or

17, as previously described (58). Dams from wild type mice were fed Cu-deficient or Cu-adequate diets, consisting of a Cu-deficient purified diet (TD.80388, Envigo) and either sterilized distilled low-Cu drinking water or Cu-supplemented drinking water (20 μg $CuCl_2$/mL), respectively. Pups were sacrificed at P15 due to clear evidence of severe Cu deficiency. All procedures involving animals were carried out in accordance with the National Institutes of Health Guide for the Care and Use of Laboratory Animals and have been approved by the Institutional Animal Care and Use Committee at the University of Maryland, College Park (protocol number R-15-14). Tissues were dissected following washing with ice-cold PBS, frozen in liquid nitrogen, and stored at −80°C until use. For the isolation of intestinal epithelial cells, the small intestine was opened along the long axis, washed in ice-cold PBS, and soaked in PBS containing 1.5 mM EDTA and protease inhibitors at 4°C for 30 min with gentle agitation (96). After incubation, the mesenchymal layer was removed, and intestinal epithelial cells were washed three times with ice-cold PBS with protease inhibitors and recovered by centrifugation at 2000 x*g* for 3 min.

Dissected tissues or purified intestinal epithelial cells were homogenized in ice-cold cell lysis buffer (PBS pH 7.4, 1% Triton X-100, 0.1% SDS, 1 mM EDTA) containing Halt protease inhibitor cocktail (Thermo Scientific) in 1.5 mL centrifuge tubes by pellet mixer (VWR) on ice. Homogenates were incubated on ice for 1 h followed by centrifugation at 16,000 x*g* for 15 min at 4˚C. The supernatants were used as total extracts for immunoblotting. Protein concentrations were measured by the BCA Protein Assay Kit (Thermo Scientific) with bovine serum albumin as a

standard and equal amounts of protein (100 μg/lane) were fractionated on a 4-20% gradient gel (Bio-Rad).

Confocal Immunofluorescence Microscopy

For the immunofluorescence analysis, intestines were washed with PBS and fixed in 4% (w/v) paraformaldehyde/PBS immediately following dissection. A 2 cm section of upper jejunum, positioned 1 cm from the stomach, was dissected and fixed with the same fixative solution overnight at 4°C with gentle shaking. Fixed tissue samples were processed and embedded into a paraffin block and sectioned at a thickness of 5 μm for immunofluorescence staining. The deparaffinized sections were heated at a sub-boiling temperature in 1 mM EDTA buffer (pH 8.0) for 15 min to expose the antigen. Samples were blocked with 2% (w/v) BSA and 0.2% Triton X-100 in PBS for 1 h and incubated with primary antibody (as described in the figure legends) for 1 h at room temperature. After washing with 0.2% BSA and 0.02% Triton X-100 in PBS, sections were incubated with Alexa Fluor 488 anti-rabbit IgG or Alexa Fluor 568 anti-mouse IgG (1:250 dilution in 1% (w/v) BSA in PBS) for 1 h at room temperature and washed with PBS. Then, the procedure of blocking and incubation with primary and secondary antibody was repeated as described above. Following incubation with Alexa Fluor 647 Conjugate of WGA for 1 h at room temperature followed by washing, sections were mounted with Gold antifade reagent with DAPI, incubated overnight at 4°C, and visualized with a Leica SP5 confocal microscope.

Reverse transcription quantitative PCR (RT-qPCR)

Total RNA was isolated from intestinal epithelial cells or liver tissues by TRIzol reagent (Ambion). After eliminating genomic DNA using DNA-free DNA Removal Kit (Ambion), first strand cDNA was synthesized using SuperScript VILO Master Mix (Invitrogen). RT-qPCR was performed on an Agilent Mx3005P QPCR System Thermocycler (Agilent Genomics) using SYBR Green qPCR Master Mixes (Applied Biosystems). Levels of *Atp7a, Ctr1, Mt1,* and *Mt2* mRNA were compared to an internal *Gapdh* control in mouse tissues, and rat *Atp7a* transcript levels were compared to *18s rRNA* control in IEC-6 cells, and the fold change was determined using the $2^{(-\Delta\Delta Ct)}$ method (90). The oligonucleotide primer sequences used for PCR can be found in Appendix III.

Tissue Metal Measurements

Cu and Fe concentrations were measured from nitric acid-digested cells or tissues by inductively coupled plasma mass spectrometry (ICP-MS) as described (97). Tissues were collected into acid-washed 1.5-mL microcentrifuge tubes and weighed, and the harvested cultured cells were washed with PBS three times and weighed. The values were normalized by wet weight (g) of cells or mouse tissues. More extensive details can be found in previous reports (97).

General Methods

Bioinformatics and Statistics

Clustal Omega and ClustalW2 were used to generate a multiple sequence alignment and phylogenetic tree of a subset of *cua-1* homologs (98). Transmembrane helices and Cu-binding motifs of CUA-1 homologs were predicted using TMHMM and the Conserved Domain Database (CDD) (99). Statistical significance was determined using a one-way or two-way ANOVA followed by Tukey's post hoc test or two-tailed unpaired Student's t-test in GraphPad Prism, Version 6 (GraphPad Software). All data are presented as mean ± SEM (standard error of the mean) or mean ± SD (standard deviation), and P-values less than 0.05 were considered to be statistically significant.

Chapter 3: The Role of the Intestinal Cu Exporter CUA-1 in Systemic Cu Homeostasis in *Caenorhabditis elegans*

Summary

Cu is essential for catalytic and regulatory functions in a wide range of biochemical reactions involved in mitochondrial respiration, connective tissue formation, and iron (Fe) metabolism (2,7). Cu deficiency is associated with pathologies that include anemia, neutropenia, and cardiomyopathy (2,100). Additionally, if its homeostasis is not properly regulated, Cu can be extremely toxic due to its stimulation of free radical production. Organisms finely tune Cu homeostasis through a combination of absorption, distribution, and efflux in multiple tissues. In many species, a key aspect of Cu homeostasis is facilitated by membrane-bound Cu efflux pumps. Mammals have two primary Cu exporters which are structurally related: ATP7A and ATP7B P-type ATPases. In tissue-culture models, both proteins deliver Cu to the lumen of the secretory machinery for incorporation into various Cu-dependent enzymes at basal or low intracellular Cu concentrations. At elevated cellular Cu levels, ATP7A traffics to the plasma membrane to remove excess Cu from cells, and ATP7B relocates to the plasma membrane and endosomes to excrete Cu (7,50). In humans, mutations in the genes encoding ATP7A and ATP7B result in severe systemic Cu deficiency (Menkes disease) and hepatic/neuronal hyperaccumulation of Cu (Wilson's disease), respectively (2). However, to date, Cu-

responsive steady-state distributions of ATP7A/B have been studied predominantly at the cellular level in tissue-culture models, and regulation of their trafficking by dietary Cu has not yet been thoroughly elucidated within an intact animal model (50,101,102).

While the optically transparent roundworm *C. elegans* has emerged as a highly amenable model of micronutrient metabolism (73-75), the *C. elegans* model system has been relatively unexploited for questions related to Cu homeostasis, despite the fact that these worms have a defined and highly versatile intestinal capacity for nutrient absorption (76-78). To examine the effects of Cu deprivation and overload on the development of animals *in vivo*, we utilized *C. elegans*, which has been widely used in the study of the metabolism of metals including Fe, heme, and zinc (Zn) (74,79-83). While mammals have two Cu exporters, serving complementary functions in different tissues such as the gut and liver, lower metazoans (including nematodes [*Caenorhabditis elegans*] and insects [*Drosophila melanogaster*]) have only a single homolog of ATP7A/B (7,85,103). The protein product of *C. elegans cua-1* shares very high sequence similarity with human ATP7A/B. Previous studies have used yeast to demonstrate that *cua-1* has Cu efflux function, as the gene encoding *C. elegans* CUA-1 could rescue a yeast strain lacking *CCC2* gene, which encodes a functional counterpart (86). In worms, transcriptional reporters have been used to detect *cua-1* expression in several tissues, including the intestine. An essential role for *cua-1* for Cu transport in *C. elegans* has been suggested, as deletion of *cua-1* results in embryonic lethality (85,87), however how CUA-1 in the intestine responds

to systemic Cu status is not understood, and its intracellular location and Cu responsiveness has not been determined.

Here, we report the importance of Cu in *C. elegans* development and a distinct role for CUA-1 in mediating Cu transport. Expression of *cua-1* specifically in the intestine is sufficient to rescue the embryonic lethal phenotype of the *cua-1* mutant. A CUA-1 translational fusion protein primarily localizes to the basolateral membrane of the intestine under basal and Cu-deficient conditions, but redistributes to lysosome-related organelles (gut granules) in response to elevated Cu levels in the diet. Moreover, Cu-injection into the pseudocoelom, a fluid-filled body cavity between the intestine and the body wall, leads to a significant endosomal re-localization of intestinal CUA-1 even in dietary Cu-deprived worms. Our studies show that intestinal CUA-1 is a key component regulating Cu supply and detoxification to maintain systemic Cu homeostasis in the intact animal.

Results

Dietary Cu levels affect worm growth

Living organisms have an optimal range of Cu concentrations, and dietary excess or deficiency of Cu causes various diseases and developmental defects in a broad range of organisms (2,7,104). To determine the dietary Cu requirements of *C. elegans* grown on NGM plates fed with the *Escherichia coli* strain OP50, we followed worm growth over eight days under Cu restriction using the Cu(I)-specific chelator bathocuproinedisulfonic acid (BCS), or with Cu supplementation using $CuCl_2$. Worm growth showed a biphasic curve over dietary Cu levels (Fig. 3.1A).

Figure 3.1. Growth of *C. elegans* is affected by dietary Cu. (A) Population growth rates of wild-type N2 worms cultured in the presence of increasing amounts of $CuCl_2$ or BCS on NGM dishes. Fifty synchronized L1 stage worms were grown on 10 cm plates for eight days under specified conditions and quantified by microscopy. Error bars are mean ± SEM of three independent experiments. (B) Synchronized L1 worms were cultured on plates supplemented with different levels of Cu or BCS for three days. Representative DIC images of worms three days post-hatch are shown. Scale bar, 50 μm. (C) Synchronized L1 larvae grown on NGM plates for 2.5 days were sorted by a COPAS Biosort. Time of flight (TOF) and extinction (EXT) denote the length and optical density (width) of worms, respectively.

A

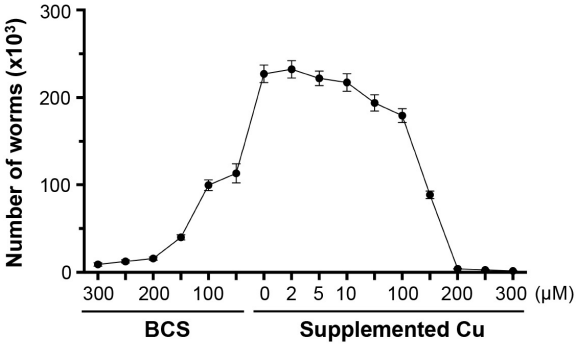
Number of worms (x10³)
300
200
100
0
300 200 100 0 2 5 10 100 200 300 (μM)
BCS
Supplemented Cu

B

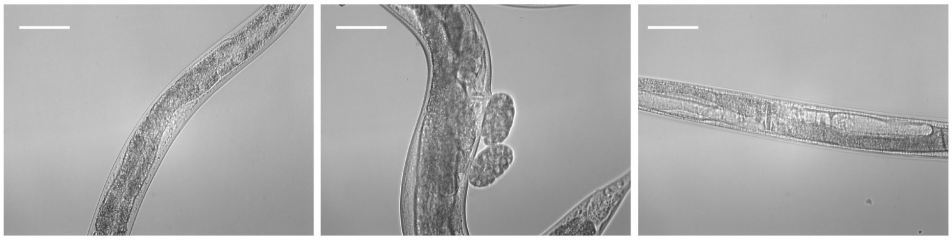
100 μM BCS
0 μM CuCl2
150 μM CuCl2

C

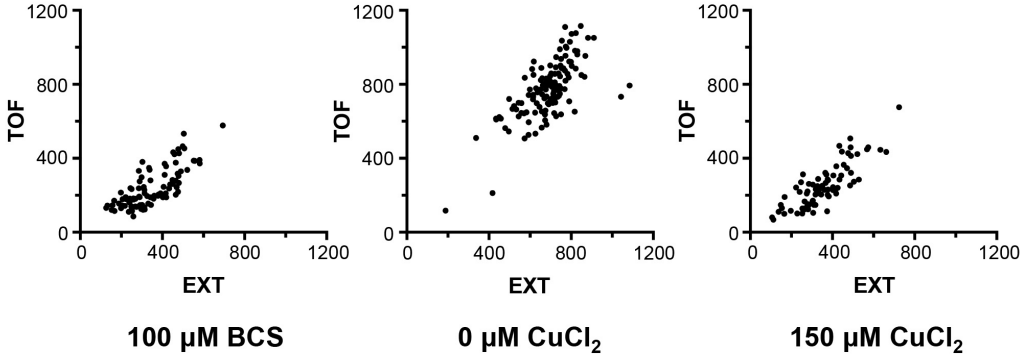
TOF
EXT
1200
800
400
0
0 400 800 1200
100 μM BCS
0 μM CuCl2
150 μM CuCl2

Figure 3.2. Metal levels of *C. elegans* in response to dietary Cu. Total Cu (A), Fe (B), Zn (C) levels of L4 stage wild-type worms grown on agar plates with varying levels of dietary Cu were determined by ICP-MS. Error bars indicate mean ± SEM of 3-6 independent experiments, and different letters indicate significantly different means ($P<0.05$) (one-way ANOVA, Tukey's post hoc test).

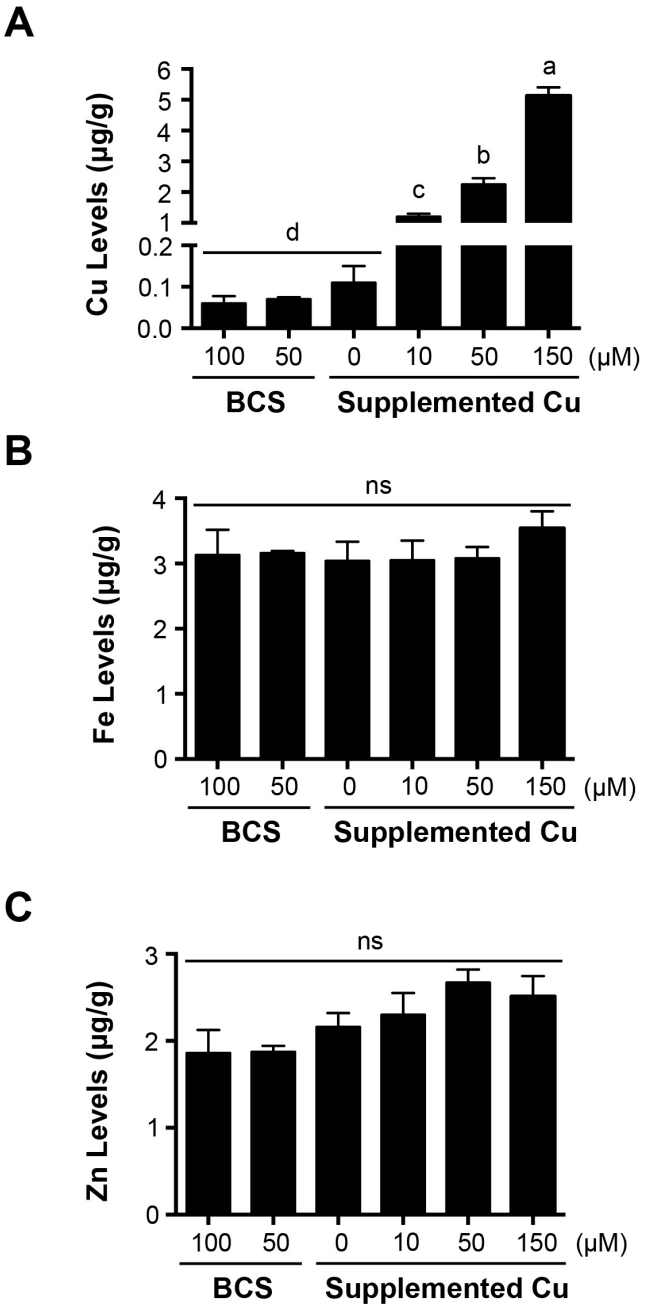
A
Cu Levels (µg/g)
6
5
4
3
2
1
0.2
0.1
0.0
a
b
c
d
100 50 0 10 50 150 (µM)
BCS
Supplemented Cu
B
Fe Levels (µg/g)
4
3
2
1
0
ns
100 50 0 10 50 150 (µM)
BCS
Supplemented Cu
C
Zn Levels (µg/g)
3
2
1
0
ns
100 50 0 10 50 150 (µM)
BCS
Supplemented Cu

C. elegans displayed maximal growth in the low micromolar range of supplemental Cu and impaired growth at either end of the Cu spectrum, 100 μM BCS and 150 μM Cu, with smaller brood size and delayed development. Large amounts of Cu (≥ 200 μM) resulted in growth arrest at the L3 stage, likely due to Cu toxicity. Monitoring of animal development revealed that at optimal Cu (~2 μM), worms became gravid adults in 3 days, while most animals grown at high or low Cu conditions only reached the L3 to young adult stage at this time point (Fig. 3.1B).

To quantify the effect of dietary Cu on each animal within a mixed population, we used a COPAS Biosort instrument. Animal development was significantly delayed by supplementation of high doses of either Cu or BCS (Fig. 3.1C). To complement the analysis of how dietary Cu influences worm growth, whole animal Cu content was measured using inductively coupled plasma mass spectrometry (ICP-MS). Worms cultured with high Cu (150 μM) had only a 5-fold increase in Cu content as compared to animals grown on 10 μM Cu supplementation, whereas the relative ratio of supplemental Cu concentrations (15-folds) is higher, implying the existence of a homeostatic regulatory mechanism for maintaining optimal Cu levels in *C. elegans* (Fig. 3.2A). BCS treatment resulted in ~ 40% reduction in total Cu content as compared to no supplementation. No significant changes in Fe and Zn content were observed in worms treated with Cu or BCS (Fig. 3.2B-C). Collectively, these data indicate that dietary Cu levels impact growth and development within one generation in *C. elegans*.

CUA-1 is essential for larval development in *C. elegans*

While vertebrates have two Cu exporters, unicellular organisms and invertebrates have a single Cu exporter, suggesting that the Cu exporter gene duplication to ATP7A and ATP7B occurred following the branching off of the vertebrate phyla (Fig. 3.3A-B). In worms, *cua-1* encodes a putative Cu exporter (86), which shares about 45% sequence identity at the amino acid level with human ATP7A and ATP7B. Importantly, the motifs known to be essential for Cu transport and protein trafficking in the human ATP7A/B are highly conserved in CUA-1 (Fig. 3.3B and Fig. 3.4B). The genomic structure of *cua-1* consists of 16 exons, and it is predicted to encode two splice isoforms. The first isoform, *cua-1.1* (Y76A2A.2a), contains all exons, whereas the *cua-1.2* (Y76A2A.2b) isoform lacks the first two exons, which encode the first metal-binding domain (Fig. 3.4A-B).

To ascertain the physiological function of *cua-1*, worms were analyzed for growth and developmental phenotypes after knockdown of *cua-1*. Without Cu supplementation, animals treated with *cua-1* RNAi at the L1 stage became gravid adults in four days, but failed to lay eggs. For worms grown in the presence of 100 μM BCS, treatment with *cua-1* RNAi resulted in near total lethality, while vector control worms only showed a delayed F_1 hatching (Fig. 3.5A). Together, these results indicate that *cua-1* is required for normal growth in *C. elegans*. To further explore the importance of *cua-1* in fecundity, total brood size was quantified. Regardless of RNAi conditions, addition of 100 μM BCS resulted in reduced brood sizes, indicating that dietary Cu uptake is essential for normal reproduction (Fig. 3.5B).

Figure 3.3. Phylogenetic analysis of CUA-1 orthologs. Phylogenetic analysis (A) and multiple sequence alignments (B) of CUA-1 orthologs in *Caenorhabditis elegans* (Ce), *Arabidopsis thaliana* (At), *Saccharomyces cerevisiae* (Sc), *Drosophila melanogaster* (Dm), *Danio rerio* (Dr), *and Homo sapiens* (Hs). Evolutionary distances (sequence changes) were used to infer the phylogenetic tree. (C) Sequencing results showing inserted and deleted molecular regions in the wild-type and *cua-1(ok904)* mutant worms. Numbers indicate the base pair location within the *cua-1* cDNA.

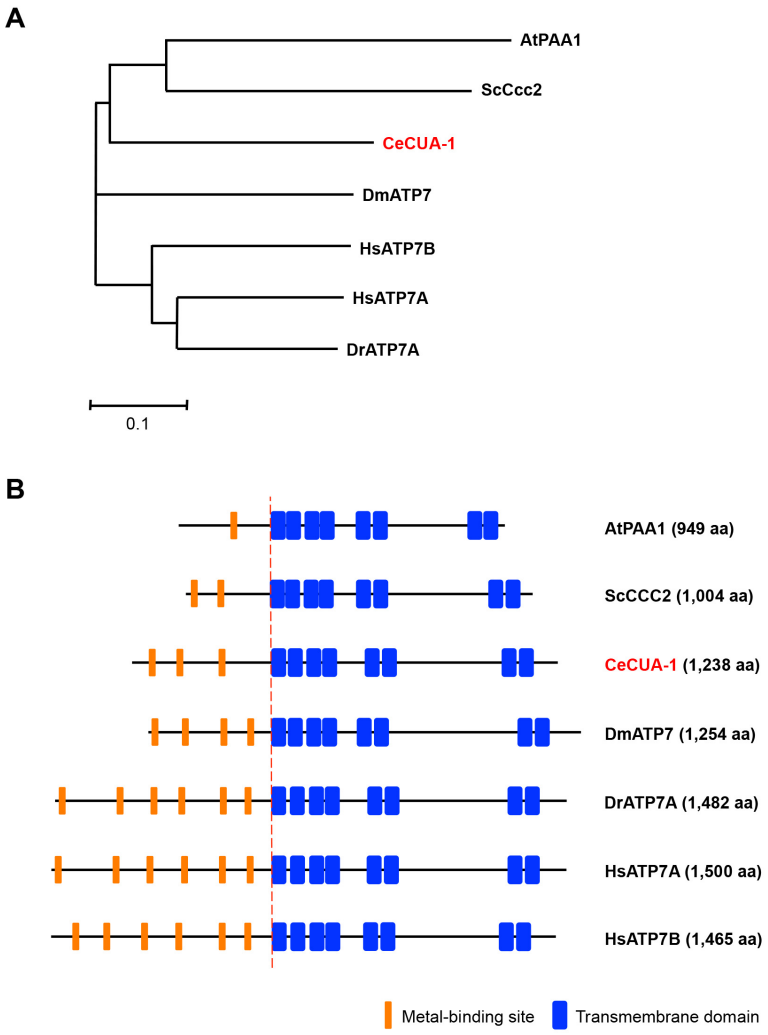
A
AtPAA1
ScCcc2
CeCUA-1
DmATP7
HsATP7B
HsATP7A
DrATP7A
0.1
B
AtPAA1 (949 aa)
ScCCC2 (1,004 aa)
CeCUA-1 (1,238 aa)
DmATP7 (1,254 aa)
DrATP7A (1,482 aa)
HsATP7A (1,500 aa)
HsATP7B (1,465 aa)
Metal-binding site
Transmembrane domain
C
Wild Type
+2923
+2502
cDNA (bp)
cua-1
(ok904)

Figure 3.4. Gene structure and protein topology of *cua-1*. (A) Schematic diagram of the *C. elegans cua-1* gene. The straight line indicates genomic DNA on *C. elegans* chromosome III. The *cua-1.2* transcript lacks the first two exons as compared to the full-length *cua-1.1* isoform. (B) Predicted CUA-1 membrane topology. Domains required for Cu transport activity, including metal- binding sites, a phosphatase domain, a CPC motif (Cys-Pro-Cys), a phosphorylation domain, an ATP- binding motif, and a dileucine-based sorting signal present in human ATP7A/B are highly conserved in CUA-1. The genomic regions of *cua-1* that are deleted in the *ok904* allele are shown in the red box, and the N-terminal truncation in CUA-1.2 is shown in the blue box.

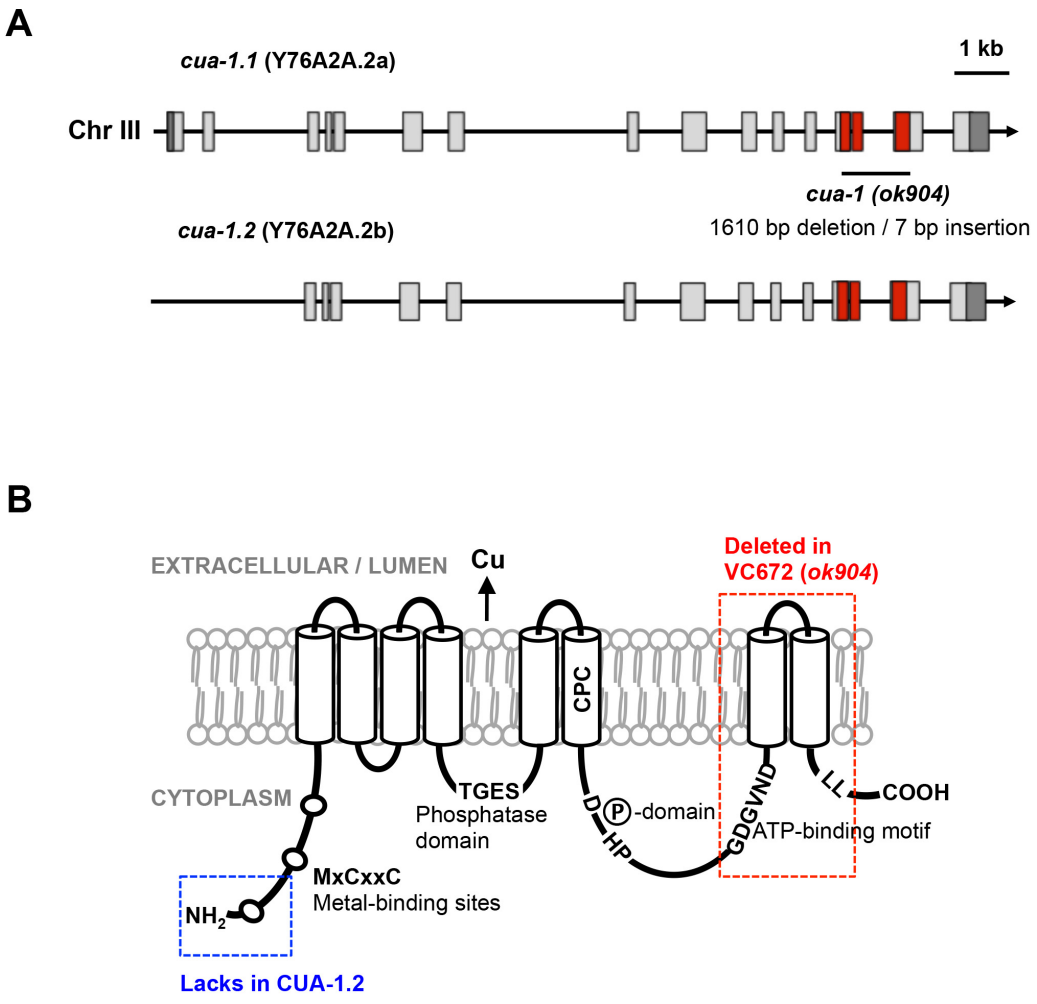
A
cua-1.1 (Y76A2A.2a)
1 kb
Chr III
cua-1 (ok904)
cua-1.2 (Y76A2A.2b)
1610 bp deletion / 7 bp insertion
B
EXTRACELLULAR / LUMEN
Cu
Deleted in
VC672 (ok904)
CPC
CYTOPLASM
TGES
Phosphatase
domain
D-HP
Ⓟ-domain
GDGVND
LL
COOH
ATP-binding motif
MxCxxC
Metal-binding sites
NH2
Lacks in CUA-1.2

Figure 3.5. *cua-1* is required for larval development under low Cu conditions. (A) L1 worms were exposed to RNAi for 4 days with or without 100 μM BCS treatment; representative microscope images are shown. Note that *cua-1* RNAi used in this study targets the last two exons of both *cua-1.1* and *cua-1.2*. Arrowhead indicates eggs that have already been laid. (B) L4 larval stage worms grown under varying RNAi and BCS conditions were picked to individual plates, allowed to lay eggs, and transferred to fresh plates every 24 hours for three days. Eggs were counted for each brood treatment, and progeny number for each brood was determined as the sum of total eggs and larvae, n=5 (two-way ANOVA, Tukey's post hoc test). Error bars represent average ± SEM. Values with different letters are significantly different from each other ($P<0.05$). (C) Wild-type P_0 animals were precultured for three days on NGM plates containing 0 or 10 μM supplemental Cu, and synchronized F_1 progeny were cultured from the L1 stage for two days on plates with the indicated levels of BCS. TOF was determined by a COPAS Biosort. Lower values indicate more severely retarded growth of worms under dietary Cu deficient conditions as compared to controls (no BCS supplementation). Three independent experiments were performed with ~200 worms for each sample. Error bars represent average ± SEM, and different letters indicate significantly different means ($P<0.05$) (two-way ANOVA, Tukey's post hoc test).

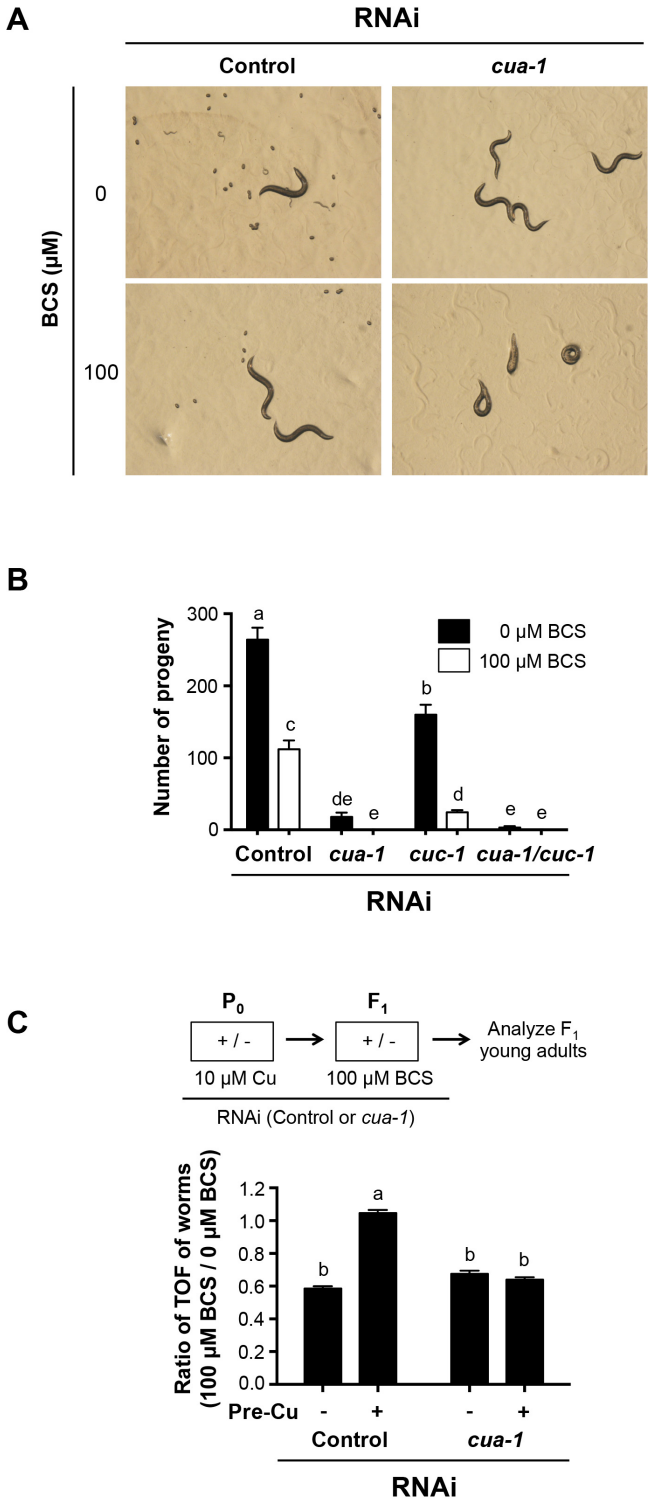
A
RNAi
Control
cua-1
BCS (μM)
0
100
B
Number of progeny
300
200
100
0
a
c
de
e
b
d
e
e
0 μM BCS
100 μM BCS
Control
cua-1
cuc-1
cua-1/cuc-1
RNAi
C
P0
F1
+ / -
+ / -
Analyze F1 young adults
10 μM Cu
100 μM BCS
RNAi (Control or cua-1)
Ratio of TOF of worms (100 μM BCS / 0 μM BCS)
1.2
1.0
0.8
0.6
0.4
0.2
0.0
b
a
b
b
Pre-Cu
-
+
-
+
Control
cua-1
RNAi

In mammals, cytosolic Cu is delivered to either ATP7A or ATP7B by the Cu chaperone ATOX1. In *C. elegans*, *cuc-1* is a putative ATOX1 homolog that has been previously identified by yeast complementation assay (85). Depletion of *cua-1* or *cuc-1* by RNAi resulted in a decrease in brood size as compared to vector control RNAi (Fig. 3.5B). Double knockdown of *cua-1/cuc-1* led to a severe egg-laying defect, suggesting that a CUC-1/CUA-1 Cu relay and transport pathway is conserved in *C. elegans*, analogous to the ATOX1-ATP7A/B pathway in mammals.

To investigate the physiological significance of maternal Cu availability to progeny, RNAi against *cua-1* with either 0 or 10 μM supplemental Cu was conducted for 3 days until parental animals (P_0) reached adulthood, and their synchronized L1 progeny (F_1) were cultured under identical RNAi knockdown conditions in the presence or absence of BCS for 2.5 days. Worms treated with *cua-1* RNAi whose parents were grown in 0 μM supplemental Cu displayed delayed growth rates in the presence of BCS as compared to those treated with vector control (data not shown). When mothers were provided with 10 μM supplemental Cu, the growth rate of F_1 progeny treated with control RNAi was faster than that of progeny from mothers that received no supplemental Cu (Fig. 3.5C). However, the growth rate of the *cua-1* knockdown progeny was not strongly affected when the mothers were cultured in 10 μM supplemental Cu (Fig. 3.5C). These results suggest that viability of embryos is both dependent upon maternal Cu status and upon *cua-1* activity.

CUA-1 expression is regulated by dietary Cu

To determine whether *cua-1* is transcriptionally regulated by dietary Cu, wild-type N2 worms were cultured with no supplementation, with 150 μM Cu, or with 100 μM BCS, and mRNA levels were measured by reverse transcription quantitative PCR (RT-qPCR). Levels of *cua-1* mRNA were modestly elevated under Cu-limited conditions compared to Cu supplementations (Fig. 3.6A). To further analyze *cua-1* expression and localization, we generated transgenic animals expressing CUA-1::GFP translational fusions under the control of an endogenous promoter using the CUA-1.1 isoform, as this isoform is the full-length form of the CUA-1 gene. P_{cua-1}*::CUA-1.1::GFP* transgenic animals showed similar tissue distribution patterns to the previously reported transcriptional reporter worms, which was primarily intestine, neurons, hypodermis, and pharynx (85), although the intestinal expression was concentrated mainly in the anterior of the intestine (Fig. 3.6B).

The strain VC672 contains a deletion in *cua-1(ok904)*, spanning exons 13 through 15 (Fig. 2A; Supplemental Fig. S2C), which is genetically balanced due to the embryonic lethality of *cua-1* mutant worms (87,105). The *cua-1(ok904)* deletion removes a region containing the last two transmembrane helices as well as an ATP-binding motif and a dileucine-based sorting signal (Fig. 3.4A). The *cua-1(ok904)* mutant is rescued with the transgene P_{cua-1}*::CUA-1.1::GFP*, indicating that the CUA-1.1::GFP translational fusion protein is functional (Fig. 3.7A). To further confirm whether the CUA-1.1::GFP translational fusion protein can transport Cu, we exploited previously established assays in *Atp7a*$^{+/+}$ and *Atp7a*$^{-/-}$ mouse embryonic fibroblasts (MEFs) (106). *Atp7a*$^{-/-}$ MEFs transiently transfected with CUA-1.1::GFP

Figure 3.6. *cua-1* is expressed in multiple tissues in *C. elegans*. (A) Wild-type L1 worms were cultivated with no supplemental Cu, 150 μM Cu, or 100 μM BCS for 2.5 days. The relative fold changes of *cua-1* mRNA levels were determined by RT-qPCR. Bars indicate mean ± SEM of three independent experiments. Means followed by different letters are significantly different at p=0.05 (one-way ANOVA, Tukey's post hoc test). (B) Live transgenic animals expressing a *cua-1.1* translational reporter [P*cua-1::CUA- 1.1::GFP::unc-54 3'UTR*] were imaged by confocal microscopy. I, intestine; N, neurons; P, pharynx; H, hypodermis. Scale bar, 50 μm.

A

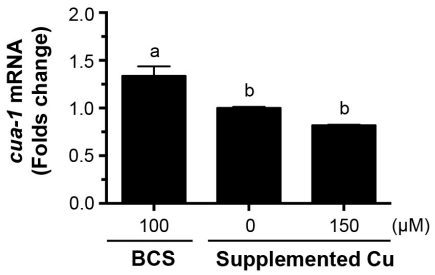
cua-1 mRNA
(Folds change)
2.0
1.5
1.0
0.5
0.0
a
b
b
100
0
150
(μM)
BCS
Supplemented Cu

B

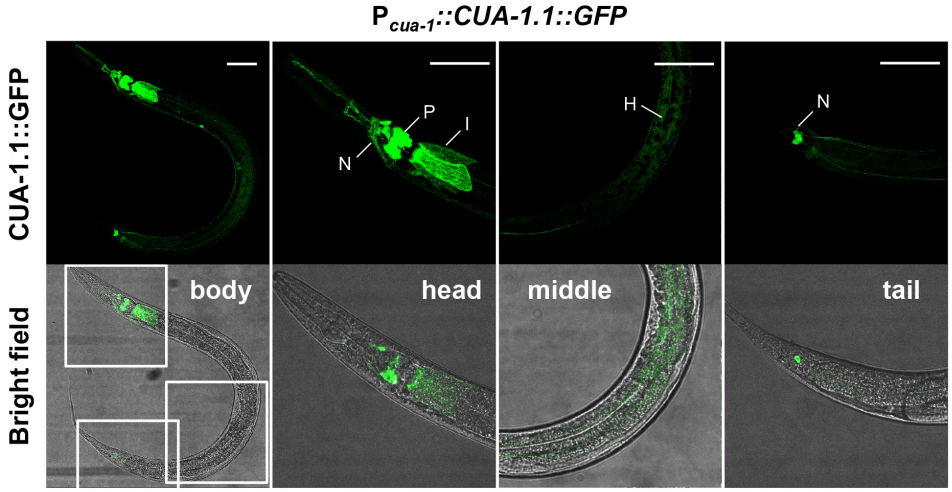
P cua-1::CUA-1.1::GFP
CUA-1.1::GFP
Bright field
P
I
N
H
N
body
head
middle
tail

Figure 3.7. Cu deficiency induces *cua-1* in *C. elegans*. (A) Elevated CUA-1.1::GFP expression in the hypodermis by BCS supplementation was detected in transgenic animals [P*cua-1::CUA-1.1::GFP::unc-54 3'UTR; cua-1(ok904)*]. The arrowheads and dashed circles indicate the anterior intestinal cells and hypodermis, respectively. Note that b, c, e, and f are magnified images. Scale bars, 200 μm (a and d) and 25 μm (b, c, e, and f). (B-C) Immunoblot (B) and ICP-MS (C) analysis of *Atp7a*$^{+/+}$ and *Atp7a*$^{-/-}$ MEFs transfected with either vector or CUA-1.1::GFP. Error bars represent mean ± SEM of three independent experiments. Means which share the same letters are not significantly different (P>0.05) (one-way ANOVA, Tukey's post hoc test). (D) Normalized GFP was analyzed using a COPAS Biosort. Background fluorescence and neuronal CUA-1.1::GFP fluorescence (which is refractory to RNAi knockdown), are indicated by a' and b', respectively. As such, c' represents CUA-1.1::GFP expression specifically in the intestine, hypodermis, and pharynx. Error bars show mean ± SEM of a single experiment with ~200 worms. Groups that do not share the same letter are significantly different (P<0.05) (one-way ANOVA, Tukey's post hoc test). (E) Immunoblot analysis of CUA-1.1::GFP in transgenic worms [P*cua-1::CUA-1.1::GFP::unc-54 3'UTR; cua-1(ok904)*]. Worm lysates were subjected to SDS-PAGE followed by immunoblotting using anti-GFP and anti-tubulin antibodies. Tubulin is shown as a loading control.

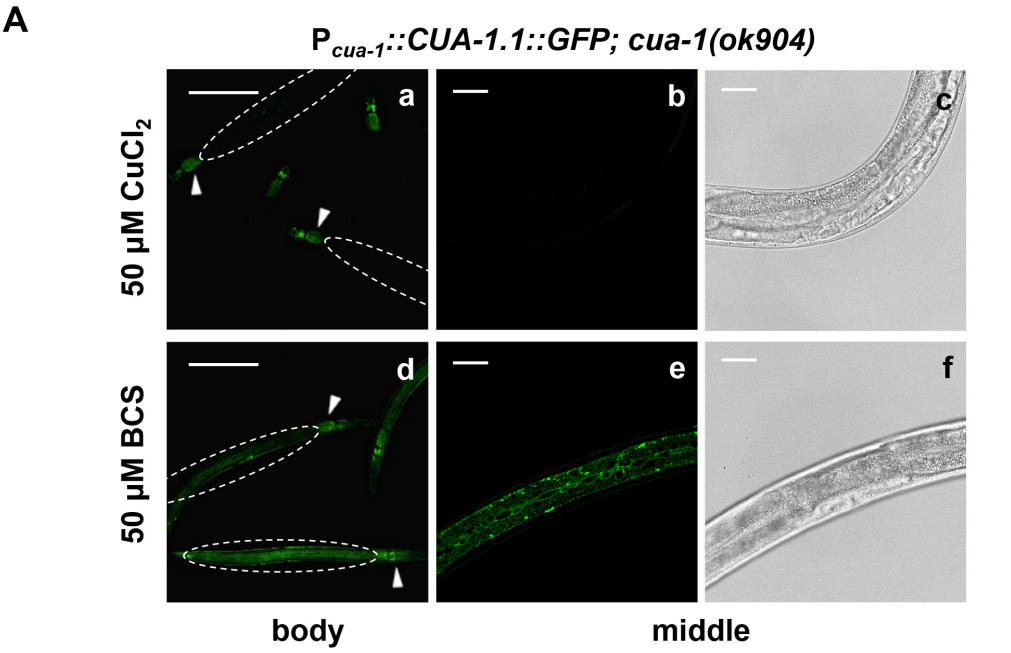
A
P cua-1::CUA-1.1::GFP; cua-1(ok904)
50 µM CuCl2
50 µM BCS
a
b
c
d
e
f
body
middle

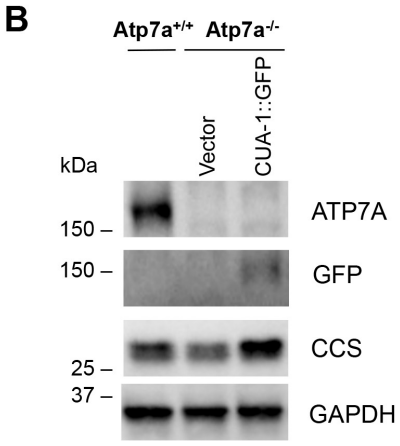
B
Atp7a+/+
Atp7a-/-
Vector
CUA-1::GFP
kDa
150 –
150 –
25 –
37 –
ATP7A
GFP
CCS
GAPDH

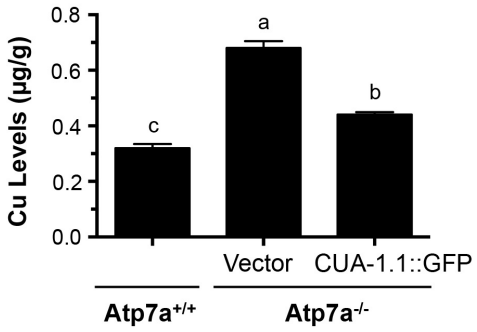
C
Cu Levels (µg/g)
0.8
0.6
0.4
0.2
0.0
a
b
c
Vector
CUA-1.1::GFP
Atp7a+/+
Atp7a-/-

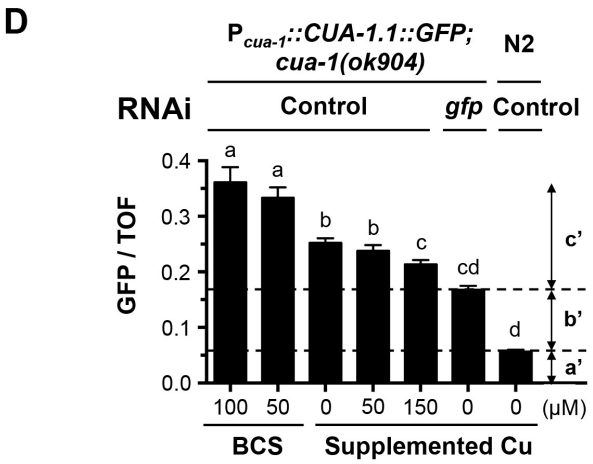
D
P cua-1::CUA-1.1::GFP; cua-1(ok904)
N2
RNAi
Control
gfp
Control
GFP / TOF
0.4
0.3
0.2
0.1
0.0
a
a
b
b
c
cd
d
c'
b'
a'
100 50 0 50 150 0 0 (µM)
BCS
Supplemented Cu

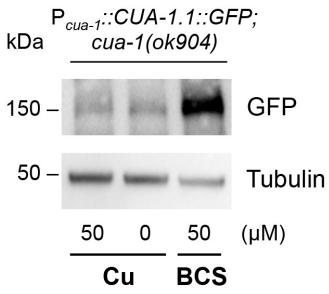
E
P cua-1::CUA-1.1::GFP; cua-1(ok904)
kDa
150 –
50 –
GFP
Tubulin
50 0 50 (µM)
Cu
BCS

Figure 3.8. Loss of *cua-1* specifically in the intestine causes embryonic lethality. Depletion of *cua-1* in the intestine recapitulated the reduced fecundity of whole-animal RNAi. Wild-type N2, RNAi resistant worm strain (*rde-1*), and tissue-specific RNAi lines were cultured on RNAi dishes with indicated concentration of Cu or BCS. Int, intestine-specific RNAi; Mus, muscle-specific RNAi; Hyp, hypodermis-specific RNAi; Error bars represent mean ± SEM. Values with one different letter superscript are significantly different from each other ($P<0.05$). n=3 (two-way ANOVA, Tukey's post hoc test).

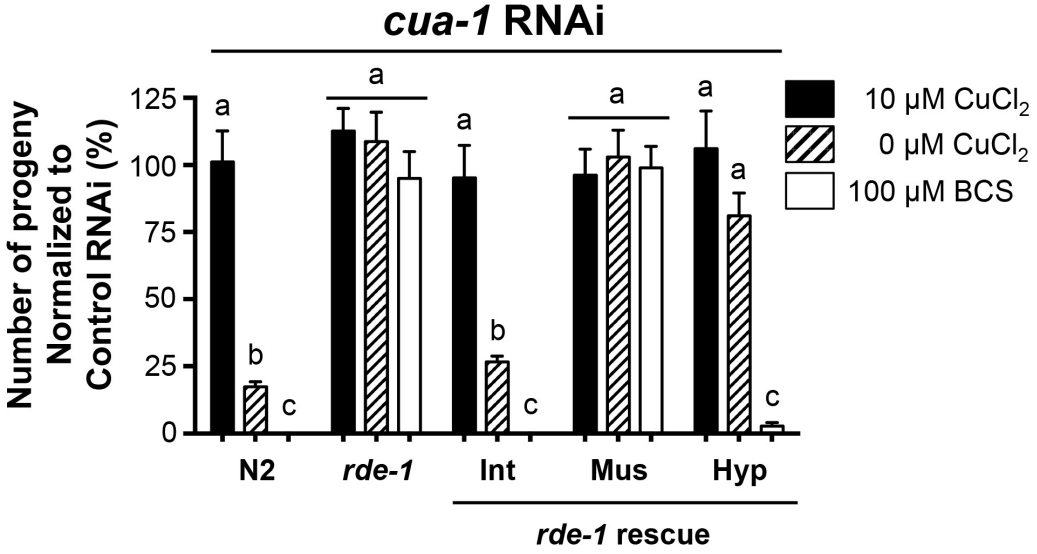
cua-1 RNAi
Number of progeny Normalized to Control RNAi (%)
125
100
75
50
25
0
a
b
c
a
a
b
c
a
a
a
c
N2
rde-1
Int
Mus
Hyp
rde-1 rescue
10 μM CuCl2
0 μM CuCl2
100 μM BCS

showed increased expression of Cu chaperone for superoxide dismutase (CCS), indicating decreased levels of cellular Cu (33,34) as compared to *Atp7a*$^{-/-}$ MEFs transfected with an empty vector (Fig. 3.7B). Over-accumulated Cu in *Atp7a*$^{-/-}$ MEFs was rescued by ectopic expression of CUA-1.1::GFP (Fig. 3.7C), further indicating that CUA-1.1 can export Cu. Moreover, these results demonstrate that a C-terminal GFP tag does not significantly interfere with CUA-1 function.

Unexpectedly, when transgenic worms (P_{cua-1}*::CUA-1.1::GFP*) were maintained at low Cu concentrations (50 μM BCS), stronger CUA-1.1::GFP expression was observed in the hypodermis, while GFP expression levels were not altered in other tissues such as the intestine and neurons (Fig. 3.7A). Indeed, quantification of CUA-1.1::GFP by COPAS Biosort and immunoblotting assay showed significantly enhanced CUA-1.1::GFP levels under low Cu conditions, suggesting that Cu-dependent regulation in the hypodermal cells contributes to the overall steady state abundance of CUA-1.1. (Fig. 3.7D-E).

To determine the contribution of each tissue to the embryonic lethal phenotype of *cua-1* mutant worms, we carried out tissue-specific RNAi experiments. Mutant *rde-1* worms are resistant to RNAi, but restoring tissue-specific expression of the wild-type *rde-1* cDNA in these mutants confers RNAi sensitivity to a specific tissue (107). We depleted *cua-1* in wild-type N2, WM27 (*rde-1* mutant, RNAi insensitive), VP303 (P_{nhx-2}*::RDE-1*, intestine only RNAi), WM118 (P_{myo-3}*::RDE-1*, muscle only RNAi), and NR222 (P_{lin-26}*::RDE-1*, hypodermis only RNAi) worm strains (82). Knockdown of *cua-1* in the intestine resulted in reduced fecundity similar to that of whole-body RNAi (Fig. 3.7A), indicating that intestinal CUA-1 is

crucial for the survival of worms. While significant effects were not observed when *cua-1* was knocked down in muscle, depletion of *cua-1* in the hypodermis caused a severe reduction in brood size under low dietary Cu conditions (Fig. 3.8). Cu supplementation (10 μM) was able to rescue the brood sizes phenotype caused by *cua-1* RNAi in each of these strains (Fig. 3.8). These results imply a critical role of both intestinal and hypodermal CUA-1 in worm growth under Cu-deficient conditions.

Intestinal expression of *cua-1.1* is sufficient to rescue the lethal phenotype of *cua-1(ok904)*

Given that targeted depletion of *cua-1* in the intestine caused similar phenotypes as whole-body RNAi, we examined the subcellular localization of CUA-1.1 by driving the expression of CUA-1.1::GFP from the strong constitutive intestine-specific *vha-6* promoter (108). $P_{vha\text{-}6}$*::CUA-1.1::GFP* localized to basolateral membranes and to intracellular compartments, reminiscent of basolateral sorting and recycling endosomes in the *C. elegans* intestine (Fig. 3.9A) (109). Importantly, the embryonic lethal phenotype of the *cua-1* (ok904) mutant can be rescued by intestine-specific expression of CUA-1.1::GFP (Fig. 3.9B-C) suggesting that the intestine is the key site of Cu regulation in *C. elegans*. These results are further corroborated by the fact that RNAi depletion of either *cuc-1* or *cua*-1 in $P_{vha\text{-}6}$*::CUA-1.1::GFP; cua-1(ok904)* transgenic animals grown in low Cu results in a lethal phenotype that can be rescued by Cu supplementation. These observations suggest that a CUC-1/CUA-1 Cu delivery pathway from intestine to peripheral tissues is essential for worms under

dietary Cu restriction (Fig. 3.9B-C). To further assess the significance of intestinal CUA-1 function under varying Cu availability, F_1 progeny of N2 wild-type, P_{vha-6}*::CUA-1.1::GFP*, and P_{vha-6}*::CUA-1.1::GFP; cua-1(ok904)* worms derived from P_0 worms exposed to 10 μM Cu were grown to the L4/young adult stage under different dietary Cu conditions and then analyzed by COPAS Biosort. Transgenic animals expressing CUA-1.1::GFP under control of the *vha-6* promoter exhibited a reduced growth phenotype when exposed to high Cu, and enhanced growth under Cu restriction in a dose-dependent manner (Fig. 3.9C and 3.10A). We attribute the Cu hypersensitivity to the constitutive overexpression of CUA-1.1 in the intestine, which would lead to export Cu into the worm body. In line with the assertion that intestinal CUA-1 is crucial for Cu delivery to extraintestinal tissues, depletion of *cua-1* by RNAi in both wild-type and P_{vha-6}*::CUA-1.1::GFP; cua-1(ok904)* worms resulted in improved growth under toxic Cu conditions and growth inhibition under Cu restriction as compared to vector RNAi (Fig. 3.9C and 3.10A-B). To further understand the role of *cua-1* in Cu metabolism, we measured total worm Cu content using ICP-MS. In the presence of 50 μM Cu, either *cua-1* or *cuc-1* RNAi knockdown in wild-type worms resulted in approximately 30% lower total Cu content than in control worms, whereas worms without Cu supplementation exhibited similar total Cu contents under both RNAi conditions (Fig. 3.10C). These results suggest that accumulation of Cu under high dietary Cu conditions is dependent on *cua-1*.

Figure 3.9. CUA-1 localizes to the basolateral membrane of the intestine and is crucial for survival in Cu-deficient condition. (A) Transgenic worms expressing a *cua-1.1* translational reporter [P*vha-6::CUA-1.1::GFP::unc-54 3'UTR*] were imaged by confocal microscopy. The bright field image (a) shows the morphology of the worm intestine, and the green signal (b) shows CUA-1.1::GFP expression therein. Dotted lines indicate apical membrane, solid lines indicate basal membrane, and arrowheads indicate lateral membranes in polarized intestinal cells. Scale bar, 20 μm. (B-C) Survival rates (B) and images (C) of transgenic worms [P*vha-6::CUA-1.1::GFP::unc-54 3'UTR; cua-1(ok904)*] cultured on RNAi plates supplemented with either Cu or BCS 48 h post-hatch. Error bars indicate average ± SEM. Means that do not share a letter are significantly different ($P<0.05$). n=3 (two- way ANOVA, Tukey's post hoc test).

.

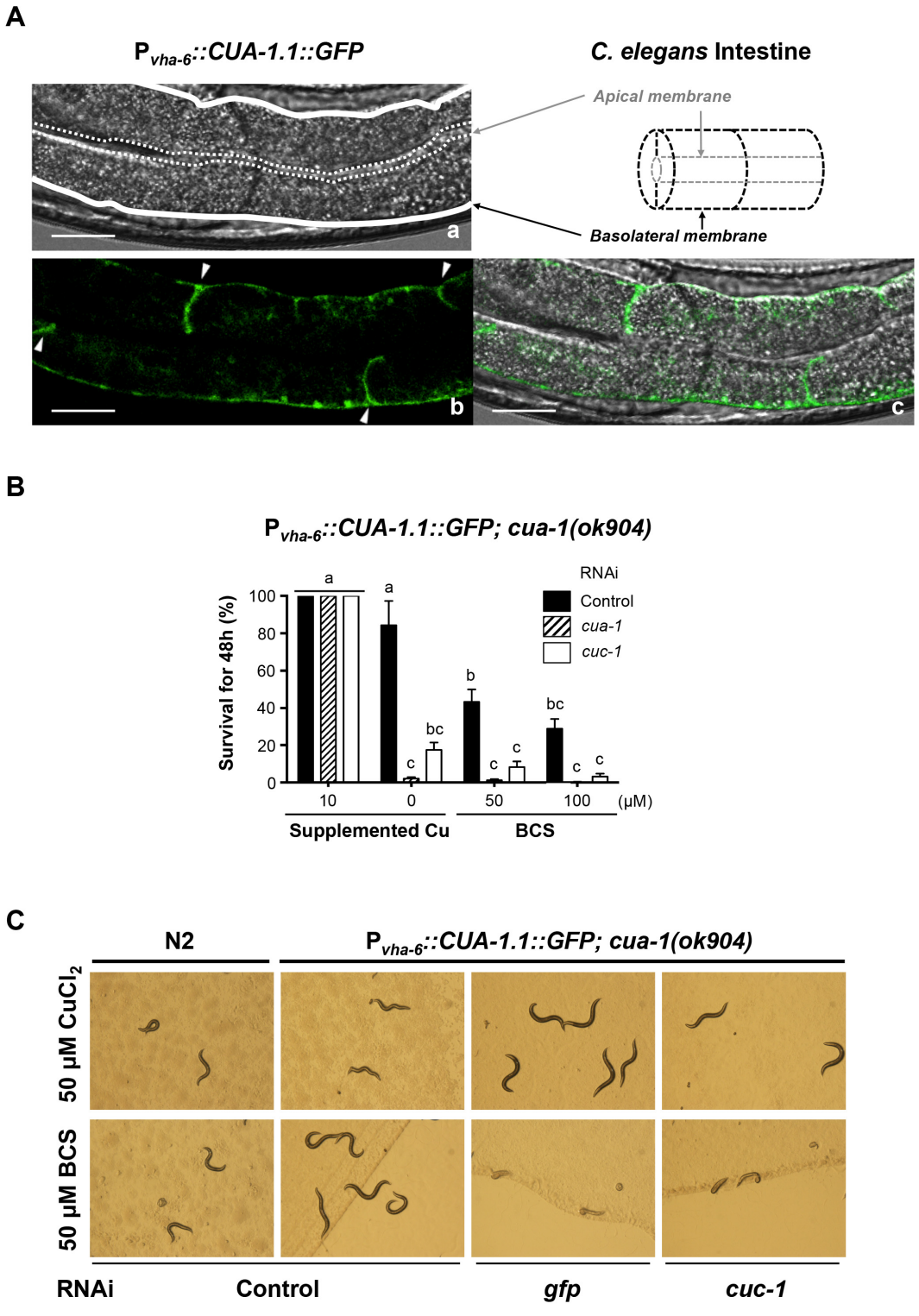
A
P vha-6::CUA-1.1::GFP
C. elegans Intestine
Apical membrane
Basolateral membrane
a
b
c
B
P vha-6::CUA-1.1::GFP; cua-1(ok904)
RNAi
Control
cua-1
cuc-1
Survival for 48h (%)
100
80
60
40
20
0
a
a
c
bc
b
c
c
bc
c
c
10
0
50
100
(μM)
Supplemented Cu
BCS
C
N2
P vha-6::CUA-1.1::GFP; cua-1(ok904)
50 μM CuCl2
50 μM BCS
RNAi
Control
gfp
cuc-1

Figure 3.10. Cu export by intestinal CUA-1 is essential for survival. (A) P_0 worms were treated with 10 μM supplemental Cu on NGM plates with *E. coli* OP50. Synchronized L1 stage wild-type N2 worms and transgenic worms ([P*vha-6::CUA-1.1::GFP::unc-54 3'UTR*] and [P*vha-6::CUA-1.1::GFP::unc-54 3'UTR; cua-1(ok904)*]) were grown for 2-2.5 days on NGM plates and analyzed using a COPAS Biosort. Error bars indicate mean ± SEM of ~200 worms (**P* < 0.05, ***P* < 0.01, and ****P* < 0.001) (two-way ANOVA, Tukey's post hoc test). (B) Synchronized L1 stage wild-type N2 worms and transgenic worms [P*vha-6::CUA-1.1::GFP::unc-54 3'UTR; cua-1(ok904)*] were fed control or *cua-1* RNAi bacteria and analyzed using a COPAS Biosort. TOF equivalent to zero indicates lethal phenotype. Error bars represent mean ± SEM of ~200 worms (****P* < 0.001) (two-way ANOVA, Tukey's post hoc test). (C) Total Cu levels of L4/young adult stage wild-type worms grown on NGM plates with 0 or 50 μM supplemental Cu as determined by ICP-MS. Error bars indicate mean ± SEM of six independent experiments. Means that do not share letters are significantly different from each other at p=0.05 (two-way ANOVA, Tukey's post hoc test).

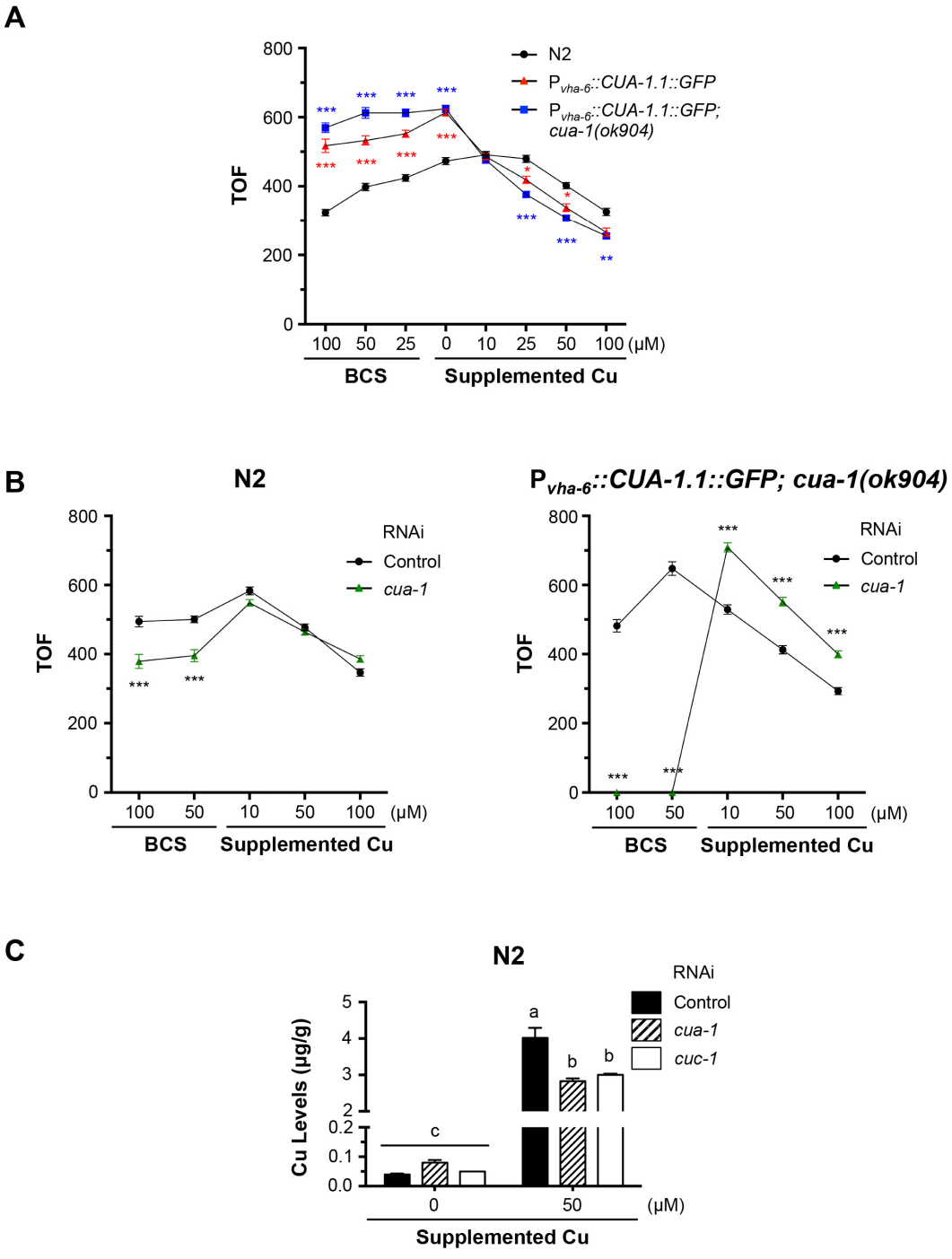
A
800
600
400
200
0
TOF
N2
P vha-6::CUA-1.1::GFP
P vha-6::CUA-1.1::GFP; cua-1(ok904)
100 50 25 0 10 25 50 100 (μM)
BCS
Supplemented Cu
B
N2
P vha-6::CUA-1.1::GFP; cua-1(ok904)
RNAi
Control
cua-1
100 50 10 50 100 (μM)
BCS
Supplemented Cu
C
N2
RNAi
Control
cua-1
cuc-1
Cu Levels (μg/g)
5
4
3
2
0.2
0.1
0.0
a
b
b
c
0
50
(μM)
Supplemented Cu

Intestinal CUA-1.1 distribution is regulated by Cu levels

Cu-responsive fluorescent probes have been used to visualize the distribution of Cu in a variety of model systems (93,110-112). After conducting several pilot studies with a number of different Cu probes in *C. elegans*, we selected the newly developed Cu(I) probe CF4 based on its high specificity (see Materials and Methods for details). To investigate the dynamics of Cu levels in the intestine, we pre-exposed worms expressing CUA-1.1::GFP in the intestine to either 50 μM $CuCl_2$ or 50 μM BCS followed by incubation with CF4. We observed that worms exposed to supplemental Cu accumulated more fluorescence puncta in the intestine than worms treated with BCS, while a control CF4 probe, which lacks the Cu-binding atoms but retains the same lipophilic dye platform, displayed weaker staining (Fig. 3.11). These results indicate that CF4 detects labile Cu levels in vesicles of the intestine in *C. elegans*.

To test if dietary Cu alters CUA-1.1 localization, transgenic animals harboring a *cua-1.1* translational reporter driven by the *vha-6* promoter were grown under varying Cu concentrations and then imaged using confocal microscopy. In the presence of 50 μM BCS (Fig. 3.12 and 3.13A) or no supplemental Cu (data not shown), intestinal CUA-1.1::GFP localized predominantly to basolateral membranes (Fig. 3.12, a and f), as well as low levels being detectable in intracellular compartments. We identified these compartments as Golgi, as some of them overlapped with the Golgi marker MANS::mCherry (Fig. 3.13A). Strikingly, in the presence of 25 μM supplemental Cu, CUA-1.1::GFP was redistributed to a cellular compartment which was distinct from the Golgi (Fig. 3.12, g and l, and 3.13A). CUA-

1.1::GFP containing vesicles overlapped with the autofluorescence of gut granules (Fig. 3.12, j), an intestine-specific lysosome-related organelle, indicating that Cu may be concentrated at these sites (113,114).

To examine the relationship between CUA-1.1 and Cu, transgenic animals expressing CUA-1.1::GFP were cultured with the Cu probe CF4. In worms cultured with 25 μM Cu, CF4 and CUA-1.1::GFP fluorescence overlapped almost completely, suggesting that CUA-1.1 localizes to the gut granules that concentrate Cu in response to toxic levels of environmental Cu (Fig. 3.12, k). Additionally, intestinal CUA-1.1::GFP localization shifted from punctate staining to larger vesicles as worms were exposed to increasing concentrations of dietary Cu (Fig. 3.13B). CUA-1.1::GFP expression in the intestine driven by the endogenous *cua-1* promoter rather than the *vha-6* promoter also showed similar trafficking in response to changes in dietary Cu (Fig. 3.13C). Worms in which *cua-1* had been depleted by RNAi showed dramatically decreased levels of CF4 fluorescence in the intestine as compared to control worms (Fig. 3.12, i and u) suggesting that CUA-1.1 acts to export Cu to gut granules. In summary, CUA-1.1 mainly resides on the basolateral membranes under basal and Cu-deficient conditions, but localizes to gut granules in response to increasing dietary Cu. Note that these changes are not due to Cu-responsive elevation in protein abundance of intestinal CUA-1.1 ($P_{vha\text{-}6}$*::CUA-1.1::GFP*) in transgenic worms, as immunoblotting and COPAS Biosort analysis showed no significant differences in GFP levels when these worms were grown at varying Cu levels (Fig. 3.13D-E).

Figure 3.11. Cu accumulation in worms is monitored by CF4 Cu probe. Fluorescence images of control-CF4 or CF4 Cu probe staining in transgenic animals [P*vha-6::CUA-1.1::GFP::unc-54 3'UTR*] cultured with 50 μM supplemental Cu or BCS on NGM agar. Scale bar, 10 μm.

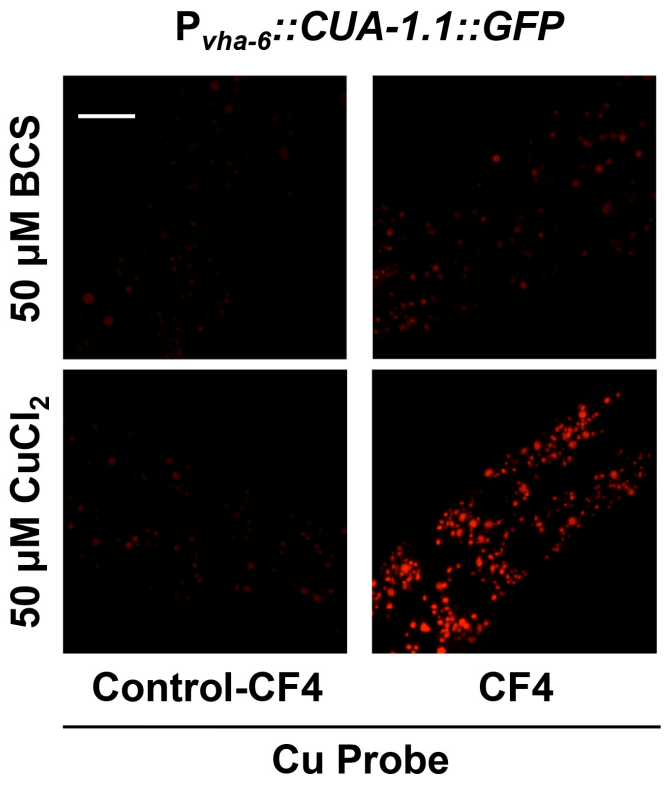
P vha-6::CUA-1.1::GFP
50 µM BCS
50 µM CuCl2
Control-CF4
CF4
Cu Probe

Figure 3.12. Localization of intestinal CUA-1.1 is altered by Cu levels. Confocal images of transgenic animals [P*vha-6::CUA-1.1::GFP::unc-54 3'UTR*] expressing CUA-1.1::GFP in the intestine cultured with the Cu probe CF4 or the control CF4 probe, the indicated levels of supplemental Cu or BCS, and control or *cua-1* RNAi. Images show intestinal cells, and arrowheads indicate representative gut granules and Cu probe positive vesicles overlapping with CUA-1.1::GFP. Scale bar, 10 μm.

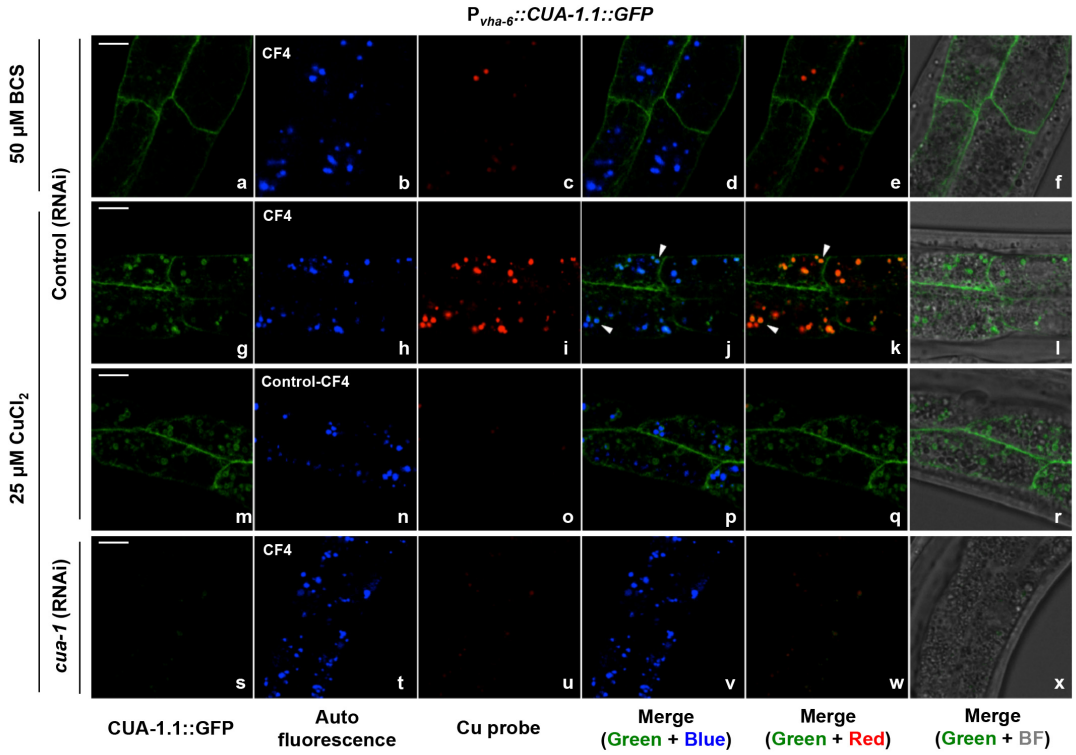
P vha-6::CUA-1.1::GFP
50 µM BCS
25 µM CuCl2
Control (RNAi)
cua-1 (RNAi)
CF4
Control-CF4
a
b
c
d
e
f
g
h
i
j
k
l
m
n
o
p
q
r
s
t
u
v
w
x
CUA-1.1::GFP
Auto fluorescence
Cu probe
Merge (Green + Blue)
Merge (Green + Red)
Merge (Green + BF)

Figure 3.13. Subcellular localization of intestinal CUA-1.1 is changed by Cu supplementation. (A) Confocal images of transgenic animals expressing both CUA-1.1::GFP and MANS::mCherry (a Golgi-localized mannosidase-mCherry fusion protein) in the intestine. Arrowheads indicate colocalization of CUA-1.1::GFP with MANS::mCherry, and insets are magnified images of boxed regions. Scale bar, 20 μm. (B) Confocal images were taken of transgenic animals [P*vha-6::CUA-1.1::GFP::unc-54 3'UTR*] under varying Cu conditions. Arrowheads indicate representative CUA-1.1::GFP puncta. Scale bar, 10 μm. (C) Confocal images of the intestinal cells (arrowheads) of transgenic worms [P*cua- 1::CUA-1.1::GFP::unc-54 3'UTR; cua-1(ok904)]* grown with Cu or BCS supplementation. Scale bar, 20 μm. (D-E) Intestinal CUA-1.1::GFP expression levels were determined by immunoblotting (D) and a COPAS Biosort (E). Tubulin is shown as a loading control. Note that a' represents background fluorescence and b' represents CUA-1.1::GFP expression in the intestine. Error bars indicate mean ± SEM of a single experiment with ~200 worms. Means followed by different letters are significantly different at p=0.05 (one-way ANOVA, Tukey's post hoc test).

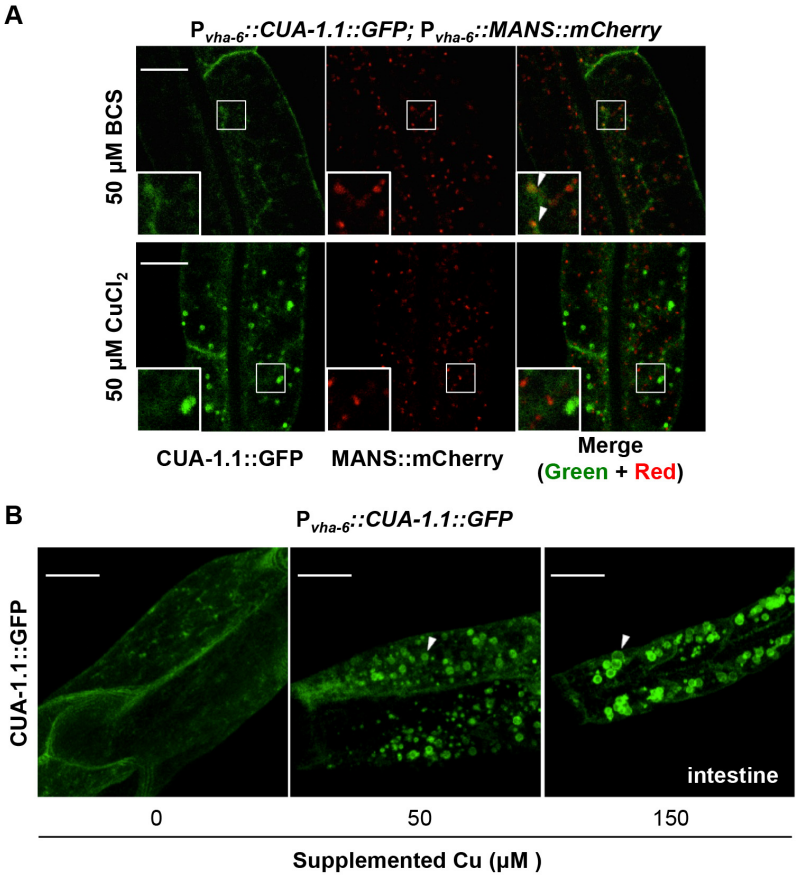
A
P vha-6::CUA-1.1::GFP; P vha-6::MANS::mCherry
50 µM BCS
50 µM CuCl2
CUA-1.1::GFP
MANS::mCherry
Merge
(Green + Red)
B
P vha-6::CUA-1.1::GFP
CUA-1.1::GFP
intestine
0
50
150
Supplemented Cu (µM)
C
P cua-1::CUA-1.1::GFP; cua-1(ok904)
50 µM CuCl2
50 µM BCS
CUA-1.1::GFP
Auto
fluorescence
Merge
(Green + Blue)
Merge
(Green + BF)
D
kDa
P vha-6::CUA-1.1::GFP;
cua-1(ok904)
150 –
GFP
50 –
Tubulin
50 0 50 (µM)
Cu
BCS
E
P vha-6::CUA-1.1::GFP;
P vha-6::mCherry; cua-1(ok904)
RNAi
Control
gfp
GFP / mCherry
a
b
b'
a'
100 50 0 50 150 0 (µM)
BCS
Supplemented Cu

Figure 3.14. Localization of CUA-1.1 in hypodermis is not affected by Cu levels. Lateral view of transgenic animals [P*dpy-7::CUA-1.1::GFP::unc-54 3'UTR*] expressing CUA-1.1::GFP in the hypodermis. Seam cells are mostly embedded in the hyp7 syncytium. Note that images in the first and second columns are from independent worms. Scale bars, 100 μm (first column) and 10 μm (second and third columns).

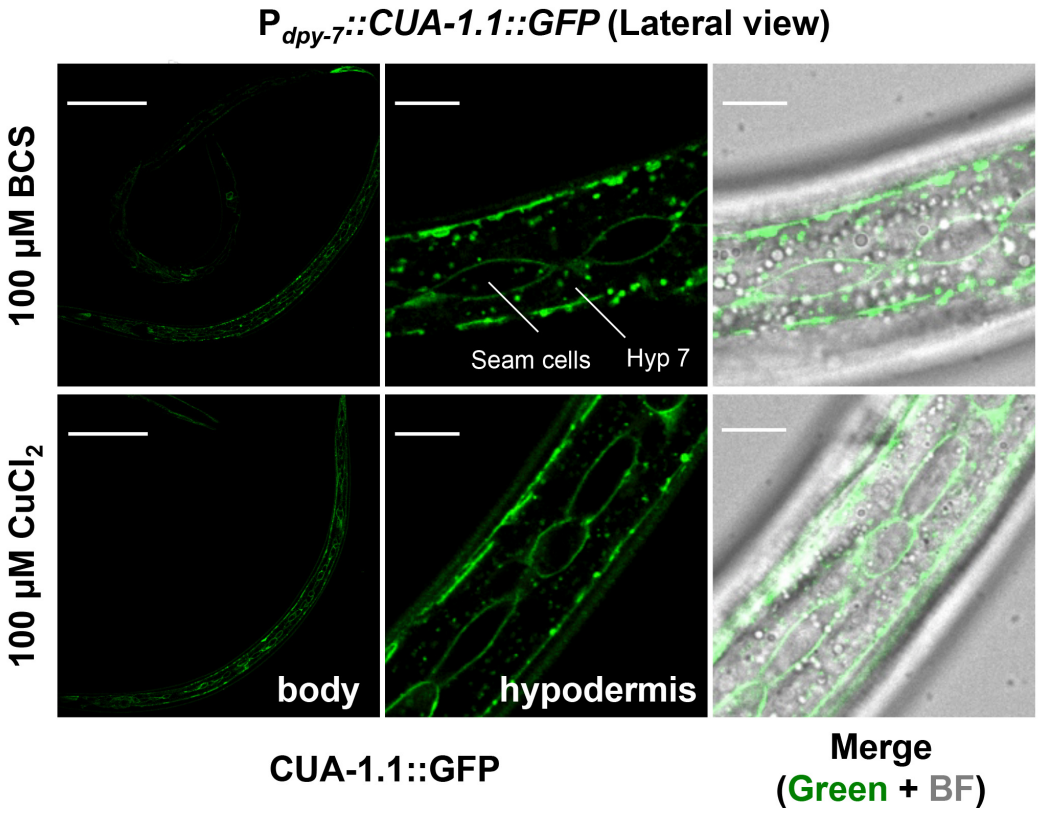
P dpy-7::CUA-1.1::GFP (Lateral view)
100 µM BCS
100 µM CuCl2
Seam cells
Hyp 7
body
hypodermis
CUA-1.1::GFP
Merge
(Green + BF)

We next expressed CUA-1.1::GFP in the specialized epithelial cells of the *C. elegans* hypodermis using the hypodermis-specific *dpy-7* promoter (113). Confocal microscopy studies in transgenic worms expressing $P_{dpy\text{-}7}$*::CUA-1.1::GFP* showed that in hypodermal tissues, plasma membrane localization of CUA-1.1::GFP was not affected by dietary Cu, suggesting that Cu-responsive trafficking of CUA-1.1 protein is intestine-specific (Fig. 3.14).

To further explore if the intracellular localization of intestinal CUA-1.1::GFP is altered by elevated Cu status in the pseudocoelom, approximately 100 μg $CuCl_2$ per g of worm (wet weight) in M9 buffer was injected into the pseudocoelom of adult worms harboring the CUA-1.1::GFP transgene, which had been preincubated with 50 μM BCS. Interestingly, we observed a punctate pattern of CUA-1.1::GFP in the intestine of animals injected with Cu, while M9-injected controls showed predominately basolateral membrane localization (Appendix IV), implying the existence of a systemic Cu homeostasis mediated by the trafficking of intestinal CUA-1.1.

CUA-1.1 is required for Cu detoxification in the intestine

To further investigate the dynamics of CUA-1.1 localization in response to sub-toxic doses of Cu supplementation, we assayed CUA-1.1 colocalization with LysoTracker, a lysosome-specific fluorescent dye (114,115). In the presence of 50 μM Cu, LysoTracker was observed in intestinal vesicles surrounded by membrane-bound CUA-1.1::GFP (Fig. 3.15A). Upon RNAi knockdown of *cua-1*, the number and morphology of LysoTracker-positive compartments did not change. However,

RNAi knockdown *pgp-2*, which encodes an ABC transporter that is required for gut granule biogenesis and localizes to the gut granule membrane (114,116), significantly reduced LysoTracker staining and prevented CUA-1.1::GFP-containing vesicle formation, while CUA-1.1::GFP was detected on the basolateral membrane (Fig. 3.15A). These results further suggest that CUA-1.1 localizes to the membranes of gut granules and gut granules are the destination of Cu sequestered by CUA-1.1 in the intestine when animals are exposed to high dietary Cu.

To determine whether Cu sequestration into gut granules by CUA-1.1 contributes to Cu detoxification, we tested Cu sensitivity by measuring the growth rate of *C. elegans* in the presence of increasing concentrations of Cu. When compared to control worms, *pgp-2* depleted worms showed increased sensitivity to high Cu, as they displayed a dose-dependent decrease in growth rate in response to Cu (Fig. 3.15B). To quantify Cu sequestration defects in gut granule-deficient worms, we measured total Cu content in worms by ICP-MS. *pgp-2* mutant worms cultured in 50 μM Cu displayed reduced total Cu content as compared to wild-type worms (Fig. 3.15C). Consistent with previous reports, *pgp-2* mutant worms displayed lower Zn content independent of Cu supplementation (Fig. 3.15D-E) (74). These results indicate that Cu deposition accounts for a significant proportion of total body Cu in *C. elegans,* and that gut granules are at least partially required for Cu detoxification.

Figure 3.15. CUA-1.1 sequesters excess Cu to gut granules. (A) Confocal images of transgenic animals [P*vha-6::CUA-1.1::GFP::unc-54 3'UTR*] exposed to varying RNAi conditions in the presence of 50 μM supplemental Cu, followed by incubation with LysoTracker. Boxed images in the top row are enlarged at the corner of each panel. Scale bar, 10 μm. (B) Synchronized wild-type L1 larvae were cultured on RNAi plates supplemented with the indicated concentrations of Cu for 2.5 days. TOF was determined using a COPAS Biosort. Error bars indicate average ± SEM of two independent experiments. (**$P < 0.01$) (two- way ANOVA, Tukey's post hoc test). (C-E) ICP-MS was used to measure total Cu (C), Fe (D), and Zn (E) levels in wild-type and *pgp-2(kx48)* worms grown in the presence of 0 or 50 μM supplemental Cu. Error bars indicate mean ± SEM of three independent experiments. Values with one different letter are significantly different from each other ($P<0.05$) (two-way ANOVA, Tukey's post hoc test).

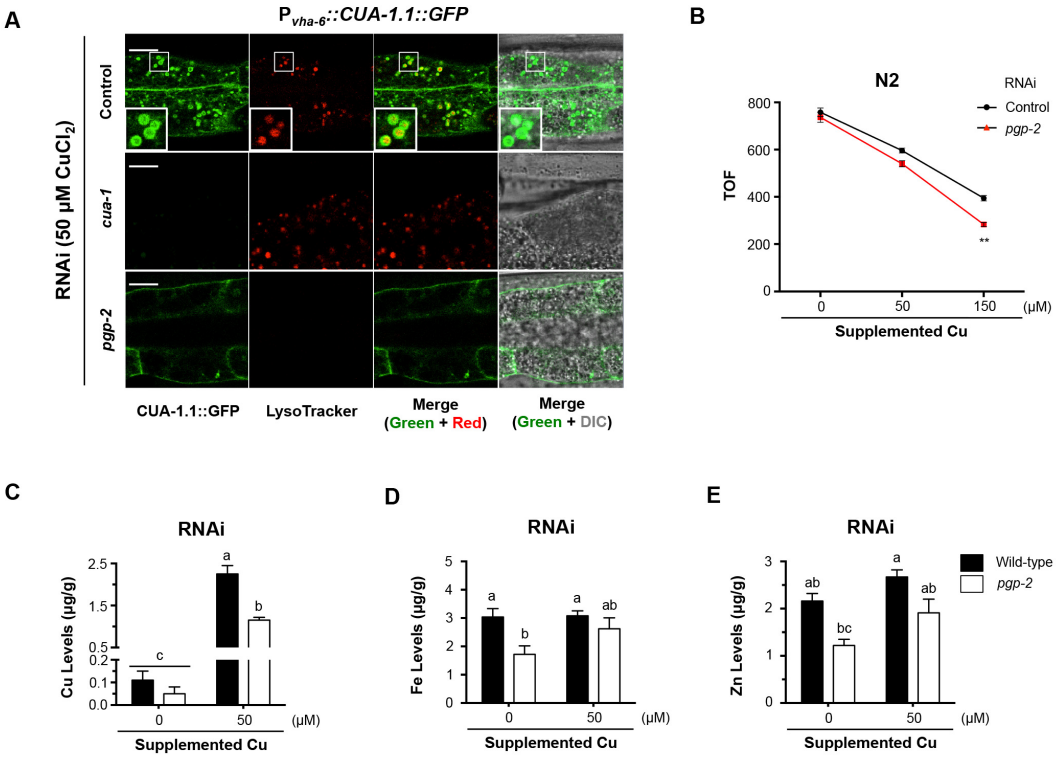
A
P vha-6::CUA-1.1::GFP
RNAi (50 µM CuCl2)
Control
cua-1
pgp-2
CUA-1.1::GFP
LysoTracker
Merge (Green + Red)
Merge (Green + DIC)
B
N2
RNAi
Control
pgp-2
TOF
800
600
400
200
0
0
50
150
(µM)
**
Supplemented Cu
C
RNAi
Cu Levels (µg/g)
2.5
1.5
0.5
0.2
0.1
0.0
a
b
c
0
50
(µM)
Supplemented Cu
D
RNAi
Fe Levels (µg/g)
5
4
3
2
1
0
a
b
a
ab
0
50
(µM)
Supplemented Cu
E
RNAi
Zn Levels (µg/g)
3
2
1
0
ab
bc
a
ab
Wild-type
pgp-2
0
50
(µM)
Supplemented Cu

CUA-1 isoforms function coordinately to maintain systemic Cu levels

RNAseq assays with synchronized populations of worms treated with different Cu or BCS levels revealed the existence of *cua-1.2* variant as annotated (Fig. 3.4A), though relative levels of the two isoforms have not been established (unpublished work). To examine whether intestinal CUA-1.2 also retains the capacity to traffic in response to a high Cu diet, we generated transgenic worms expressing a CUA-1.2::GFP translational fusion driven from the intestinal *vha-6* promoter. Confocal microscopy analysis showed that CUA-1.2::GFP is localized to the basolateral membranes irrespective of dietary Cu concentration (Fig. 3.16A). Additionally, CUA-1.2::GFP did not colocalize with autofluorescent gut granules under high Cu conditions suggesting CUA-1.2 functions constantly at basolateral membranes. Since CUA-1.1 has additional 122 amino acid sequences at the N-terminus end compared to CUA-1.2, it is plausible that Cu-dependent trafficking of CUA-1.1 to gut granules is dependent on trafficking motifs within this N-terminal segment.

Figure 3.16. Cu homeostasis in worms is maintained by distinctly localized intestinal CUA-1 isoforms. (A) Confocal images of transgenic animals [P*vha-6::CUA-1.2::GFP::unc-54 3'UTR*] expressing CUA-1.2::GFP in the intestine in the presence of 50 μM of supplemental Cu or BCS. Scale bar, 10 μm. (B) A model of Cu homeostasis in *C. elegans* is shown. Dietary Cu ions are transported from the lumen of the intestine to the enterocytes by an unidentified Cu importer, and CUC-1 delivers Cu to CUA-1. Under basal Cu or Cu-deficient conditions, CUA-1.1 isoform localizes to the basolateral membrane and Golgi to either export Cu ions to peripheral tissues, or to direct Cu into the secretory pathway. CUA-1.2 consistently localizes to the basolateral membrane of enterocytes regardless of Cu conditions. CUA-1.1 is redistributed to the gut-granule membranes in response to elevated Cu levels in order to promote Cu detoxification in *C. elegans.*

A

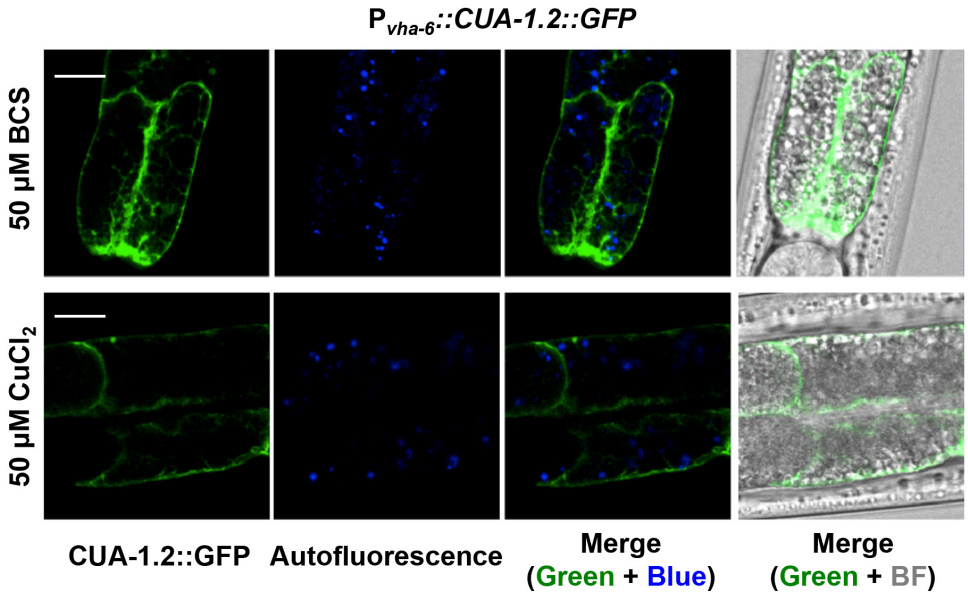
P vha-6::CUA-1.2::GFP
50 µM BCS
50 µM CuCl2
CUA-1.2::GFP
Autofluorescence
Merge (Green + Blue)
Merge (Green + BF)

B

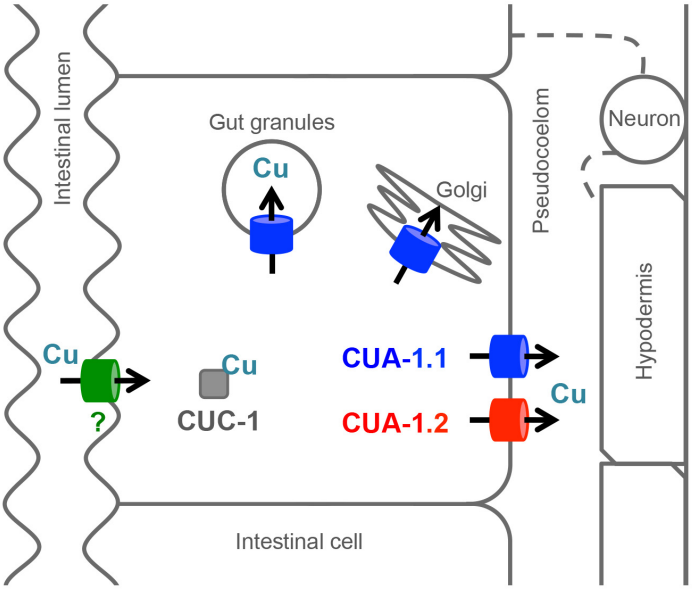
Intestinal lumen
Gut granules
Cu
Golgi
Pseudocoelom
Neuron
Hypodermis
Cu
?
Cu
CUC-1
CUA-1.1
CUA-1.2
Cu
Intestinal cell

Discussion

Dietary Cu availability can fluctuate widely depending upon an organism's immediate environment, as would be the case in *C. elegans* that lives in soil. In the current study, we show that CUA-1.1 is expressed in intestinal cells and normally localizes to the basolateral membrane and intracellular compartments, such as the Golgi. When worms are exposed to higher Cu levels, redistribution of intestinal CUA-1.1 promotes Cu sequestration into lysosome-related organelles called gut granules. Defects in gut granule biogenesis lead to decreased Cu accumulation and increased susceptibility to toxic Cu levels. Together, these results suggest that Cu homeostasis is regulated by altering the localization of intestinal CUA-1.1 to either the basolateral membrane for delivery of Cu to peripheral tissues, or to the gut granule membrane to prevent Cu toxicity (Fig. 3.16B).

In *C. elegans*, which lack a liver, the intestine has been thought to perform functions associated with both the intestine and the liver (117). Worms encode only one Cu exporter gene, *cua-1*, raising the question as to whether CUA-1 accomplishes some or all of the similar functions as ATP7A/B in the intestine and liver of mammals (86). We found that CUA-1 protein abundance in the intestine was not changed by dietary Cu. Instead, both CUA-1 isoforms localize to basolateral membranes and intracellular compartments including the Golgi under basal and Cu-limiting conditions. The CUA-1.1 isoform alone redistributes to the gut granules when worms are exposed to high levels of Cu, indicating that CUA-1 shares physiological features of mammalian ATP7A and ATP7B. Enrichment of CUA-1.1 to the membrane of gut granules rather than the basolateral membrane of the intestine

suggests a distinct role for intestinal CUA-1.1 in detoxification of excess Cu in *C. elegans*. Although relocation of CUA-1.1 and ATP7B to the gut granules and apical membrane, respectively, in polarized cells is not identical, the direction of trafficking towards preventing systemic Cu toxicity is similar. Taken together, these data indicate that intestinal CUA-1 functions as Cu exporters in worms like ATP7A/B in both the intestine and liver of mammals in order to maintain Cu balance in the body.

Given that CUA-1.2 lacks a portion of the N-terminal intracellular domain of CUA-1.1 and is targeted constitutively to the basolateral membrane even under Cu-loaded conditions, necessary trafficking information may exist in the first 122 amino acids of CUA-1.1 for Cu responsiveness and correct targeting to gut granules. Several intriguing questions arise from this observation. What route does CUA-1.1 take to reach gut granules when intracellular Cu is increased? Where within the first 122 amino acids is the crucial targeting signal? What cellular machinery recognizes the Cu signal? One possible sorting complex is the Biogenesis of Lysosome-related Organelles Complex-1 (BLOC-1), which is a known regulator of intracellular trafficking to lysosome-related organelles in mammals, *Drosophila*, and *C. elegans (118-120)*. ATP7A is known to supply Cu to melanosomes in a BLOC-1-dependent manner in mammalian cells, and BLOC-1 subunits are also required for the proper trafficking of gut granule cargo in worms (118,121). Given that CUA-1.1 localizes to gut granules, and that ATP7A localizes to melanosomes in response to elevated levels of Cu, redistribution of the Cu exporter may require the BLOC-1 complex and related sorting proteins in metazoans.

We have determined that gut granules function to sequester excess Cu via CUA-1.1 in the intestine. Ablation of *cua-1* by RNAi does not interfere with the formation of gut granules, but Cu was not readily detected by a Cu probe in gut granules upon the loss of CUA-1.1. RNAi depletion of *pgp-2* genes resulted in significantly reduced numbers of gut granules and increased sensitivity to Cu toxicity. However, whether stored Cu is capable of being reutilized under Cu-limiting conditions was not determined. Studies by the Kornfeld group have shown that gut granules act to detoxify and store dietary Zn via the CDF-2 Zn exporter (74). When worms were exposed to high concentrations of dietary Zn, gut granules displayed a bilobed morphology, which was not observed in our studies with CUA-1.1 and high dietary Cu. We speculate that gut granules may function as a central site of metal storage to prevent its cytotoxicity. This is specifically relevant since depletion of the metallothionein genes *mtl-1* and *mtl-2* by RNAi does not result in the expected enhanced susceptibility to Cu toxicity (122,123), raising the possibility that *C. elegans* may adopt a protective mechanism to withstand an environmental challenge of toxic Cu by sequestering Cu to an intracellular location via CUA-1.1.

Unexpectedly, we observed that CUA-1.1 expression is upregulated in response to dietary Cu deficiency in the hypodermis when expressed under the control of an endogenous promoter. Given that CUA-1.1 abundance was not altered under the *dpy-7* promoter, and that *cua-1* transcript levels increased under Cu-limiting conditions, hypodermal *cua-1* may respond to Cu deficiency transcriptionally. MTF-1 is known to transcriptionally induce both ATP7 and metallothionein expression in *Drosophila*, but no MTF-1 homolog has been defined in *C. elegans* (124-127). MTF-

1 independent metal-responsive transcription factors have been identified, suggesting the existence of other Cu-responsive transcription factors that could regulate *cua-1* expression in the hypodermis (68,122). CUA-1 in the hypodermis may deliver Cu to the secretory pathway for Cu incorporation into Cu-dependent enzymes. Another possibility is that the hypodermis acts as a Cu storage compartment that can release Cu to peripheral tissues by increasing CUA-1.1 expression when worms are in a Cu-deficient environment. When CUA-1.1 is highly expressed in the hypodermis under dietary Cu restriction, most CUA-1.1 localizes to plasma membranes. Notably, the hypodermis is known to act as a major fat storage site in worms by accumulation of lipid droplets (128,129).

Organs communicate to ensure that intestinally derived micronutrients are distributed appropriately throughout tissues in the body, balancing cellular requirements against toxicity (8,9). We injected Cu into the pseudocoelom of adult worms expressing CUA-1.1::GFP that had been precultured with BCS. Interestingly, worms injected with Cu showed a punctate distribution of CUA-1.1::GFP, implying that the mechanism of CUA-1.1 responds to Cu status in the pseudocoelom, or/and Cu overload peripheral tissues. In mammals, Fe overload results in the liver producing elevated levels of secreted hepcidin peptide that interacts with the ferroportin Fe exporter on the basolateral membrane of intestinal epithelial cells as well as on macrophages, decreasing Fe entry into blood through internalization of ferroportin (9,130). In *C. elegans*, several neuropeptides are known to mediate intestinal function to regulate metabolism and development (131-133), while a hepcidin homolog is not found. Cardiac Cu deficiency caused by depletion of *Ctr1* Cu

importer in the heart induced a significant upregulation of ATP7A in the intestine of mice, which may lead to increased Cu supply into circulation (61). This study suggested that a cross-talk may take place among tissue types for systemic Cu homeostasis. In *C. elegans*, while enterocyte-autonomous Cu homeostasis regulation may result in a sufficient organismal Cu balance in general, another possibility is that intestinal CUA-1.1 is regulated via an inter-organ communication network. A cellular component responsible for Cu-induced CUA-1.1 trafficking in the intestine may be the molecular link by which the enterocytes sense and respond to extraintestinal Cu status. Future studies to characterize how intestinal Cu acquisition and distribution is regulated at the systemic level may lead to the discovery of new pathways of organismal Cu trafficking.

Chapter 4: Organ-specific Regulation of ATP7A Abundance is Coordinated with Systemic Cu Homeostasis

Summary

Cu is an essential trace element required for a vast array of cellular processes in organisms from bacteria to humans. Cu serves as a redox-reactive, catalytic cofactor in the enzymatic reactions that drive oxidative phosphorylation, iron (Fe) acquisition, protection from oxidative stress, neuropeptide maturation, blood clotting, and angiogenesis(1-3). However, the ability of Cu to undergo reversible redox changes also makes this element deleterious to the organism when present in excess (4,5). Because of its dichotomous potential as both an essential cofactor and a toxic agent, cells have evolved sophisticated mechanisms for the regulation of Cu acquisition, storage, and distribution (6,7). As all organismal Cu must pass through the intestine prior to distribution to other tissues (15,58), cross-talk must take place among tissue types to ensure that import and export of Cu from the intestine are coordinated with extraintestinal Cu requirements.

Cu is taken up by intestinal epithelial cells (IECs), routed for incorporation into Cu-dependent proteins, and mobilized across the basolateral membrane into peripheral circulation. Ctr1 is a homotrimeric integral membrane protein conserved in eukaryotes ranging from yeast to humans that drives intestinal Cu absorption with high affinity and specificity (11,57). Once Cu is imported into IECs, the Cu-

transporting P-type ATPase known as ATP7A conveys it across the basolateral membrane of the enterocyte, where it is delivered into portal circulation. The ATP7B Cu exporter, which is structurally related to ATP7A, is expressed in the liver and removes excess Cu via transport across the apical membrane into the bile (134).

In humans, mutations in the ATP7A gene are known to cause Menkes disease (100), which often leads to early childhood mortality as a consequence of reduced Cu efflux from enterocytes into the bloodstream (135,136). ATP7A is normally localized to the trans-Golgi network (TGN) (137) where it is essential for the insertion of Cu into important secreted enzymes such as tyrosinase (138) and lysyl oxidase (139). When Cu is abundant, ATP7A-containing vesicles traffic to the plasma membrane for Cu efflux (137). The Cu-induced trafficking of ATP7A has presumably evolved to allow this transporter to shift its function from metallation of secreted cuproenzymes in the TGN to the cellular-protective export of excess cellular Cu across the plasma membrane, as well as for absorption of dietary Cu by enterocytes in the intestine.

In contrast to other organisms, systemic Cu fluctuations in mammalian cells do not alter expression of Cu homeostasis genes at the transcriptional level (7). While it is generally accepted that regulation of mammalian Cu homeostasis at the cellular level occurs predominantly via posttranscriptional mechanisms, these mechanisms have not yet been shown to play a role in organism-wide systemic Cu homeostasis. In this study, we present evidence that low Cu levels stimulate a reduction in ATP7A protein abundance in tissue cultures and a whole animal model. Specifically, Cu-deficient mice exhibited substantially reduced ATP7A steady-state protein levels in peripheral tissues, including the heart, spleen, and liver, consistent with results from

cell culture data. Compared to peripheral tissues, however, ATP7A expression in the intestine was inversely regulated in response to Cu levels, hinting at a distinct regulatory role for intestinal ATP7A in organismal Cu homeostasis. Our data suggest that this intestine-specific regulation of ATP7A protein levels may serve as a key homeostatic mechanism for control of the efflux of this essential, yet potentially toxic, trace element into circulation, thus providing new molecular insights into how intestinal Cu export is regulated for systemic Cu homeostasis in response to peripheral Cu deficiency.

Results

Elevated Cu increases ATP7A protein levels in cultured cells

To explore Cu-responsive regulation of ATP7A, non-polarized rat intestinal epithelial cells (IEC-6) were grown in basal media and treated with $CuCl_2$ (100 μM), the membrane impermeable Cu(I)-specific chelator bathocuproine disulfonic acid (BCS, 300 μM), or 300 μM BCS together with 100 μM $CuCl_2$, and analyzed for ATP7A abundance by immunoblotting. A significant elevation in ATP7A protein levels was observed in media containing 100 μM Cu, whereas ATP7A levels were decreased in BCS-treated cells (Fig. 4.1A-B). Notably, mRNA levels of *Atp7a* were not altered by either treatment (Fig. 4.1C). ATP7A levels were enhanced in cells treated simultaneously with BCS and $CuCl_2$ indicating that the BCS-induced ATP7A decrease is caused by a Cu-limitation. Increased levels of the Cu chaperone for superoxide dismutase (CCS) observed in BCS-treated cells (Fig. 4.1A) suggested that

available cellular Cu was limited, as CCS is elevated when Cu is scarce (33,34). ATP7A levels in IEC-6 cells were increased in response to 100 μM $CuCl_2$ in a time-dependent manner (Fig. 4.3A), in agreement with a previous report by the Collins group (140). Abundance of an ectopically-expressed recombinant-tagged (HA-GFP) ATP7A by Cu and BCS was regulated similarly to endogenous ATP7A (Fig. 4.2).

To determine the sensitivity of ATP7A elevation during Cu surplus conditions, IEC-6 cells were pre-grown in BCS-treated media for 6 h, washed with phosphate-buffered saline (PBS), and exposed to a range of Cu concentrations for 2 h, followed by assessment of ATP7A levels. Cu levels as low as 1 μM were sufficient to enhance expression of ATP7A as compared to cells in BCS-treated media, and ATP7A levels progressively increased until reaching saturation at treatment with 10 μM of Cu (Fig. 4.3B), which is within the physiological range of Cu concentrations in plasma (141).

To test the specificity of ATP7A metal-responsiveness, ATP7A levels were investigated in media containing 200 μM $FeCl_3$, $ZnCl_2$, $MnCl_2$, or 10 μM $AgNO_3$; exposure to iron, zinc, and manganese at a 2:1 molar excess over Cu resulted in no substantial increase in ATP7A protein levels (Fig. 4.3C). However, ATP7A levels were increased by treatment with 10 μM Ag with similar efficiency to equimolar concentrations of Cu. As Ag(I) is isoelectronic to Cu(I), these findings suggest that Cu(I), rather than Cu(II), is the primary driver of this process.

To further explore this phenomenon in primary cells, hepatocytes were isolated from the livers of C57BL/6 mice at postnatal day 12 (P12), as hepatic Cu content and ATP7A expression levels in perinatal mice are higher than those in adult mice, suggesting a role for ATP7A in the livers of neonatal mice (61,142-144).

Figure 4.1. Cu levels affect ATP7A protein abundance. (A) IEC-6 cells were exposed to basal medium, 100 μM $CuCl_2$ for 3 h, 300 μM BCS for 6 h, or 300 μM BCS plus 100 μM $CuCl_2$ for 6 h. Total protein extracts were probed with an anti-ATP7A antibody, anti-CCS, and anti-GAPDH as a loading control. A representative immunoblot of seven independent experiments is shown here. (B-C) Relative expression levels of ATP7A protein (B) and *Atp7a* mRNA (C) in IEC-6 cells exposed to $CuCl_2$, BCS, or BCS with $CuCl_2$ were normalized to basal media conditions from four independent immunoblot and RT-qPCR experiments. GAPDH protein and *18S rRNA* mRNA, respectively, were used as internal controls in these experiments. Error bars indicate mean ± SD of four independent experiments. Means that do not share a letter are significantly different ($P<0.05$); ns, not significant ($P>0.05$) (one-way ANOVA, Tukey's post hoc test).

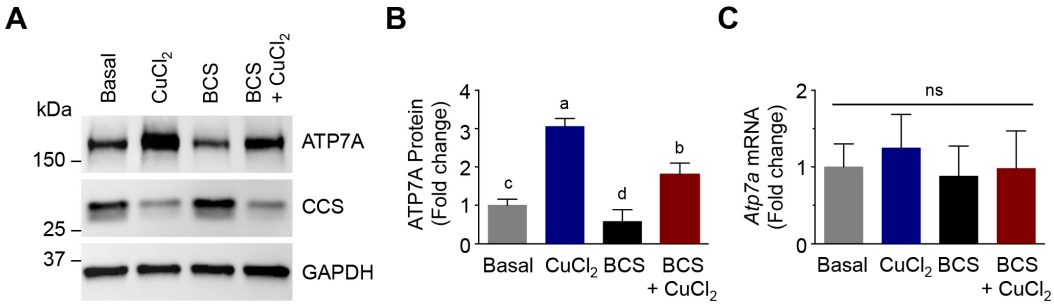
A
Basal
CuCl2
BCS
BCS + CuCl2
kDa
150
25
37
ATP7A
CCS
GAPDH
B
ATP7A Protein (Fold change)
c
a
d
b
Basal
CuCl2
BCS
BCS + CuCl2
C
Atp7a mRNA (Fold change)
ns
Basal
CuCl2
BCS
BCS + CuCl2

Figure 4.2. Evaluation of anti-ATP7A antibody specificity and the regulation of recombinant-tagged ATP7A abundance by Cu. (A) Immunoblotting with anti-ATP7A antibody. Total protein extracts from mouse embryonic fibroblasts (MEFs) of WT ($ATP7A^{+/+}$) and ATP7A knock-out ($ATP7A^{-/-}$) mice (106) were assayed. The upper panel shows immunoblot results with the anti-ATP7A antibody. The lower panel shows immunoblot results with anti-GAPDH antibody as a loading control. (B) HEK293 cells transiently transfected with an empty vector or a CMV-driven plasmid expressing a HA-GFP-ATP7A were exposed to basal medium, basal medium containing 100 μM $CuCl_2$, or 300 μM BCS for 10 h. Whole cell lysates were processed for immunoblotting analysis using antibodies as indicated. Representative immunoblots of three and two independent experiments are shown in (A) and (B), respectively.

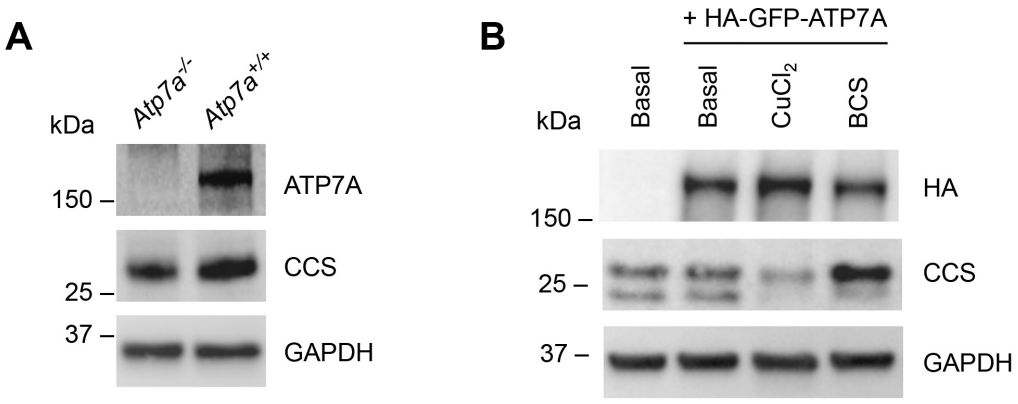
A
kDa
Atp7a-/-
Atp7a+/+
150 –
ATP7A
CCS
25 –
37 –
GAPDH
B
+ HA-GFP-ATP7A
kDa
Basal
Basal
CuCl2
BCS
150 –
HA
25 –
CCS
37 –
GAPDH

Figure 4.3. Cu stimulates the elevation of ATP7A. (A-B) IEC-6 cells at ~60% confluence were preincubated with 300 μM BCS-treated medium for 6 h to minimize expression levels of ATP7A. Cells were further supplemented with 100 μM $CuCl_2$ for the indicated time (A) or with the indicated Cu concentrations for 2 h (B). β-actin and GAPDH levels shown in the lower panel demonstrate equal protein loading. Data are representative of two (A) and three (B) independent experiments. (C) IEC-6 cells were preincubated with 300 μM BCS for 3 h before switching to media containing 200 μM of $FeCl_3$ (*Fe*), $ZnCl_2$ (*Zn*), $MnCl_2$ (*Mn*), 10 μM of $AgNO_3$ (*Ag*), or 10 or 100 μM of $CuCl_2$ (*Cu*) for 2 h, and 100 μg of protein extracts were subjected to immunoblotting. Reduced levels of CCS indicate increased bioavailable Cu levels, and GAPDH levels are shown to indicate protein loading of samples. Immunoblots are representative results of four independent experiments.

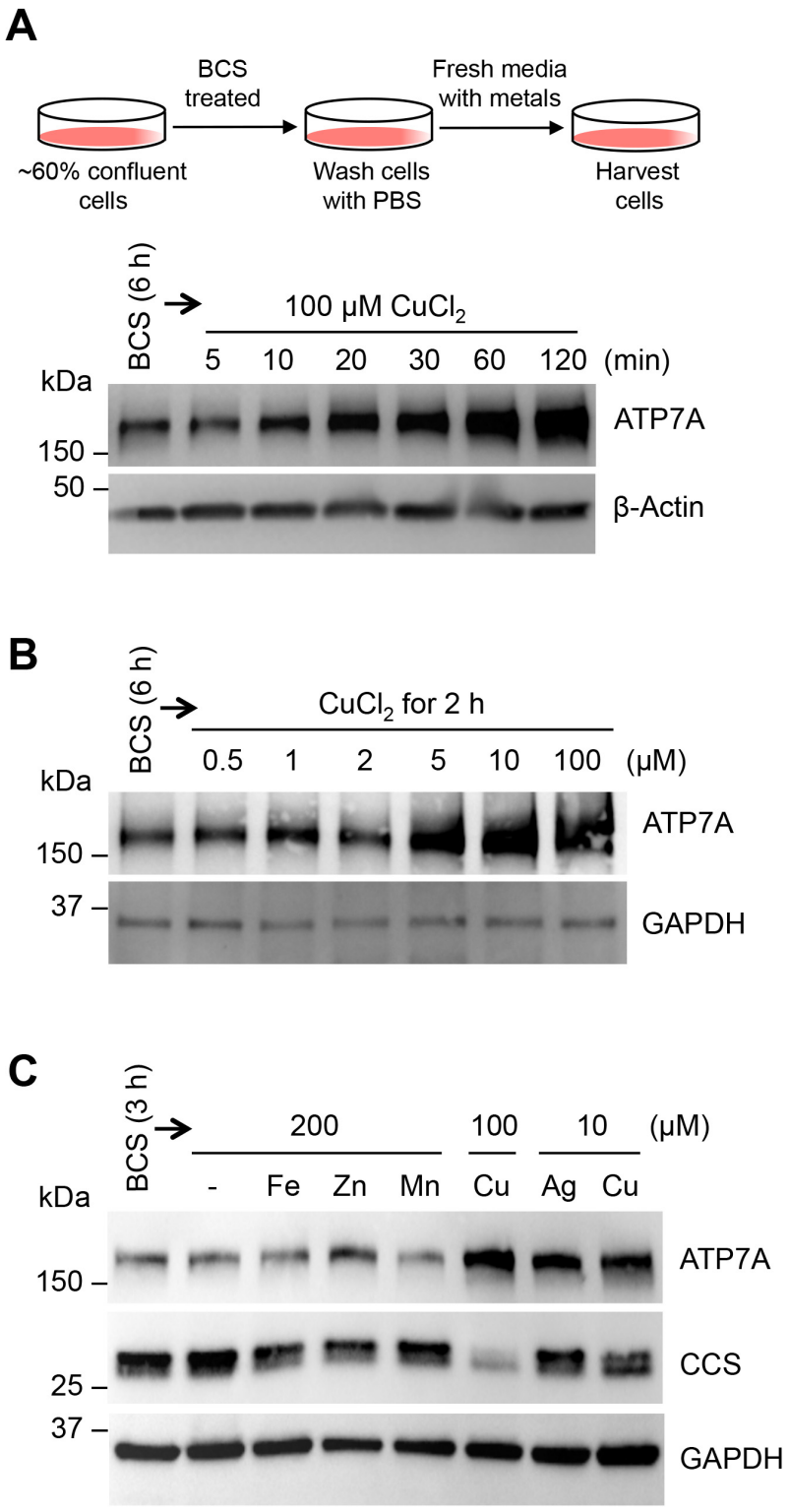
A
BCS treated
Fresh media with metals
~60% confluent cells
Wash cells with PBS
Harvest cells
BCS (6 h)
100 μM CuCl2
5 10 20 30 60 120 (min)
kDa
150
50
ATP7A
β-Actin
B
BCS (6 h)
CuCl2 for 2 h
0.5 1 2 5 10 100 (μM)
kDa
150
37
ATP7A
GAPDH
C
BCS (3 h)
200 100 10 (μM)
- Fe Zn Mn Cu Ag Cu
kDa
150
25
37
ATP7A
CCS
GAPDH

Figure 4.4. ATP7A abundance is increased by Cu in primary cell lines. (A) Mouse primary hepatocytes treated with Cu supplementation were analyzed by immunoblotting. Mouse hepatocytes were pretreated for 12 h in BCS-containing medium and then exposed to medium containing indicated concentrations of $CuCl_2$ for additional 12 h. GAPDH levels were assayed as a loading control. Immunoblots are representative results of four independent experiments. (B) Total Cu levels in mouse primary hepatocytes were measured by ICP-MS upon supplementation with 100 μM BCS or the indicated Cu concentrations. Data are presented as mean ± SD from four biological replicates. Values with one different letter are significantly different from each other ($P<0.05$) (One-way ANOVA, Tukey's post hoc test). (C) Immunoblotting of ATP7A and Ctr1 levels in HUVEC cells treated with a range of concentrations of $CuCl_2$ for 12 h. The arrowheads labeled *g* and *t* indicate the full-length glycosylated monomer and the amino-terminal truncation forms of Ctr1, respectively. The glycosylated and truncated form of Ctr1 have previously been demonstrated to represent mature glycosylated Ctr1 species, and amino-terminal cleaved truncated Ctr1, respectively (23). Data are representative of three independent experiments.

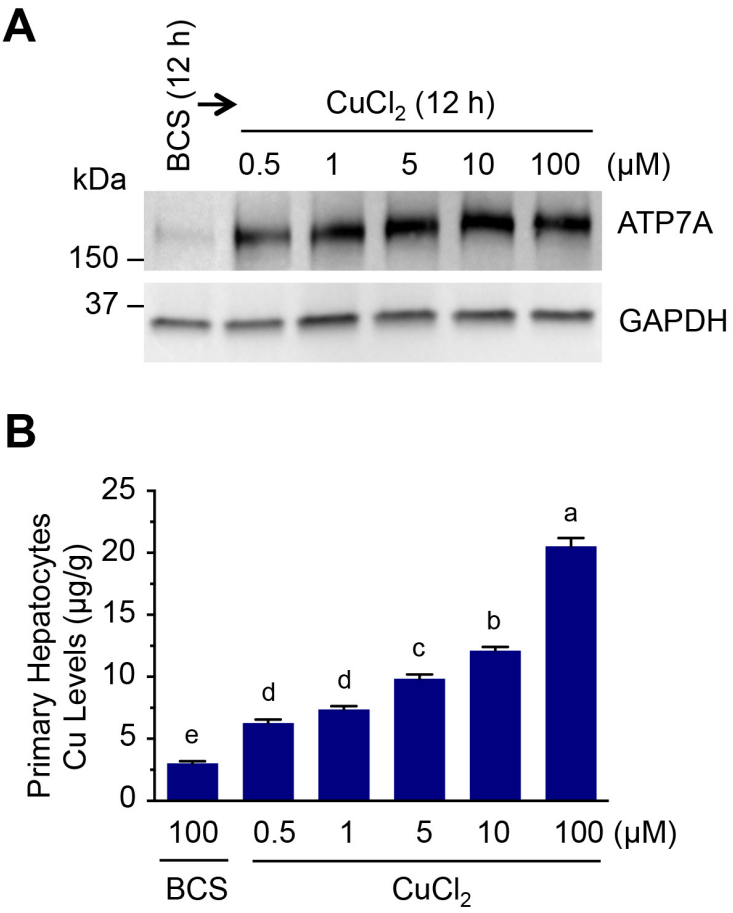
A
BCS (12 h)
CuCl2 (12 h)
0.5 1 5 10 100 (μM)
kDa
150
37
ATP7A
GAPDH
B
Primary Hepatocytes Cu Levels (μg/g)
25
20
15
10
5
0
a
b
c
d
d
e
100 0.5 1 5 10 100 (μM)
BCS
CuCl2
C
Basal
CuCl2 (12 h)
1 2 5 (μM)
kDa
150
37
20
ATP7A
g
Ctr1
t

Figure 4.5. ATP7A protein levels in *Ctr1*$^{+/+}$ and *Ctr1*$^{-/-}$ MEFs. Total protein extracts isolated from wild type (*Ctr1*$^{+/+}$) MEFs, *Ctr1*$^{-/-}$ MEFs transfected with empty vector (vec) exposed to basal media or 100 μM $CuCl_2$ for overnight (vec+Cu), and *Ctr1*$^{-/-}$ MEFs transfected with a plasmid expressing Ctr1 were resolved by SDS-PAGE and analyzed by immunoblotting. Data are representative for three independent experiments.

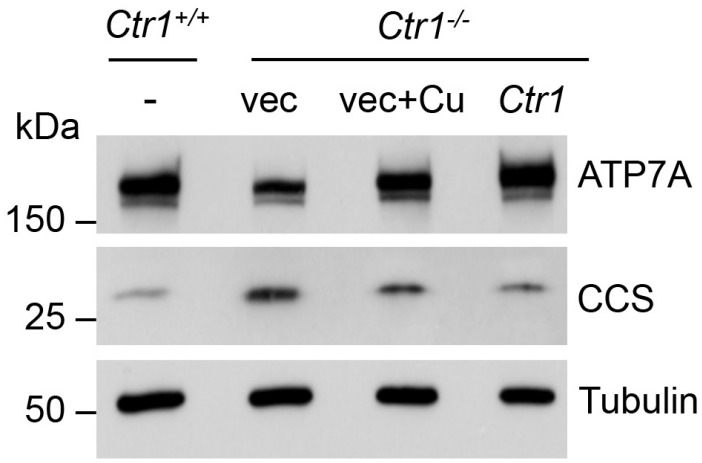
Ctr1+/+
Ctr1-/-
-
vec
vec+Cu
Ctr1
kDa
150
25
50
ATP7A
CCS
Tubulin

Isolated hepatocytes were pretreated with BCS overnight and exposed to a range of Cu concentrations. The primary cells treated with as low as 0.5 μM Cu showed significantly increased ATP7A protein abundance (Fig. 4.4A) demonstrating that increased cellular Cu levels, as shown by ICP-MS analysis (Fig. 4.4B), are associated with elevated ATP7A expression. Moreover, low micromolar Cu (1 μM) was also sufficient to induce ATP7A expression in human umbilical vein endothelial cell (HUVEC) cultures (Fig. 4.4C), and levels of the Ctr1 Cu importer were significantly decreased upon Cu treatment, as described previously in HEK293 cells (15). These results demonstrate that cells harbor a mechanism for regulation of ATP7A protein levels to adjust the export of Cu in response to exogenous Cu. Although elevation of ATP7A occurs in response to Cu media supplementation, it is unclear whether extracellular Cu triggers this process indirectly, or whether Cu in the growth media enters cells and elevates intracellular Cu, thereby triggering ATP7A stabilization.

In order to clarify the mechanism, we investigated the degradation of ATP7A in mouse embryonic fibroblasts (MEFs) lacking the high-affinity Cu importer Ctr1 (*Ctr1*$^{-/-}$) (22), along with *Ctr1*$^{+/+}$ wild type cells, and *Ctr1*$^{-/-}$ cells transfected with a wild type Ctr1-expressing plasmid, grown in Cu-supplemented media (Fig. 4.5). ATP7A protein levels in *Ctr1*$^{-/-}$ MEF cells transfected with vector plasmid were lower than those in *Ctr1*$^{+/+}$ MEFs and *Ctr1*$^{-/-}$ MEFs treated with exogenous Cu, indicating that the intracellular Cu pool modulates ATP7A abundance.

Post-translational control of ATP7A abundance in response to Cu

A previous report showing no changes in ATP7A mRNA levels in response to supplemental Cu in rat IECs (140) suggests steady-state ATP7A protein levels are regulated post-transcriptionally. ATP7A is very stable protein, with a reported half-life over 40 h in a variety of cells (140,145-147). To further explore Cu-dependent ATP7A regulation, IEC-6 cells were treated with Cu or BCS in the presence of the translation inhibitor cycloheximide (CHX), and steady-state levels of ATP7A were analyzed by immunoblotting over time. In IEC-6 cells, elevated steady-state levels of ATP7A by Cu treatment were significantly diminished within an hour of exposure to 300 μM BCS; no reduction in ATP7A was observed under Cu-excess conditions upon 100 μM Cu treatment (Fig. 4.6A).

To test whether this enhanced turnover of ATP7A occurs through the proteasome pathway, IEC-6 cells pretreated with Cu were exposed to BCS along with the proteasome inhibitors MG132 and bortezomib, alone or in combination. These proteasome inhibitors partially abrogated the decrease in steady-state levels of ATP7A protein in response to cellular Cu deprivation (Fig. 4.6B), suggesting that the reduction in ATP7A protein levels was due, at least in part, to increased proteolysis via a proteasomal pathway.

Figure 4.6. Cu-deficiency stimulates the degradation of ATP7A protein. (A) IEC-6 cells pretreated with media containing 100 μM $CuCl_2$ for 2.5 h were further treated with 50 μg/mL cycloheximide (CHX). Following 30 min incubation, cells were exposed to fresh culture media containing 300 μM BCS and 50 μg/ml CHX and then lysed after 0.5, 1, 3, or 6 h (lanes 3-6). Whole cell lysates were processed for immunoblotting analysis using antibodies as indicated. Immunoblot images are representative results of four independent experiments. (B) IEC-6 cells were pretreated with media containing 100 μM $CuCl_2$ for 1 h before addition of 20 μM MG132, 100 nM bortezomib, or DMSO (vehicle control) and treated for another 90 min. Cells were further treated with 50 μg/mL CHX for 30 min, and then the media was replaced with fresh media containing 300 μM BCS and 50 μg/mL CHX for 2 h in the presence of MG132 and/or bortezomib, or DMSO. Na^+/K^+-ATPase served as a loading control. Representative immunoblots of four independent experiments are shown.

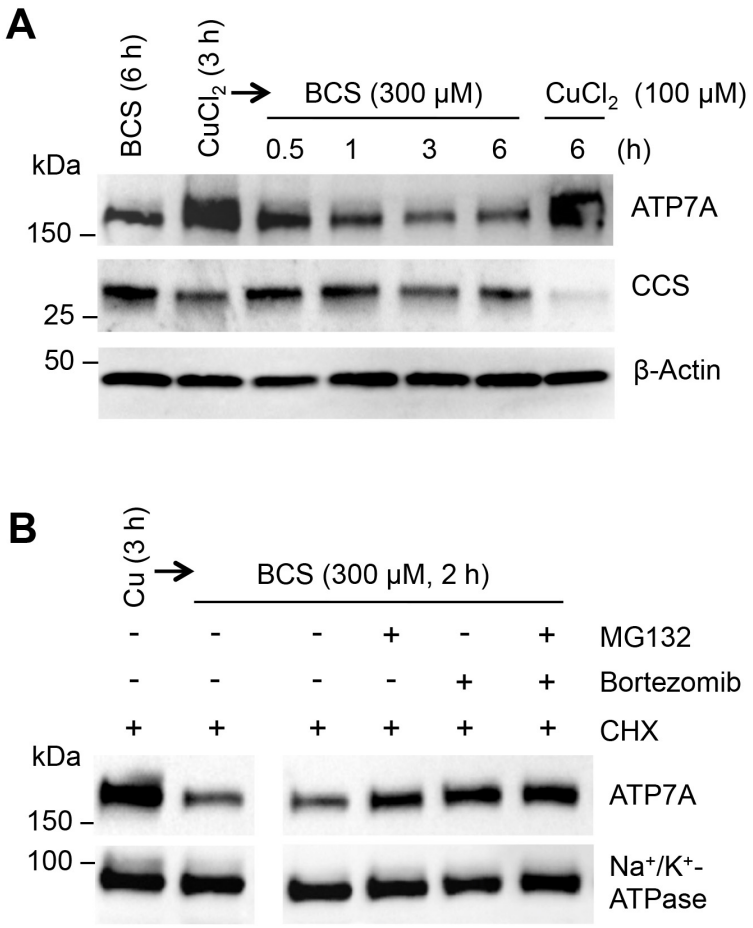
A
BCS (6 h)
CuCl2 (3 h)
BCS (300 μM)
CuCl2 (100 μM)
0.5 1 3 6 6 (h)
kDa
150 –
ATP7A
CCS
25 –
50 –
β-Actin
B
Cu (3 h)
BCS (300 μM, 2 h)
- - - + - + MG132
- - - - + + Bortezomib
+ + + + + + CHX
kDa
150 –
ATP7A
100 –
Na+/K+-
ATPase

A liver-specific role for active Cu sequestration

To test the physiological significance of Cu-responsive ATP7A abundance regulation, C57BL/6 mice were subcutaneously (SQ) administered Cu or saline (15) at P7 for three consecutive days. Mice were dissected at P10 and assayed for Cu accumulation in tissues by ICP-MS. While no marked Cu accumulation was observed in the serum or the heart, the liver showed highly elevated Cu accumulation in a dose-dependent manner (Fig. 4.7A-C). As metallothionein (MT) genes are induced by high Cu exposure (148), mRNA levels of MT-1 and MT-2 genes were assessed to explore whether these correlate with hepatic Cu accumulation. As expected, while expression of MT-1 was modestly increased only in mice administered Cu at the concentration of 10 μg/g BW, MT-2 gene was significantly elevated in mice administered SQ Cu compared to control mice (Fig. 4.7D-E). Hepatic ATP7A expression was enhanced only in mice administered Cu at the concentration of 10 μg/g total body weight (BW) (Fig. 4.8A). Elevated serum Cu levels were also detected only in mice treated with 10 μg Cu/g BW (Fig. 4.7A), suggesting that this level of Cu exceeds the capacity of the liver to excrete surplus Cu.

As the Cu-specific importer Ctr1 is inactivated through endocytosis and degradation in cultured cells in response to Cu treatment (Fig. 4.4C) (25), and the mature glycosylated form of Ctr1 was increased in the intestines and hearts of wild type mice fed a Cu-deficient diet (23), we performed immunoblot analysis of Ctr1 protein levels in the livers of mice administered with Cu. Unexpectedly, whereas mRNA levels of Ctr1 were not changed (Fig. 4.7F), the glycosylated full-length form

Figure 4.7. Hepatic Cu accumulation is preferentially elevated by subcutaneous Cu administration. (A-C) Cu levels measured by ICP-MS in serum (A), hearts (B), and livers (C) from C57BL/6 mice (P10) SQ administered indicated amounts of Cu-histidine for three consecutive days beginning at P7. Data (means ± SD) are from seven to nine mice of each condition (n = 2-5 mice for males and females per Cu dose), and means marked with different letter superscripts are significantly different at p=0.05 (one-way ANOVA, Tukey's post hoc test). (D-F) Quantitative RT-qPCR analysis of mRNA levels of *Mt1, Mt2, and Ctr1*. Levels of *Mt1* (D), *Mt2* (E), *Ctr1* (F) transcripts were measured relative to *Gapdh* mRNA levels in the livers of individual mice at P10 (male, n = 2; female, n = 2) for each condition, which were SQ administered Cu or saline at P7 for three consecutive days. Bars indicate mean ± SD for each condition. Means that do not share a letter are significantly different ($P<0.05$). ns, not significant ($P>0.05$) (one-way ANOVA, Tukey's post hoc test).

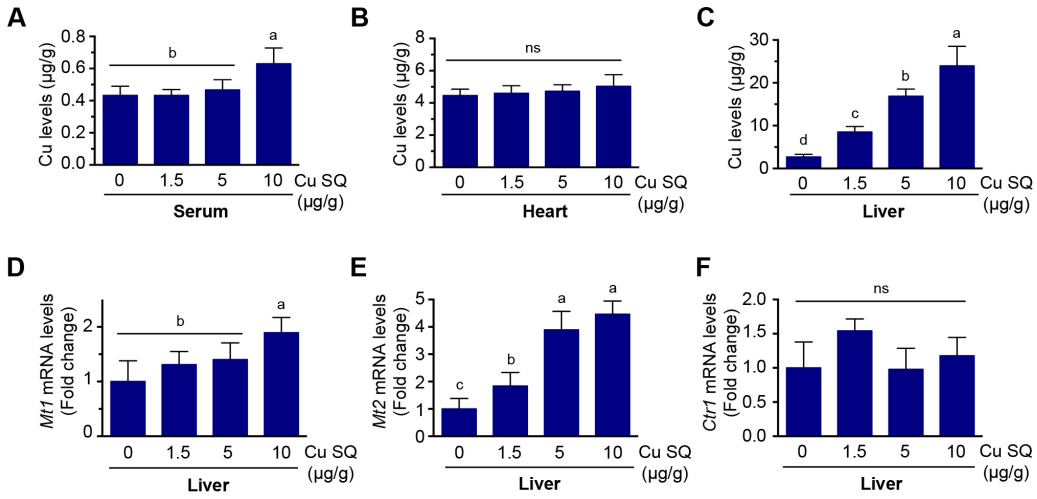
A
Cu levels (µg/g)
0.8
0.6
0.4
0.2
0.0
b
a
0
1.5
5
10
Cu SQ (µg/g)
Serum
B
Cu levels (µg/g)
8
6
4
2
0
ns
0
1.5
5
10
Cu SQ (µg/g)
Heart
C
Cu levels (µg/g)
30
20
10
0
d
c
b
a
0
1.5
5
10
Cu SQ (µg/g)
Liver
D
Mt1 mRNA levels (Fold change)
2
1
0
b
a
0
1.5
5
10
Cu SQ (µg/g)
Liver
E
Mt2 mRNA levels (Fold change)
5
4
3
2
1
0
c
b
a
a
0
1.5
5
10
Cu SQ (µg/g)
Liver
F
Ctr1 mRNA levels (Fold change)
2.0
1.5
1.0
0.5
0.0
ns
0
1.5
5
10
Cu SQ (µg/g)
Liver

Figure 4.8. Hepatic Ctr1 protein levels are elevated by subcutaneous Cu administration. (A-B) Immunoblot analysis of ATP7A, Ctr1, CCS, and GAPDH in liver (A) and heart (B) extracts from two representative mice administered saline or indicated amounts of Cu-histidine per body weight (μg/g) for three consecutive days beginning at P7. The arrowheads indicate the glycosylated full-length (*g*) and truncated form (*t*) of Ctr1, respectively. GAPDH levels were assayed as a loading control. Results are representative of three to four independent experiments performed on a total of male (liver, n = 5, 4, 4, and 6; heart, n = 5, 3, 5 and 6) and female mice (liver, n = 6, 4, 4, and 5; heart, n = 6, 4, 2, and 5), which were SQ administered with 0, 1.5, 5, and 10 μg $CuCl_2$–histidine per body weight (g).

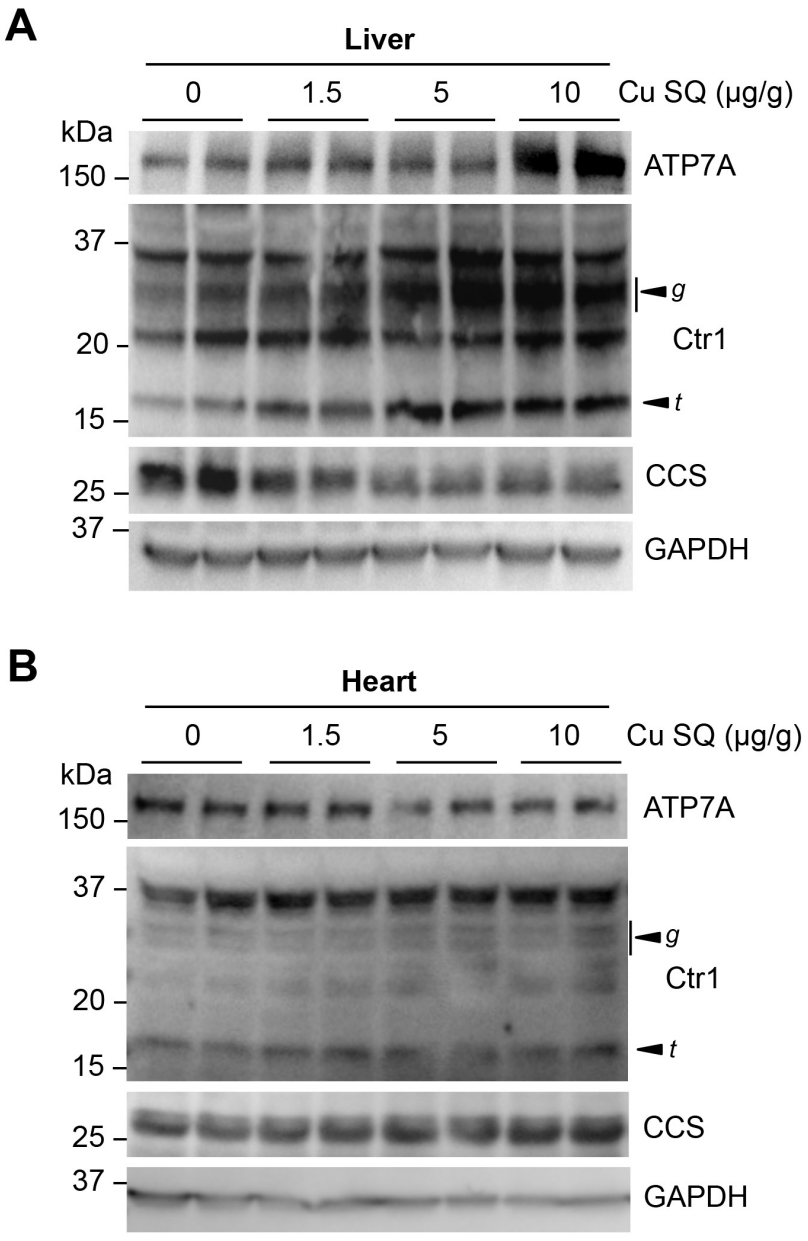
A
Liver
0
1.5
5
10
Cu SQ (μg/g)
kDa
150
ATP7A
37
g
20
Ctr1
t
15
25
CCS
37
GAPDH
B
Heart
0
1.5
5
10
Cu SQ (μg/g)
kDa
150
ATP7A
37
g
20
Ctr1
t
15
25
CCS
37
GAPDH

Figure 4.9. Ctr1 protein levels in the heart, spleen, brain, and liver from WT mice SQ administered saline or Cu. Immunoblot analysis of ATP7A, Ctr1, CCS, and β-actin in the heart, spleen, brain, and liver extracts from two representative mice administered with saline or 10 μg of Cu-histidine per body weight (g) for three consecutive days beginning at P7. The arrowheads indicate the full-length glycosylated (*g*) and truncated form (*t*) of Ctr1, respectively. β-actin levels were assayed as a loading control. Data shown here are representative of three to four independent experiments performed for each tissue of male (M) (liver, n = 5 and 6; heart, n = 5 and 6; brain, n = 2 and 2; spleen, n = 3 and 4) and female (F) mice (liver, n = 6 and 5; heart, n = 6 and 5; brain, n = 2 and 2; spleen, n = 3 and 2), which were SQ administered saline or Cu.

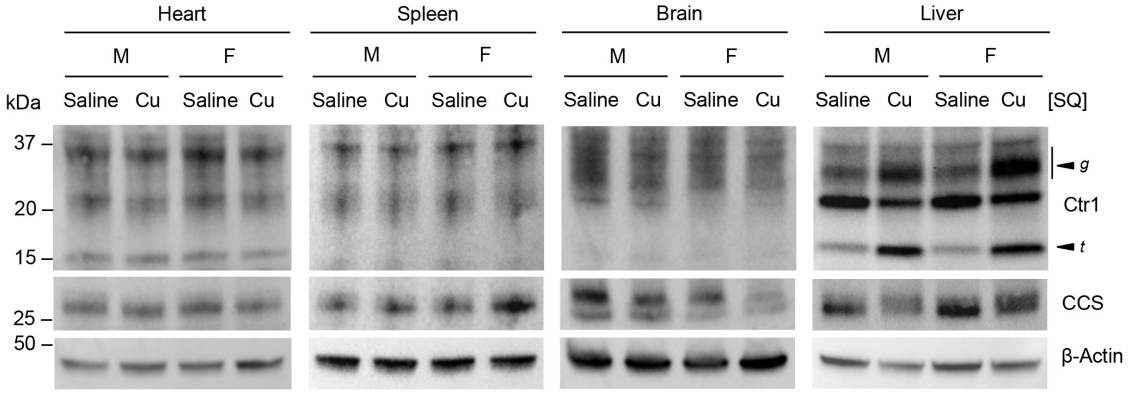
Heart
Spleen
Brain
Liver
M
F
kDa
Saline
Cu
[SQ]
37
20
15
25
50
g
Ctr1
t
CCS
β-Actin

of Ctr1 protein was strongly elevated in the livers of Cu-treated mice, with a concomitant increase in hepatic Cu accumulation and a reduction in CCS levels, in a dose-dependent manner (Fig. 4.7C and Fig. 4.8A). However, peripheral tissues such as the heart, spleen and brain showed no obvious changes in protein abundances of Ctr1 and ATP7A (Fig. 4.8B and Fig. 4.9). These data suggest that Cu-responsive elevation of the mature glycosylated Ctr1 protein is liver-specific, suggesting a mechanism by which Cu can be sequestered in the liver under Cu-excess conditions. Taken together, these findings suggest the existence of a liver-specific role for Ctr1 in active Cu detoxification for systemic Cu homeostasis.

Organ-specific regulation of ATP7A abundance

The administration of Cu treatment in C57BL/6 mice did not lead to robust changes in Cu levels in the circulation (Fig. 4.7A) and resulted in an increase in ATP7A levels in the liver only in mice administered Cu at the concentration of 10 μg/g BW (Fig. 4.8A) compared to those in cell culture models (Fig. 4.4A) despite comparable cellular Cu levels between the *in vitro* (Fig. 4.4B) and *in vivo* (Fig. 4.7C) experimental conditions. We therefore postulated that the tissues of Cu-deficient mice may be more sensitive to Cu fluctuations in circulation than those from Cu-adequate wild-type mice. To test this hypothesis, we utilized the intestine-specific Ctr1 knockout mouse ($Ctr1^{int/int}$) as a Cu-deficient animal model. Ctr1 knockout in the intestine markedly reduces Cu accumulation in peripheral tissues including the liver, heart, and spleen, and results in severe Cu deficiency phenotypes at P10 (15,23). P10 $Ctr1^{int/int}$ mice were SQ administered 10 μg Cu/g BW and sacrificed after 48 h, and

the steady-state levels of Cu in several peripheral tissues of *Ctr1*$^{int/int}$ and control mice (*Ctr1*$^{flox/flox}$) administered with Cu or saline were evaluated by ICP-MS. As shown in Fig. 4.10, *Ctr1*$^{int/int}$ mice demonstrated significantly reduced Cu accumulation in all peripheral tissues tested. Consistent with previous data, the intestine of *Ctr1*$^{int/int}$ mice hyperaccumulated Cu in a non-bioavailable pool(15), as supported by elevated CCS abundance representing reduced bioavailable Cu levels (Fig. 4.14A and Fig. 4.14C).

To explore whether fluctuations in Cu concentrations in peripheral tissues are associated with changes in ATP7A protein expression levels, we examined ATP7A levels from *Ctr1*$^{int/int}$ and *Ctr1*$^{flox/flox}$ pups administered with Cu or saline injections. ATP7A levels in the peripheral tissues (such as the livers) of *Ctr1*$^{int/int}$ mice were clearly decreased as compared to those in age-matched sibling control mice (*Ctr1*$^{flox/flox}$); however, this decrease in ATP7A levels was rescued to the levels found in control *Ctr1*$^{flox/flox}$ mice by SQ Cu administration (Fig. 4.11A-B). Hyper-accumulated Fe levels in the intestine and liver, likely due to a reduction of Fe efflux facilitated by the Cu-dependent ferroxidase hephaestin and ceruloplasmin (15), were also rescued by Cu administrations in these mice (Fig. 4.12). The abundance of hepatic ATP7B protein was not changed by Cu injection or Cu deficiency (Fig. 4.11A), which is consistent with recent observations that elevated Cu levels in the body alters the cellular localization of ATP7B from the TGN to lysosomes without any concomitant change in ATP7B protein levels (149).

While Cu deficiency did not affect Ctr1 abundance in the livers of *Ctr1*$^{int/int}$ mice, glycosylated full-length form of hepatic Ctr1 was highly expressed in both Cu-

Figure 4.10. Relative Cu levels in control and *Ctr1*$^{int/int}$ mice SQ administered saline or Cu-histidine. Relative Cu levels in liver extracts, serum, intestinal epithelial cells (IEC), and total brain extracts of control mice (*Ctr1*$^{flox/flox}$ or *Ctr1*$^{flox/+}$) and *Ctr1*$^{int/int}$ mice SQ administered saline or 10 µg of Cu-histidine per body weight (g) at P10, normalized to those of control (*Ctr1*$^{flox/flox}$ or *Ctr1*$^{flox/+}$) mice administered saline. Data are shown as relative fold change compared with control (means ± SD) from seven to nine mice per condition (n = 2-5 mice per sex per condition), and means followed indicated with different letter superscripts are significantly different at p=0.05 (two-way ANOVA, Tukey's post hoc test).

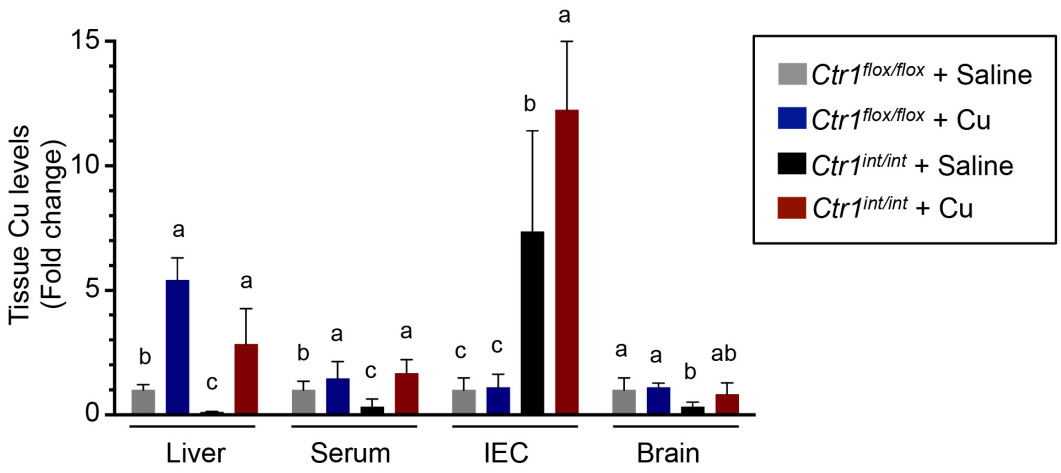
Tissue Cu levels
(Fold change)
15
10
5
0
b
a
c
a
b
a
c
a
c
c
b
a
a
a
b
ab
Liver
Serum
IEC
Brain
Ctr1flox/flox + Saline
Ctr1flox/flox + Cu
Ctr1int/int + Saline
Ctr1int/int + Cu

Figure 4.11. Systemic Cu status regulates ATP7A protein levels in the liver. (A) Representative *Ctr1*$^{flox/flox}$ and *Ctr1*$^{int/int}$ mice littermates SQ administered saline or Cu-histidine at P10 and sacrificed at P12 for analysis. Protein extracts from the indicated tissues from these mice were immunoblotted with anti-ATP7A, anti-CCS, anti-ATP7B, anti-Ctr1, and anti-GAPDH antibodies. The arrowheads labeled *g* and *t* indicate the full-length glycosylated, and truncated forms of Ctr1, respectively. Data shown here are representative of three to eleven independent experiments performed for each mouse tissue (liver, n = 12, 10, 12, and 10). (B-C) Quantification of ATP7A and CCS expression in *Ctr1*$^{flox/flox}$ and *Ctr1*$^{int/int}$ mice administered with saline or Cu. Relative protein abundances of hepatic ATP7A (B) and CCS (C) were quantified by analyzing immunoblots of 10-12 mice tissues (liver, n = 12, 10, 12, and 10) for each condition for statistical analysis. Error bars represent average ± SD, and means indicated with different letters are significantly different from each other at p=0.05 (Two-way ANOVA, Tukey's post hoc test).

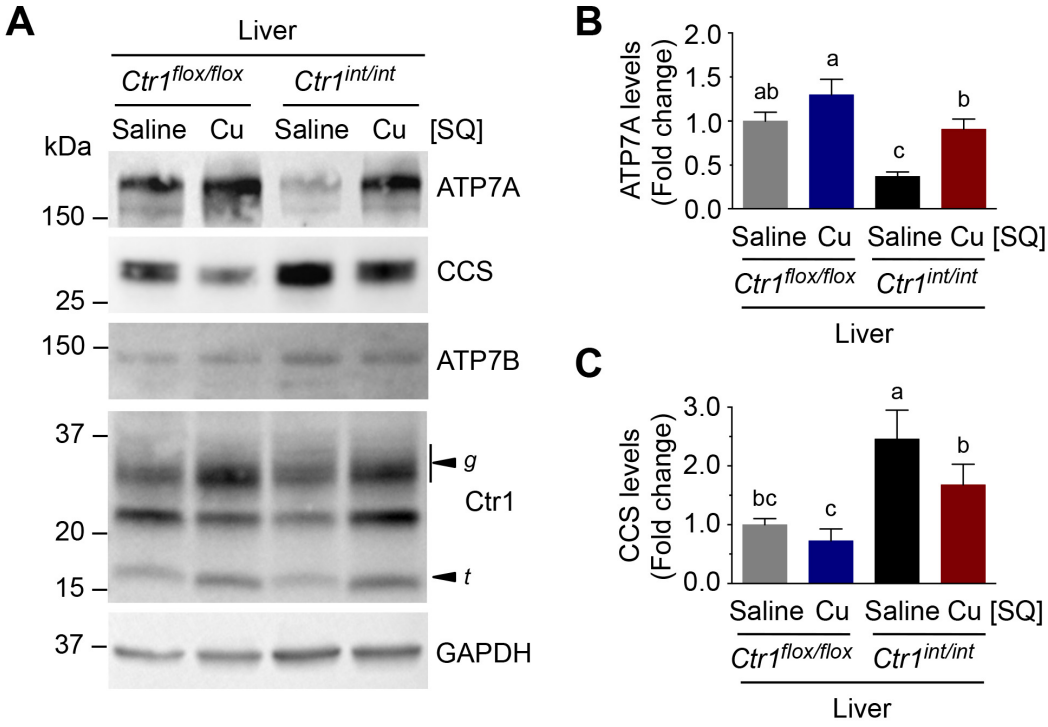
A
Liver
Ctr1flox/flox
Ctr1int/int
Saline
Cu
Saline
Cu
[SQ]
kDa
150
ATP7A
CCS
25
150
ATP7B
37
g
Ctr1
20
15
t
37
GAPDH
B
ATP7A levels
(Fold change)
2.0
1.5
1.0
0.5
0.0
ab
a
c
b
Saline
Cu
Saline
Cu
[SQ]
Ctr1flox/flox
Ctr1int/int
Liver
C
CCS levels
(Fold change)
3.0
2.0
1.0
0.0
bc
c
a
b
Saline
Cu
Saline
Cu
[SQ]
Ctr1flox/flox
Ctr1int/int
Liver

Figure 4.12. Relative Fe levels in control and *Ctr1*$^{int/int}$ mice SQ administered saline or Cu-histidine. Relative Fe levels in liver extracts, serum, intestinal epithelial cells (IEC), and total brain extracts of control mice (*Ctr1*$^{flox/flox}$ or *Ctr1*$^{flox/+}$) and *Ctr1*$^{int/int}$ mice SQ administered saline or Cu-histidine at P10, normalized to those of control (*Ctr1*$^{flox/flox}$ or *Ctr1*$^{flox/+}$) mice administered saline. Data are shown as relative fold change compared with control (means ± SD) from seven to nine mice per condition (n = 2-5 mice per sex per condition), and means indicated with different letter superscripts are significantly different at p=0.05 (two-way ANOVA, Tukey's post hoc test).

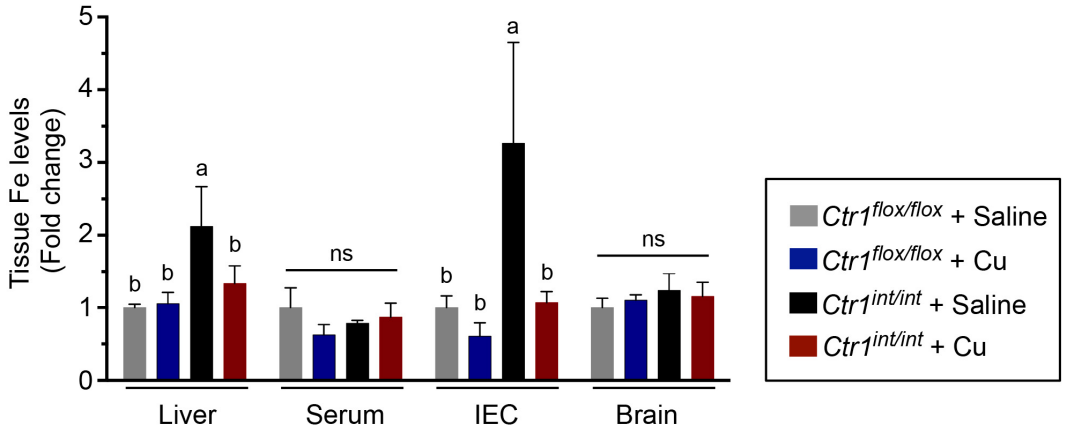
Tissue Fe levels
(Fold change)
5
4
3
2
1
0
b
b
a
b
ns
b
b
a
b
ns
Liver
Serum
IEC
Brain
Ctr1flox/flox + Saline
Ctr1flox/flox + Cu
Ctr1int/int + Saline
Ctr1int/int + Cu

Figure 4.13. Systemic Cu status regulates ATP7A protein levels in heart and spleen. (A and D) Representative *Ctr1*$^{flox/flox}$ and *Ctr1*$^{int/int}$ mice littermates SQ administered saline or Cu-histidine at P10 and sacrificed at P12 for analysis. Protein extracts from the indicated tissues from these mice were immunoblotted with anti-ATP7A, anti-CCS, and anti-GAPDH antibodies. Data shown here are representative of three to eleven independent experiments performed for each mouse tissue (heart, n = 6, 6, 4, and 4; spleen, n = 6, 4, 9, and 4). (B, C, E, and F) Relative protein abundances of ATP7A (B-C) and CCS (E-F) were quantified by analyzing immunoblots of each tissue from mice (heart, n = 6, 6, 4, and 4; spleen, n = 6, 4, 9, and 4) for each condition for statistical analysis. Error bars represent average ± SD, and means indicated with different letters are significantly different from each other at p=0.05. ns, not significant (Two-way ANOVA, Tukey's post hoc test).

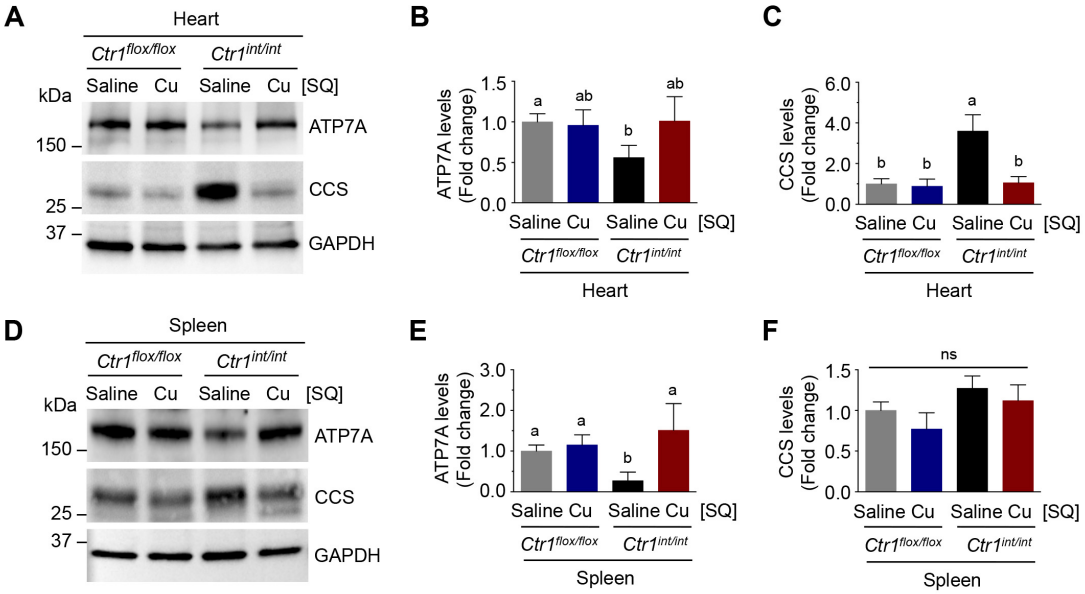
A
Heart
Ctr1flox/flox
Ctr1int/int
Saline Cu Saline Cu [SQ]
kDa
150 –
25 –
37 –
ATP7A
CCS
GAPDH
B
ATP7A levels (Fold change)
1.5
1.0
0.5
0.0
a ab b ab
Saline Cu Saline Cu [SQ]
Ctr1flox/flox Ctr1int/int
Heart
C
CCS levels (Fold change)
6.0
4.0
2.0
0.0
b b a b
Saline Cu Saline Cu [SQ]
Ctr1flox/flox Ctr1int/int
Heart
D
Spleen
Ctr1flox/flox
Ctr1int/int
Saline Cu Saline Cu [SQ]
kDa
150 –
25 –
37 –
ATP7A
CCS
GAPDH
E
ATP7A levels (Fold change)
3.0
2.0
1.0
0.0
a a b a
Saline Cu Saline Cu [SQ]
Ctr1flox/flox Ctr1int/int
Spleen
F
CCS levels (Fold change)
ns
1.5
1.0
0.5
0.0
Saline Cu Saline Cu [SQ]
Ctr1flox/flox Ctr1int/int
Spleen

treated *Ctr1*$^{int/int}$ and *Ctr1*$^{flox/flox}$ mice as compared to saline-treated *Ctr1*$^{int/int}$ and *Ctr1*$^{flox/flox}$ mice, reaffirming that the liver acts as a Cu storage and sequestration organ under Cu overload conditions. Increased CCS in the livers of *Ctr1*$^{int/int}$ pups due to Cu deficiency was suppressed by Cu administration, (Fig. 4.11A and Fig. 4.11C), consistent with the ICP-MS analysis (Fig. 4.10). ATP7A levels in several other peripheral tissues including the hearts and spleens similarly exhibited reduced ATP7A levels in *Ctr1*$^{int/int}$ mice as compared to *Ctr1*$^{flox/flox}$ mice, and these levels were restored by Cu administration (Fig. 4.13). These *in vivo* findings suggest that ATP7A protein abundance in several peripheral organs is regulated in response to Cu levels in animals.

Intestinal ATP7A protein abundance primarily responds to systemic Cu status

Since intestinal Cu absorption is the primary point at which Cu transport into circulation can be regulated, we examined the expression levels of ATP7A in intestinal enterocytes in Ctr1- and Cu-deficient mice. Interestingly, intestinal ATP7A abundance was inversely correlated with bioavailable Cu, in direct opposition to its regulation in the liver (Fig. 4.11A-B and Fig. 4.14A-B). While bioavailable Cu was limited in the intestinal epithelial cells, as indicated by increased levels of CCS (Fig. 4.14A and Fig. 4.14C) ATP7A expression was strongly elevated as compared to that in saline-treated *Ctr1*$^{flox/flox}$ mice; this elevated ATP7A was suppressed by Cu administration, leading to increases in bioavailable Cu in the intestine and other tissues as compared to that in saline-treated *Ctr1*$^{int/int}$ mice (Fig. 4.14A-C). Elevated intestinal CCS protein levels in *Ctr1*$^{int/int}$ mice were rescued by Cu-administration,

indicating that bioavailable Cu was increased in the enterocytes in *Ctr1*$^{int/int}$ mice administered with Cu (Fig. 4.10, Fig. 4.14A, and Fig. 4.14C) (2,15,150). This result was not anticipated, as our *Ctr1*$^{-/-}$ MEFs results (Fig. 4.15) indicate that bioavailable Cu levels in enterocytes are severely limited, which would lead to decreased ATP7A levels. Enterocytes displayed the opposite response when compared to that of cultured cells and peripheral tissues. These intriguing observations suggest that while ATP7A acts to manage intracellular Cu homeostasis in peripheral tissues, intestinal ATP7A levels are at least partially determined by extraintestinal Cu status.

To further explore the *in vivo* regulation of ATP7A abundance under different Cu availability, ATP7A mRNA levels in mouse tissues were measured by reverse transcription quantitative PCR (RT-qPCR). ATP7A steady-state mRNA levels did not significantly change in either the livers or the intestines of *Ctr1*$^{int/int}$ and *Ctr1*$^{flox/flox}$ mice administered Cu or saline (Fig. 4.16). This indicated that control of ATP7A abundance in response to Cu occurs post-transcriptionally, similar to regulation in cell cultures (Fig. 4.1) and reminiscent of the dramatic changes in ATP7A protein, but not mRNA, in the intestine caused by cardiac-specific loss of Ctr1 in mice (*Ctr1*$^{hrt/hrt}$) (61) (Fig. 4.17). Taken together, these results demonstrate that intestinal epithelial cells control ATP7A protein abundance via post-transcriptional regulation in response to peripheral tissue Cu deficiency.

The diametrically contrasting effects of Cu deficiency on ATP7A expression in peripheral tissues compared to enterocytes raises the question as to what mechanism underlies communication between the intestine and Cu-deficient

Figure 4.14. Reduced levels of systemic Cu increase ATP7A protein levels in enterocytes. (A) Representative *Ctr1*$^{flox/flox}$ and *Ctr1*$^{int/int}$ mice littermates SQ administered saline or Cu-histidine at P10 and sacrificed at P12 for analysis. Protein extracts from the indicated tissues from these mice were immunoblotted with anti-ATP7A, anti-CCS, anti-Ctr1, and anti-GAPDH antibodies. The arrowheads labeled *g* and *t* indicate the full-length glycosylated, and truncated forms of Ctr1, respectively. Data shown here are representative of three to eleven independent experiments performed for each mouse tissue (enterocytes, n = 22, 20, 22, and 22). (B-C) Quantification of ATP7A and CCS expression in *Ctr1*$^{flox/flox}$ and *Ctr1*$^{int/int}$ mice administered with saline or Cu. Relative protein abundances of hepatic ATP7A (B) and CCS (C) were quantified by analyzing immunoblots of 20-22 mice tissues (enterocytes, n = 22, 20, 22, and 22) for each condition for statistical analysis. Error bars represent average ± SD, and means indicated with different letters are significantly different from each other at p=0.05 (Two-way ANOVA, Tukey's post hoc test).

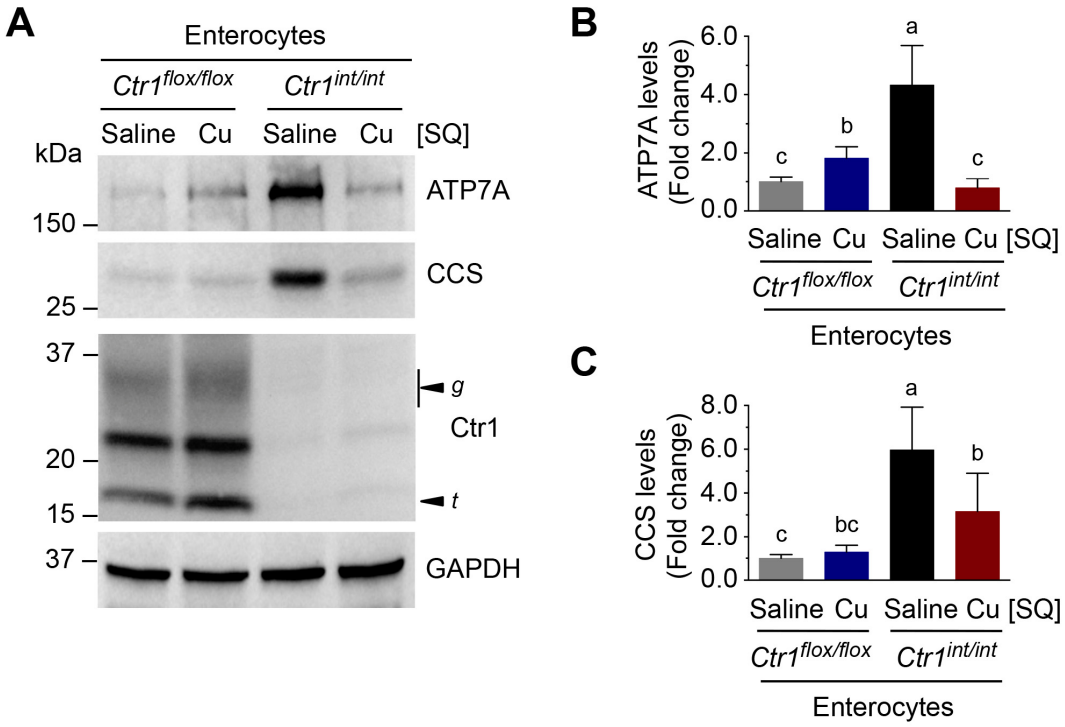
A
Enterocytes
Ctr1flox/flox
Ctr1int/int
Saline
Cu
Saline
Cu
[SQ]
kDa
150
25
37
20
15
37
ATP7A
CCS
g
Ctr1
t
GAPDH
B
ATP7A levels (Fold change)
6.0
4.0
2.0
0.0
a
b
c
c
Saline
Cu
Saline
Cu
[SQ]
Ctr1flox/flox
Ctr1int/int
Enterocytes
C
CCS levels (Fold change)
8.0
6.0
4.0
2.0
0.0
a
b
c
bc
Saline
Cu
Saline
Cu
[SQ]
Ctr1flox/flox
Ctr1int/int
Enterocytes

Figure 4.15. ATP7A protein levels in response to Cu status in isolated and cultured enterocytes. (A) Cu-responsiveness of isolated *Ctr1*$^{int/int}$ enterocytes cultures. Isolated enterocytes from *Ctr1*$^{flox/flox}$ and *Ctr1*$^{int/int}$ mice were cultured in medium containing 100 μM $CuCl_2$ or 300 μM BCS for 2 h. Total protein extracts of cultured enterocytes were subjected to SDS-PAGE and analyzed by immunoblotting. Immunoblots shown here are representative of three independent experiments performed on a total of n = 5, 5, 7, and 7. (B-C) Relative protein abundances of ATP7A (B) and CCS (C) were quantified by analyzing immunoblots of each tissue from mice (isolated enterocytes culture, n = 5, 5, 7, and 7) for each condition for statistical analysis. Error bars represent average ± SD, and means indicated with different letters are significantly different from each other at p=0.05. ns, not significant (Two-way ANOVA, Tukey's post hoc test).

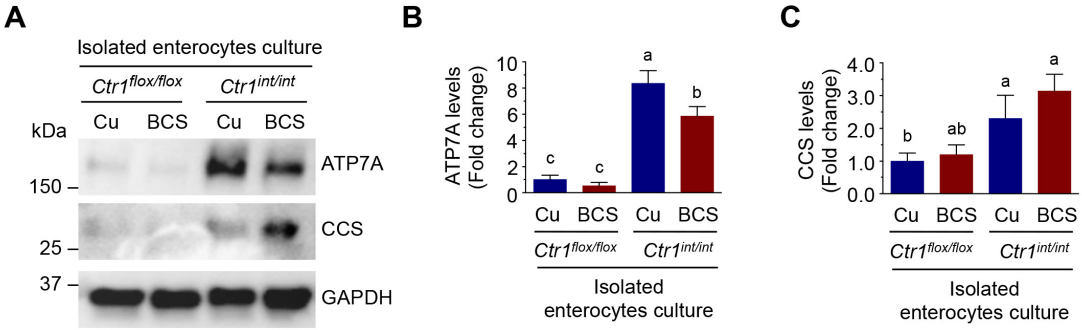
A
Isolated enterocytes culture
Ctr1flox/flox
Ctr1int/int
Cu
BCS
Cu
BCS
kDa
150 –
25 –
37 –
ATP7A
CCS
GAPDH
B
ATP7A levels (Fold change)
10
8
6
4
2
0
a
b
c
c
Cu
BCS
Cu
BCS
Ctr1flox/flox
Ctr1int/int
Isolated enterocytes culture
C
CCS levels (Fold change)
4.0
3.0
2.0
1.0
0.0
b
ab
a
a
Cu
BCS
Cu
BCS
Ctr1flox/flox
Ctr1int/int
Isolated enterocytes culture

Figure 4.16. Quantitative RT-qPCR analysis of *Atp7a* mRNA levels in the liver and intestine of *Ctr1*$^{flox/flox}$ and *Ctr1*$^{int/int}$ mice SQ administered saline or Cu. Levels of *Atp7a* mRNA relative to *Gapdh* mRNA levels in the livers (A) and intestinal epithelial cells (B) from the *Ctr1*$^{flox/flox}$ and *Ctr1*$^{int/int}$ mice two days following SQ administration of saline or 10 µg of Cu-histidine per body weight (g) at P10 were determined on a total of male (n = 2, 3, 3, and 2) and female (n = 4, 2, 3, and 3) mice. Bars indicate mean ± SD of five to six mice for each condition. ns, not significant indicates $p>0.05$ (two-way ANOVA, Tukey's post hoc test).

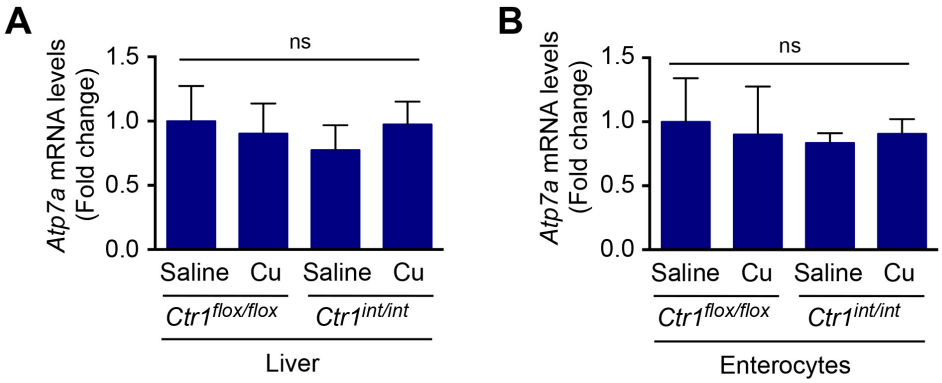
A
Atp7a mRNA levels
(Fold change)
1.5
1.0
0.5
0.0
ns
Saline
Cu
Saline
Cu
Ctr1flox/flox
Ctr1int/int
Liver
B
Atp7a mRNA levels
(Fold change)
1.5
1.0
0.5
0.0
ns
Saline
Cu
Saline
Cu
Ctr1flox/flox
Ctr1int/int
Enterocytes

Figure 4.17. Protein and mRNA levels of intestinal ATP7A in cardiac-specific Ctr1 knockout mice. Protein abundances (A) and mRNA levels (B) of ATP7A in intestinal cells in $Ctr1^{hrt/hrt}$ and $Ctr1^{flox/flox}$ mice were measured by immunoblot analysis and RT-qPCR. A representative result of three independent immunoblots for ATP7A is shown in (A). For RT-qPCR, *Atp7a* and *Gapdh* mRNA levels from five mice (male, 2 and 3; female, 3 and 2) for each condition were determined. Error bars indicate mean ± SD. Statistics: two-tailed unpaired Student's t-test (ns, $P>0.05$).

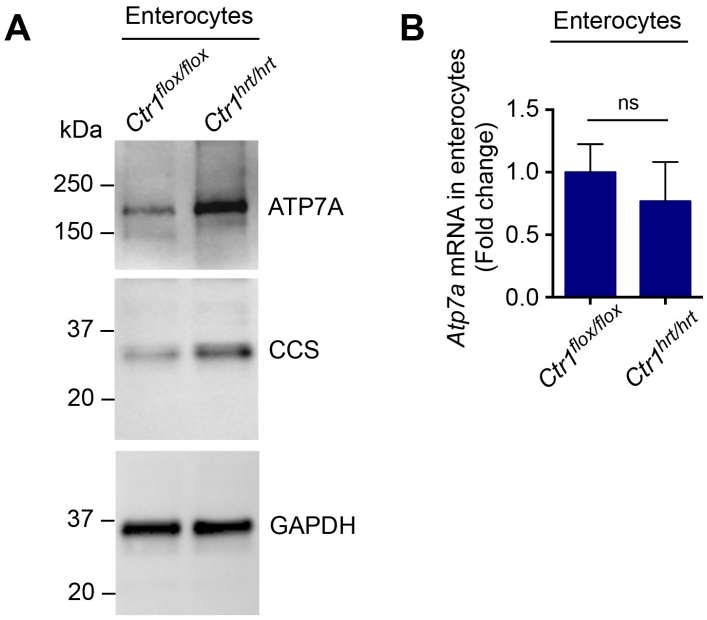
A
Enterocytes
Ctr1flox/flox
Ctr1hrt/hrt
kDa
250
150
ATP7A
37
20
CCS
37
20
GAPDH
B
Enterocytes
Atp7a mRNA in enterocytes
(Fold change)
ns
1.5
1.0
0.5
0.0
Ctr1flox/flox
Ctr1hrt/hrt

Figure 4.18. ATP7A protein levels in polarized IEC-6 cells treated with Cu or BCS. IEC-6 cells were grown on trans-well culture systems until they had formed tight junctions as a monolayer as described in Methods. Cells were treated with Cu or BCS for 12 h on either the apical or basolateral side of IEC-6 cells and cell extracts were then probed with anti-ATP7A, anti-CCS and anti-GAPDH antibodies. Shown is the representative immunoblots of two independent experiments using the indicated antibodies.

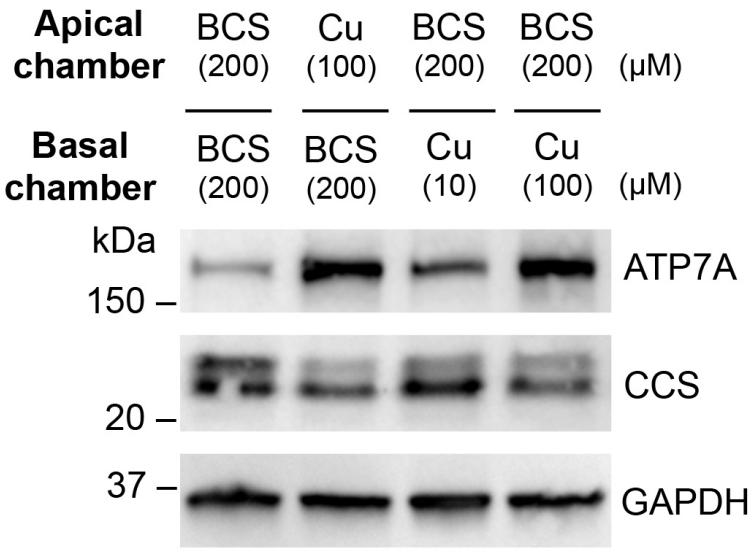
Apical chamber
BCS (200)
Cu (100)
BCS (200)
BCS (200)
(μM)
Basal chamber
BCS (200)
BCS (200)
Cu (10)
Cu (100)
(μM)
kDa
150 –
ATP7A
CCS
20 –
37 –
GAPDH

peripheral tissues. Isolated enterocytes from *Ctr1*$^{int/int}$ and *Ctr1*$^{flox/flox}$ mice were exposed to culture medium treated with Cu or BCS for 2 h. Immunoblot analysis of these cells revealed that elevated intestinal ATP7A in *Ctr1*$^{int/int}$ mice was decreased by BCS treatment, concomitant with an increase in CCS expression in isolated and cultured enterocytes when compared to those from the Cu-treated medium (Fig. 4.15). Thus, when isolated in culture, enterocytes appear to regulate ATP7A expression in response to Cu availability in a manner that more closely resembles that of peripheral tissues and cultured cells than that found in enterocytes in their native milieu. Cu treatments of either the apical or basolateral side of polarized IEC-6 cells using a trans-well system led to elevation of ATP7A levels (Fig. 4.18) suggesting polarization *per se* is not sufficient to recapitulate the ATP7A phenotype shown in the intestine of Cu-injected *Ctr1*$^{int/int}$ (Fig. 4.14).

To determine the subcellular distribution of the intestinal ATP7A protein in an *in vivo* model, we examined the localization of ATP7A across the duodenum and upper jejunum of *Ctr1*$^{int/int}$ and *Ctr1*$^{flox/flox}$ mice. Multi-label confocal immunofluorescence microscopy showed that ATP7A expression was specific to enterocytes at the villus tip (Fig. 4.19), with predominant localization of ATP7A to intracellular vesicles and little overlap with wheat germ agglutinin (WGA), an apical membrane marker (Fig. 4.20C and Fig. 4.20F). The majority of ATP7A was concentrated in intracellular puncta in both *Ctr1*$^{int/int}$ and *Ctr1*$^{flox/flox}$ mice, as opposed to the basolateral membranes (marked by the Na^+/K^+-ATPase). Highly elevated levels of ATP7A were apparent in *Ctr1*$^{int/int}$ mice as compared to control mice, confirming the Western blot data (Fig. 4.14A-B). Taken together, these findings indicate that

highly increased intestinal ATP7A in *Ctr1*$^{int/int}$ mice primarily localizes to intracellular vesicles in the enterocytes of intestinal villi, a distribution like that in *Ctr1*$^{flox/flox}$ mice.

The results from the *Ctr1*$^{int/int}$ mice support the hypothesis that ATP7A expression in the enterocyte is controlled by the need to supply Cu to peripheral tissues. Alternatively, the changes to ATP7A abundance in the intestine could also be attributed to the intestinal loss of Ctr1 in *Ctr1*$^{int/int}$ mice, independent of peripheral Cu deficiency. To separate these two possibilities, we determined if intestinal ATP7A expression was regulated by Cu deficiency in wild-type mice in a similar manner to their *Ctr1*$^{int/int}$ and *Crt1*$^{hrt/hrt}$ counterparts. We performed analysis of ATP7A levels in mice fed Cu-adequate and Cu-deficient diets. Dietary Cu-deficiency in wild type mice correlated to a reduction in hepatic ATP7A expression in parallel with increased CCS expression resulting from Cu restriction (Fig. 4.21A). However, abundance of the intestinal ATP7A Cu efflux pump was significantly enhanced, even while enterocytes demonstrated severe Cu-deficiency, as indicated by elevated levels of CCS, like the observations from *Ctr1*$^{int/int}$ mice (Fig. 4.21B). Moreover, enterocytes expressed higher amounts of the glycosylated full-length form of Ctr1 in the intestinal epithelial cells of Cu-deprived mice. Together, these findings suggest an intestinal regulatory mechanism for dietary Cu absorption via increased expression of the Ctr1 Cu importer and ATP7A Cu exporter in wild type mice, and indicate that intestinal ATP7A regulation is distinct from that in the liver and other peripheral organs.

Figure 4.19. Confocal microscopy analysis of endogenous ATP7A in the jejunum from *Ctr1*$^{flox/flox}$ and *Ctr1*$^{int/int}$ mice. Sections of upper jejunum from *Ctr1*$^{flox/flox}$ (A-B) and *Ctr1*$^{int/int}$ mice (C) were subjected to confocal immunofluorescence microscopy analysis. Image (A) is obtained without adding anit-ATP7A primary antibody. Images are representative of two independent experiments. Green, anti-ATP7A; magenta, anti-Wheat Germ Agglutinin (WGA, 15 μg/mL). Scale bars, 20 μm.

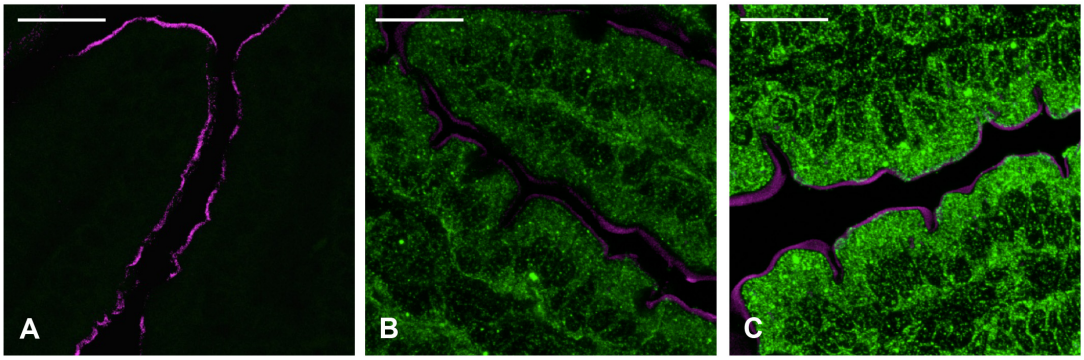
A
B
C
No primary antibody
anti-ATP7A antibody
anti-ATP7A antibody
Ctr1flox/flox
Ctr1int/int

Figure 4.20. Elevated ATP7A is enriched in intracellular vesicles in the enterocytes of *Ctr1*$^{int/int}$ mice. Confocal immunofluorescence images of endogenous ATP7A in the enterocytes of *Ctr1*$^{flox/flox}$ (A-C) and *Ctr1*$^{int/int}$ (D-F) mice (P12). Upper jejunum sections were subjected to confocal immunofluorescence microscopy analysis. Images are representative of four independent experiments. Note that B, C, E, and F are enlarged images. Green, anti-ATP7A; red, anti-Na^+/K^+-ATPase alpha-1 subunit; magenta, anti-Wheat Germ Agglutinin (WGA, 15 μg/mL); blue, DAPI. Scale bars, 50 μm (a and d) and 10 μm (b, c, e, and f).

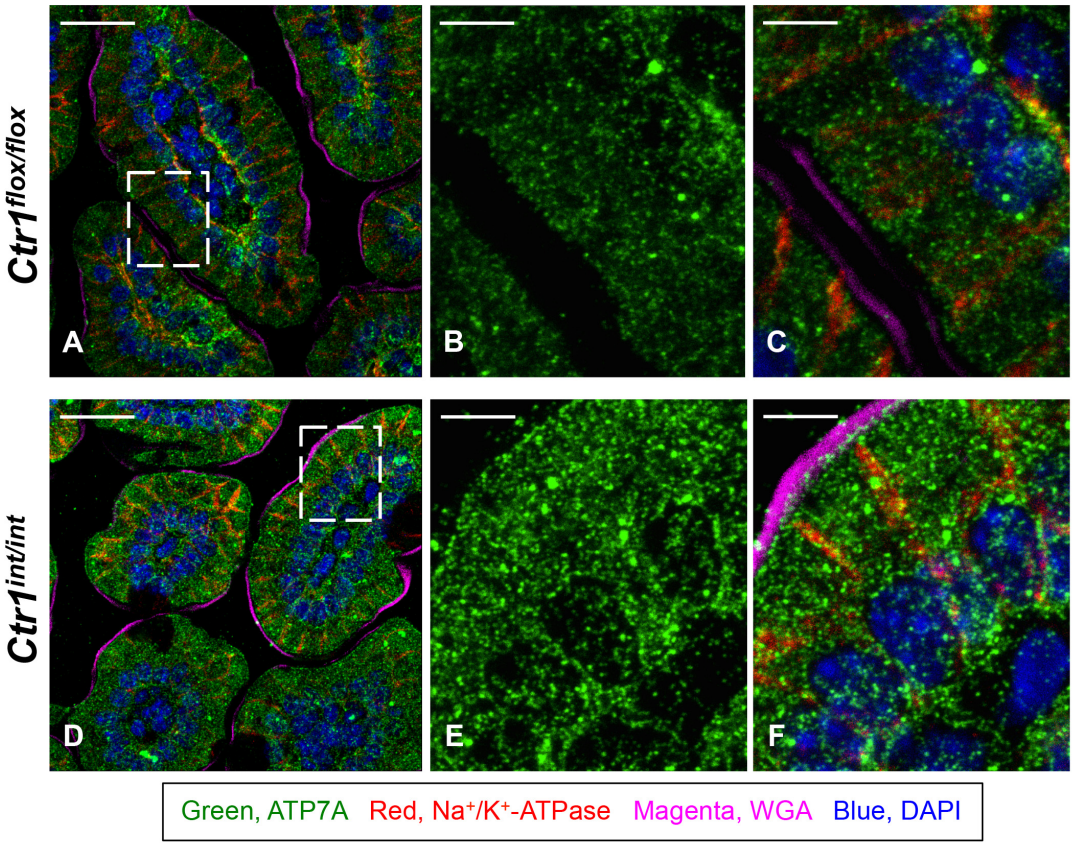
Ctr1flox/flox
Ctr1int/int
A
B
C
D
E
F
Green, ATP7A Red, Na+/K+-ATPase Magenta, WGA Blue, DAPI

Figure 4.21. Dietary Cu-deficient mice exhibit elevated protein levels of ATP7A and Ctr1 in the intestine. (A-B) Immunoblot analysis of ATP7A and CCS in the liver (A) and enterocytes (B) of three representative mice (P15) fed a control or Cu-deficient diet. GAPDH levels were assayed as a loading control. The arrowheads labeled *g* and *t* indicate the glycosylated full-length, and truncated forms of Ctr1, respectively. Data shown in here are representative of three independent experiments performed on male (n = 3 and 3) and female (n = 2 and 4) mice for Cu-adequate and Cu-deficient conditions.

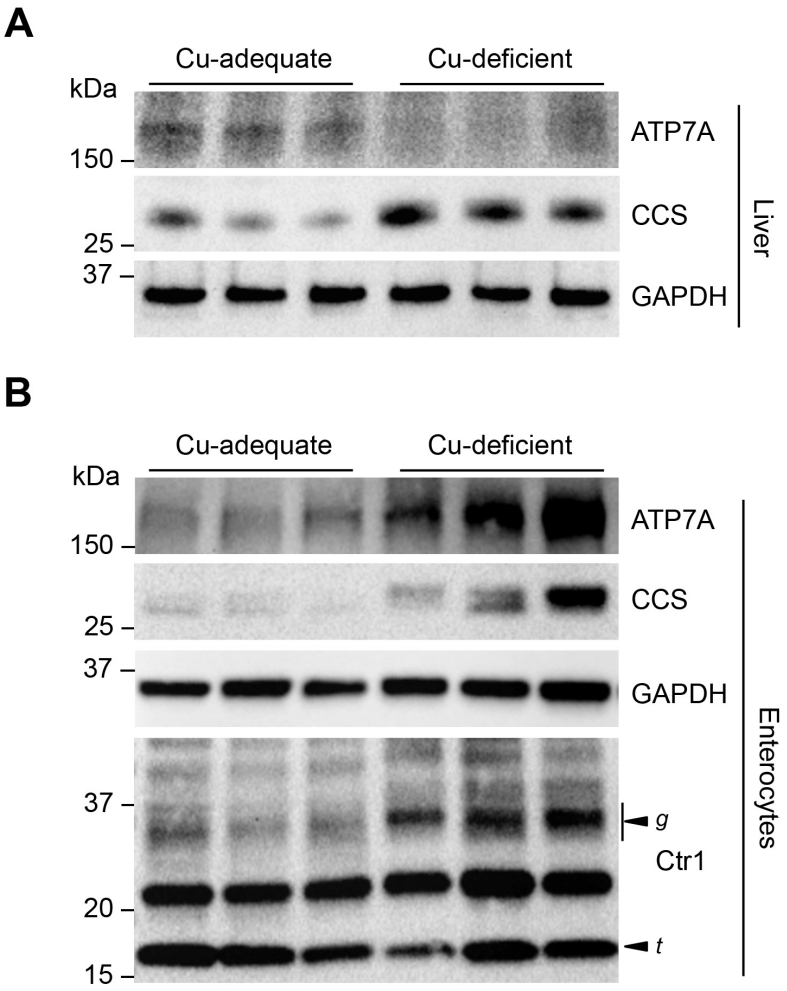
A
Cu-adequate
Cu-deficient
kDa
150
25
37
ATP7A
CCS
GAPDH
Liver
B
Cu-adequate
Cu-deficient
kDa
150
25
37
37
20
15
ATP7A
CCS
GAPDH
g
Ctr1
t
Enterocytes

Discussion

The unique physiological functions and specific cell types found in various mammalian organ systems result in differential demands for Cu. The role of the Cu exporter ATP7A in cellular Cu delivery to secretory pathways and into peripheral circulation in organisms has been well established via its Cu-responsive trafficking (7,50,101,137,151). However, the mechanisms by which ATP7A abundance in distinct tissues responds to changes in organismal Cu remain poorly understood (2,61,100). Here we present data that suggest ATP7A abundance is an important control point for Cu homeostasis in peripheral tissues including the heart and spleen; in mice, excess Cu results in increased ATP7A protein levels in liver tissue, consistent with a need to prevent over-accumulation of this metal through enhanced ATP7A-driven Cu export. Our data demonstrate that in response to potentially detrimental Cu concentrations, cell systems not only relocate ATP7A to post-Golgi vesicles and the plasma membrane (137), but also increase the protein abundance of ATP7A in order to enhance export of Cu from cells and restore intracellular Cu homeostasis (Fig. 4.1-6) (140). Conversely, under Cu deficiency, our results suggest that ATP7A protein abundance is reduced, at least in part, by the proteasome system (Fig. 4.6B), consistent with a reduced need to export Cu from the cell. It is worth noting that Cu status regulates the multi-Cu oxidase hephaestin via a proteasome-mediated pathway (152), and that XIAP targets CCS for ubiquitination through its E3 ubiquitin ligase activity, resulting in the degradation of CCS under adequate levels of Cu (35). It is possible that a similarly-regulated E3 ubiquitin ligase binds to ATP7A and targets it for degradation during Cu deficiency.

While it is known that the liver is a major Cu storage organ in mammals, little attention has been paid to the delineation of the biochemical mechanisms by which mammals regulate the detoxification, storage, and mobilization of Cu (153). We observed that Cu accumulation is drastically increased in the liver as compared to other peripheral tissues in mice administered SQ Cu (Fig. 4.7C and Fig. 4.10), supporting the concept of the liver as the principle Cu storage organ. Ctr1 is known to be internalized and degraded in response to high Cu levels in cultured cells (25), which we also observed in this study (Fig. 4.4C). Unexpectedly, the liver demonstrated an increase in Ctr1 levels in response to Cu administration when compared to levels in mice administered saline (Fig. 4.8A and Fig. 4.11A). This finding suggests that in contrast to other tissues, liver Ctr1 expression is elevated under high Cu conditions; this is possibly to facilitate removal of Cu from the circulation and prevent build up in other Cu-susceptible peripheral tissues. The mechanisms underlying the contrasting responses of Ctr1 in liver versus peripheral tissues remain to be determined.

Unexpected observations from our analyses of Cu-deficient mice include the elevated protein levels of ATP7A and Ctr1 in enterocytes associated with limited levels of bioavailable intracellular Cu, while under these same conditions, peripheral tissues showed significantly diminished ATP7A expression. In addition, while Cu accumulation significantly increased in the enterocytes of $Ctr1^{int/int}$ mice, SQ Cu administration into these mutant mice suppressed intestinal ATP7A expression. A previous study revealed that cardiac-specific Ctr1 ablation in mice ($Ctr1^{hrt/hrt}$) results in a dramatic upregulation of ATP7A expression in both the intestine and liver and a

concomitant elevation of serum Cu levels (61). Our results raise the possibility that modulation of ATP7A abundance in the intestine, not the liver, is the principal means by which Cu supply to circulation is regulated depending upon Cu demands from peripheral tissues. Notably, changes in Cu levels did not alter the subcellular distribution of ATP7A in enterocytes. This suggests the possibility that *in vivo,* the intestine increases ATP7A abundance in intracellular vesicles to efflux Cu via exocytosis through basolateral membrane into circulation.

Intestinal epithelial cells in *Ctr1*$^{int/int}$ mice administered with SQ Cu exhibited profound Cu accumulation in parallel with enhanced levels of bioavailable Cu as indicated by decreased CCS, and a rescued Fe hyper-accumulation phenotype when compared with control (saline-administered) *Ctr1*$^{int/int}$ mice (Fig. 4.10, Fig. 4.12, and Fig. 4.14). Given that Ctr1 localizes to the apical membrane in enterocytes (23), and intestinal Ctr1 is poorly expressed in *Ctr1*$^{int/int}$ mice (15), these observations suggest the existence of alternative Cu uptake machinery at the basolateral membrane of intestinal epithelial cells. Such a mechanism may have its origins *in utero* where Cu delivery to enterocytes might occur via Ctr1-independent serosal-to-mucosal Cu transport. A possible pathway in this process might be an anion exchanger-dependent Cu import system (30), which remains to be identified.

Studies of cultures of isolated enterocytes from *Ctr1*$^{int/int}$ mice presented here show that elevated ATP7A expression in the enterocytes of Cu-deficient mice is suppressed in culture with BCS-treated medium (Fig. 4.15), whereas identical enterocytes showed stronger ATP7A expression concomitant with reduced serum Cu levels as compared to *Ctr1*$^{flox/flox}$ mice (Fig. 4.14). These observations underscore the

importance of the intestine as a regulator of Cu entry to the body, which must respond not only to intrinsic Cu needs, but those of peripheral tissues via the basolateral side of epithelial cells that is thought to be in direct communication with circulating effectors. As intestinal ATP7A levels in both *Ctr1*$^{int/int}$ (low serum Cu) (15), and *Ctr1*$^{hrt/hrt}$ (high serum Cu) (61) mice are elevated, the data suggest that serum Cu itself is not a direct intestinal ATP7A inducer. Instead, we speculate that a circulating factor likely regulates intestinal levels of ATP7A. Clearly, more extensive studies are required to identify such a molecule and its mode of action. Such studies will greatly expand our understanding of the regulation of systemic Cu homeostasis and human diseases caused by Cu dysregulation.

Figure 4.22. Mammalian Cu homeostasis in select organs and tissue types. Several organs where Cu homeostasis was investigated in this study are shown, including liver, IECs, and heart. In the diagram of specific tissue types, the cellular membrane localization of Cu transporters and directionality in response to systemic Cu status are indicated.

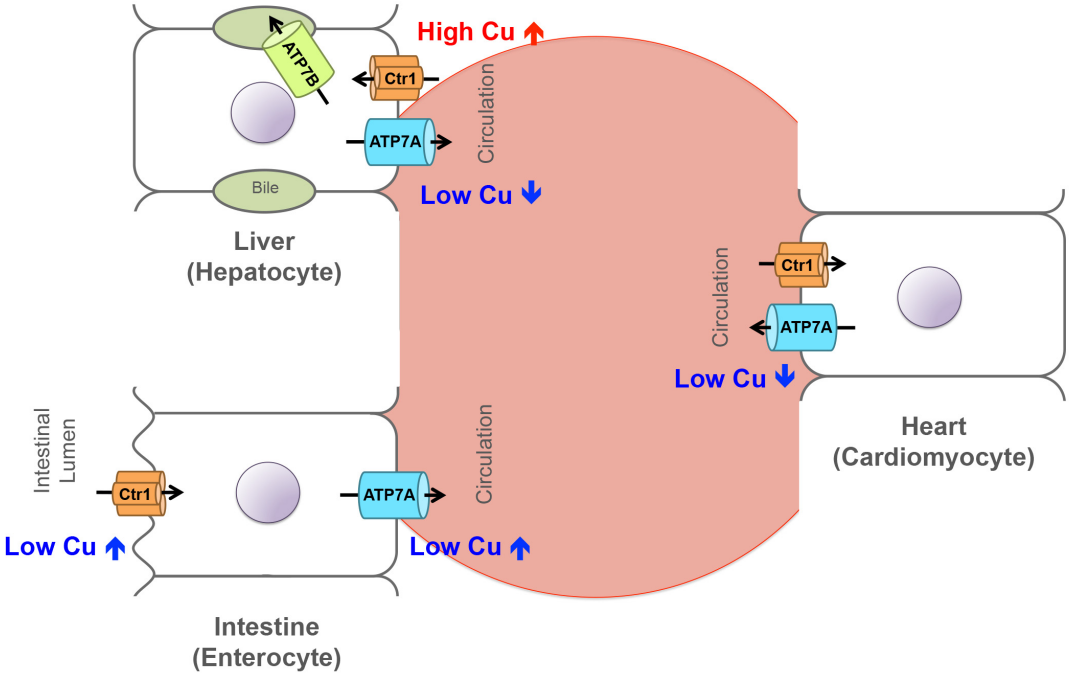
High Cu
ATP7B
Ctr1
ATP7A
Circulation
Bile
Low Cu
Liver
(Hepatocyte)
Circulation
Ctr1
ATP7A
Low Cu
Heart
(Cardiomyocyte)
Intestinal
Lumen
Ctr1
ATP7A
Circulation
Low Cu
Low Cu
Intestine
(Enterocyte)

Chapter 5: Conclusions and Future Directions

Conclusions

Understanding how Cu status is sensed and regulated at the cellular, tissue, and organismal levels is critical in the process of delineating the complicated relationship between Cu absorption, distribution, and inter-organ trafficking. The goal of this project was to determine the role that Cu exporters play in systemic Cu homeostasis in *C. elegans* and mouse. The major findings of these studies are outlined below.

1) We determined that the dietary Cu requirements of *C. elegans* showed a bell-shaped growth curve, with impaired growth, smaller brood size, and delayed development at either end of the Cu spectrum, and maximal growth in the low micromolar range of Cu.

2) CUA-1, the ortholog of human ATP7A and ATP7B, is required for normal worm growth and larval development as a regulator of Cu homeostasis. Depletion of *cua-1* under dietary Cu-deficient conditions results in lethality, which is fully rescued by supplementation of Cu in media.

3) Worms expressing *cua-1* translational fusions revealed that *cua-1* is expressed in multiple tissues, such as intestine, neurons, pharynx, and hypodermis, but that this protein is found mainly on basolateral membrane of the intestinal cells and some neurons. Dietary Cu deficiency induces an increase of *cua-1* transcript levels only in the hypodermal cells.

4) Depletion of *cua-1* in the intestine resulted in reduced fecundity similar to that of whole-body RNAi, and RNAi depletion of either *cuc-1* or *cua*-1 in P*vha-6::CUA-1.1::GFP; cua-1(ok904)* transgenic animals grown under low Cu results in a lethal phenotype that can be rescued by Cu supplementation. These results imply that a CUC-1/CUA-1 Cu delivery pathway (like Atox1/ATP7A in mammals) from intestine to peripheral tissues is essential for worms under dietary Cu restriction.

5) While CUA-1.1::GFP localized to the basolateral membranes and TGN of the intestine in BCS-treated worms, dietary Cu supplementation or Cu-injection to the pseudocoelom resulted in a redistribution of CUA-1.1 to the gut granules. These changes in localization are not associated with Cu-responsive change of CUA-1.1 abundance in the intestine. However, transgenic worms expressing P*dpy-7::CUA-1.1::GFP* showed that in hypodermal tissues, plasma membrane localization of CUA-1.1 was not affected by dietary Cu. Together these observations indicate that Cu-responsive trafficking of CUA-1.1 protein is intestine-specific.

6) Under Cu-overload conditions, CUA-1.1::GFP localized on the membrane of gut granules with stronger detection of labile Cu by Cu probe in vesicles. Inhibition of biogenesis of gut granules by *pgp-2* RNAi in worms resulted in delayed growth and reduced Cu accumulation as well as no detection of CUA-1.1 in vesicular compartments. These results imply that the existence of a systemic Cu homeostasis mediated by the trafficking of intestinal CUA-1.1 in *C. elegans*, and that gut granules are at least partially required for Cu detoxification by CUA-1.1.

7) CUA-1.2, another transcript of *cua-1*, lacking cytoplasmic N-terminus 122 amino acid residues of CUA-1.1 functions constantly at basolateral membranes in

response to varying dietary Cu levels, implying that Cu-dependent trafficking of CUA-1.1 to gut granules is dependent on trafficking motifs within this N-terminal region.

8) In mammalian cell culture, reduced Cu levels stimulate the degradation of ATP7A, and proteasomal degradation pathway is involved in the mechanism. These data indicate that, in addition to the Cu-responsive trafficking of ATP7A, regulation of ATP7A protein stability provides another layer of key homeostatic mechanism for control of the efflux of Cu.

9) While Ctr1 is known to be degraded by elevated Cu levels in cell cultures and several tissues in mice, the liver showed highly increased Ctr1 protein levels with drastically accumulated Cu levels by SQ Cu injection, suggesting the critical role of liver for facilitating removal of Cu from the blood and preventing hyperaccumulation of Cu in the other Cu-susceptible peripheral tissues.

10) *In vivo*, peripheral organs including, liver, heart, and spleen decrease ATP7A protein abundance under Cu-deficient condition as compared to those in age-matched sibling control mice. These findings indicate that ATP7A protein levels in several peripheral organs are regulated in response to Cu levels in animals similar to cell culture models.

11) In contrast to ATP7A levels in the liver, steady-state protein levels of ATP7A in the intestine were inversely correlated to intestinal Cu levels without substantial subcellular localization change; low systemic Cu increased ATP7A in the intestine but decreased ATP7A in peripheral tissues, suggesting an intestine-specific regulation for ATP7A in maintaining peripheral organismal Cu homeostasis.

12) Data from isolated and cultured enterocytes from *Ctr1*$^{int/int}$ mice show that elevated ATP7A expression in the enterocytes of Cu-deficient mice is suppressed in BCS-treated medium. Since intestinal ATP7A abundance in both *Ctr1*$^{int/int}$ (low serum Cu) (15), and *Ctr1*$^{hrt/hrt}$ (high serum Cu) (61) mice are increased, the data imply that serum Cu status itself is not a direct intestinal ATP7A inducer. These findings underscore the importance of the intestine as a regulator of Cu entry to the body, which must respond not only to intrinsic Cu needs, but those of peripheral tissues, which are thought to be in direct communication with circulating factors.

Future directions

Defining the cellular pathway for Cu-regulated trafficking of CUA-1

We found that Cu-responsive trafficking of CUA-1 in the intestine is a key regulatory mechanism to maintain systemic Cu homeostasis in worms, which raises the question as to what proteins sense high systemic Cu status and stimulate endosomal re-localization of CUA-1 in the intestine. In addition, given that CUA-1.2 lacks a portion of the N-terminal regions of CUA-1.1 and is targeted constantly to the basolateral membrane even under higher Cu conditions, the first 122 amino acids of CUA-1.1 may contain necessary trafficking information for Cu responsiveness and correct targeting to gut granules.

In this sub-aim, we propose RNAi screens for Cu-responsive regulators of CUA-1 trafficking. It has been estimated using a genome-wide screen that 657 genes are involved in endocytosis and secretion in *C. elegans* (154). To explore which of

these sorting factors might be involved in CUA-1 localization, RNAi depletion of these 657 trafficking regulators could be performed in worms expressing P*vha-6::CUA- 1.1::GFP*. Fluorescence microscopy will be used to discover which of these genes are required in Cu-dependent endocytosis of GFP-tagged CUA-1. In addition to these genes, worm orthologs of trafficking factors that are reported to facilitate human ATP7A trafficking, such as adaptor proteins and Rab GTPases, could be included (155-157). If RNAi-treated worms show intracellular accumulation of CUA-1 with decreased basolateral membrane localization under Cu-deficient conditions (and the converse at high Cu exposure), it would suggest that the knocked-down gene participates in Cu-regulated CUA-1 trafficking. This aim will define the mechanisms of Cu stimulated CUA-1 trafficking in worms, that are likely to be conserved in human cells for ATP7A and ATP7B.

Determination of the role of the hypodermis in Cu homeostasis in worms

We revealed that *cua-1* expression is elevated under Cu deficient conditions only in the hypodermis whereas subcellular localization was not altered by Cu level calling into the question as to what is the role of hypodermal CUA-1 in Cu metabolism in worms. One possible hypothesis is that CUA-1 in the hypodermis may deliver Cu to the TGN for Cu loading into newly synthesized Cu-dependent enzymes. Another possibility is that the hypodermis functions as a Cu storage tissue that can supply Cu to peripheral tissues by increasing CUA-1.1 expression when worms are undergoing Cu-deficiency. Sai Yuan, a graduate student in our laboratory, has done extensive work to characterize a Cu importer in *C. elegans* and found a strong

candidate. Future work with the worms expressing *cua-1* transcriptional or translational reporters under the endogenous promoter as well as hypodermis-specific Cu importer RNAi will determine origin of demands for Cu under Cu-limitation, which leads to the up-regulation of CUA-1 in hypodermis.

In addition, if the trafficking of intestinal CUA-1 is dependent on systemic Cu status and peripheral tissue Cu-deficiency rather than Cu status in the intestine, use of hypodermis-specific Cu importer silencing in worms expressing P*vha-6::CUA-1.1::GFP* would answer the question.

Examination of hepatic Ctr1 regulation in Cu-overload condition

It is well established that Ctr1 is inactivated through post-translational down-regulation (e.g. endocytosis and degradation) in cell culture and mouse models (25,26). Interestingly, we found that in Cu-injected mice, Ctr1 is elevated in the liver and that Cu is dramatically accumulated in the liver (~5-fold higher) as compared to control mice. Given that mRNA levels of Ctr1 in the liver were not altered by Cu-deficiency or Cu-injection, elevation of hepatic Ctr1 is regulated at post-transcriptional levels. Therefore, it is possible that Ctr1 in the liver fails to undergo endocytosis and degradation as it does in other tissues to sequester and excrete toxic levels of Cu, maintain optimal Cu homeostasis, and protect other Cu-susceptible tissues. Identifying the specific molecular mechanism for liver-specific Ctr1 regulation will provide a holistic view of the coordinated changes in Cu homeostasis proteins that result from changes in Cu demand and overload, and the constellation of tissues that respond to peripheral tissue Cu status.

Identifying Cu signals that induce elevation of intestinal ATP7A in Cu-deficient mice

A major caveat of these studies is that we have not shown the molecular mechanism by which intestinal ATP7A is increased in Cu-deficient mice. As we have observed that intestinal ATP7A expression in both *Ctr1*$^{int/int}$ (low serum Cu) (15), and *Ctr1*$^{hrt/hrt}$ (high serum Cu) (61) mice is post-transcriptionally elevated, we reason that Cu itself is not a direct intestinal ATP7A inducer. Instead, a circulating factor from plasma likely mediates ATP7A expression in the intestines of these mice. Our current hypothesis is that in mammals, tissue Cu levels are not only maintained cell-autonomously but also by an inter-organ communication network in which a systemic signal mediates crosstalk between organs and the intestine regarding Cu status in Cu-deficient mammals.

In our recent preliminary studies (unpublished work), we have evaluated mRNA profiles of hearts from P10 *Ctr1*$^{hrt/hrt}$ mice by microarray in triplicate, and found that several hundred genes were differentially regulated as compared to controls, based on the assumption that heart tissues undergoing severe Cu deficiency activate the expression of secreted proteins that directly serve as the signal, or that intracellular proteins involved in the biosynthesis of small molecules that act as the signal. As a control for transcripts that are elevated due to general cardiac hypertrophy and not related to a Cu deficiency-induced hypertrophy, we analyzed the available microarray data in heart tissues from transverse aortic constriction (TAC)-induced pressure overload mice, from exercise-induced cardiac hypertrophy model

mice, and from heart-specific transferrin receptor 1 (Tfr1) KO mice (*Tfr1*$^{hrt/hrt}$). While *Tfr1*$^{hrt/hrt}$ mice display very similar phenotypes to *Ctr1*$^{hrt/hrt}$ (i.e., mice lacking cardiac Tfr1 died at two weeks of age and demonstrated severe cardiac hypertrophy) (158), intestinal ATP7A expression of *Tfr1*$^{hrt/hrt}$ was not increased, indicating ATP7A elevation in the intestine of *Ctr1*$^{hrt/hrt}$ is not due to general cardiac hypertrophy (unpublished work). Among 250 genes, which are specifically elevated in *Ctr1*$^{hrt/hrt}$ hearts, 18 genes encoding secreted proteins were tested as primary Cu signal candidates by treating HUVEC cells with the purified mammalian recombinant proteins. Interestingly, the abundance of endogenous ATP7A protein in HUVEC cells was significantly elevated upon the one of Insulin-like Growth Factor (IGF) Binding Protein (IGFBP) family proteins treatment (0.5 μg/ml); this was accompanied by a concomitant increase in CCS levels, which is an indicator of bioavailable Cu, likely due to enhanced Cu efflux via ATP7A (unpublished work). Future studies are underway to determine whether this candidate affects the regulation of ATP7A expression in the intestine *in vivo* mice experiments.

Appendices

Appendix I. Worm strains used in this study

Strain Name	Background	Transgene
BK014	N2	P_{vha-6}*::CUA-1.1::GFP::unc-54 3' UTR*
BK015	*cua-1 (ok904) III*	P_{vha-6}*::CUA-1.1::GFP::unc-54 3' UTR*
VC672	*+/mT1 II; cua-1(ok904)/mT1 [dpy-10(e128)] III*	-
BK016	N2	P_{vha-6}*::CUA-1.1::GFP::unc-54 3' UTR;* P_{vha-6}*::mCherry::unc-54 3' UTR*
BK020	*unc-119 (ed3) III*	P_{dpy-7}*::CUA-1.1::GFP::unc-54 3' UTR; unc-119 rescue*
BK006	N2	P_{cua-1}*::CUA-1.1::GFP::unc-54 3' UTR*
BK024	N2	P_{vha-6}*::CUA-1.2::GFP::unc-54 3' UTR*
	unc-119 (ed3) III	P_{vha-6}*::MANS::mCherry::unc-54 3' UTR; unc-119 rescue*
BK018	N2	P_{vha-6}*::CUA-1::GFP::unc-54 3' UTR;* P_{vha-6}*::MANS::mCherry::unc-54 3' UTR;*
WM27	*rde-1(ne219) V*	-
VP303	*rde-1(ne219) V*	P_{nhx-2}*::RDE-1; rol-6 marker*
WM118	*rde-1(ne300) V*	P_{myo-3}*::HA::RDE-1; rol-6 marker*
NR222	*rde-1(ne219) V*	P_{lin-26}*::nls-gfp;* P_{lin-26}*::RDE-1; rol-6 marker*

Appendix II. Oligonucleotide primers used in worm study

Purpose	Name	Sequence
cua-1(ok904) genotyping	*Cua-1_gt_fwd*	CCAGCTAACCACAATTGTTTTCG
	Cua-1_gt_rev	CGAATCCTTCTCGTCGTCATTTTC
C. elegans RT-qPCR	*ceCua-1_fwd*	TGGCACAATCACCGAAGGAC
	ceCua-1_rev	CAATCGGATGCTCCGACAAA
	ceGpd-2_fwd	TGCTCACGAGGGAGACTAC
	ceGpd-2_rev	CGCTGGACTCAACGACATAG

Appendix III. Oligonucleotide primers used in mammalian study

Purpose	Name	Sequence
Mouse Ctr1 genotyping	*Ctr1_gt_fwd*	AATGTCCTGGTGCGTCTGAAA
	Ctr1_gt_rev1	GCAGTAGATAAAAGCCAAGGC
	Ctr1_gt_rev2	AAAAACCACTATTCAGAGACTG
Mouse RT-qPCR	*mAtp7a_fwd*	ATGGAGCCAAGTGTGGATG
	mAtp7a_rev	CCAAGGCAGAGTCAGTGGAG
	mGapdh_fwd	ATGGTGAAGGTCGGTGTGAA
	mGapdh_rev	AGTGGAGTCATACTGGAACA
	mMT1_fwd	CACTTGCACCAGCTCCTG
	mMT1_rev	GAAGACGCTGGGTTGGTC
	mMT2_fwd	CAAACCGATCTCTCGTCGAT
	mMT2_rev	AGGAGCAGCAGCTTTTCTTG
	mCtr1_fwd	GGGCTTACCCTGTGAAGACTTTT
	mCtr1_rev	AATGTTGTCGTCCGTGTGGT
Rat cells RT-qPCR	*rAtp7a_fwd*	TGAACAGTCATCACCTTCATCGTC
	rAtp7a_rev	TGCATCTTGTTGGACTCCTGAAAG
	r18s rRNA_fwd	GCAATTATTCCCCATGAACG
	r18s rRNA_rev	GGCCTCACTAAACCATCCAA

Appendix IV. Intestinal CUA-1 distribution is regulated by Cu status in the body. Transgenic animals [P*vha-6::CUA-1.1::GFP::unc-54 3'UTR*] were injected with M9 buffer containing either histidine alone or histidine with $CuCl_2$. (see Materials and Methods for details). Arrowheads indicate punctate of CUA-1.1::GFP. Scale bar, 20 μm.

(This experiment was conducted by Anuj Kumar Sharma)

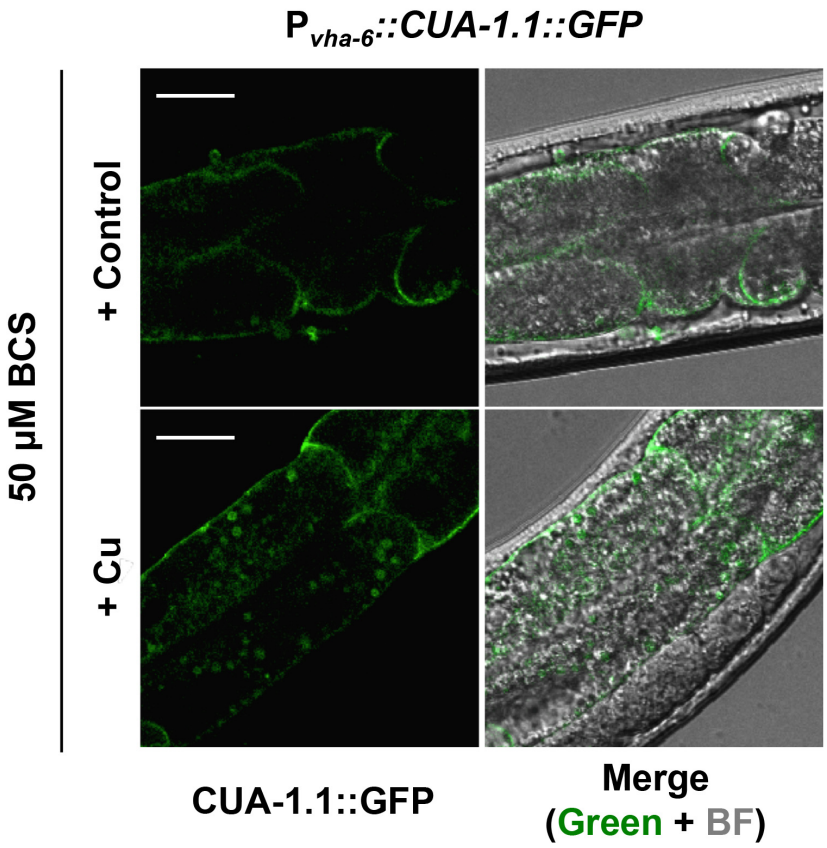
P vha-6::CUA-1.1::GFP
50 µM BCS
+ Control
+ Cu
CUA-1.1::GFP
Merge
(Green + BF)

Bibliography

1. van den Berghe, P. V., and Klomp, L. W. (2009) New developments in the regulation of intestinal copper absorption. *Nutrition reviews* **67**, 658-672
2. Kim, B. E., Nevitt, T., and Thiele, D. J. (2008) Mechanisms for copper acquisition, distribution and regulation. *Nature chemical biology* **4**, 176-185
3. Lutsenko, S., and Petris, M. J. (2003) Function and regulation of the mammalian copper-transporting ATPases: insights from biochemical and cell biological approaches. *The Journal of membrane biology* **191**, 1-12
4. Britton, R. S. (1996) Metal-induced hepatotoxicity. *Seminars in liver disease* **16**, 3-12
5. Halliwell, B., and Gutteridge, J. M. (1984) Oxygen toxicity, oxygen radicals, transition metals and disease. *The Biochemical journal* **219**, 1-14
6. Pena, M. M., Lee, J., and Thiele, D. J. (1999) A delicate balance: homeostatic control of copper uptake and distribution. *The Journal of nutrition* **129**, 1251-1260
7. Nevitt, T., Ohrvik, H., and Thiele, D. J. (2012) Charting the travels of copper in eukaryotes from yeast to mammals. *Biochimica et biophysica acta* **1823**, 1580-1593
8. Kautz, L., Jung, G., Valore, E. V., Rivella, S., Nemeth, E., and Ganz, T. (2014) Identification of erythroferrone as an erythroid regulator of iron metabolism. *Nature genetics* **46**, 678-684

9. Nemeth, E., Tuttle, M. S., Powelson, J., Vaughn, M. B., Donovan, A., Ward, D. M., Ganz, T., and Kaplan, J. (2004) Hepcidin regulates cellular iron efflux by binding to ferroportin and inducing its internalization. *Science* **306**, 2090-2093

10. Maryon, E. B., Molloy, S. A., Zimnicka, A. M., and Kaplan, J. H. (2007) Copper entry into human cells: progress and unanswered questions. *Biometals : an international journal on the role of metal ions in biology, biochemistry, and medicine* **20**, 355-364

11. Nose, Y., Rees, E. M., and Thiele, D. J. (2006) Structure of the Ctr1 copper trans'PORE'ter reveals novel architecture. *Trends in biochemical sciences* **31**, 604-607

12. Puig, S., and Thiele, D. J. (2002) Molecular mechanisms of copper uptake and distribution. *Current opinion in chemical biology* **6**, 171-180

13. Puig, S., Lee, J., Lau, M., and Thiele, D. J. (2002) Biochemical and genetic analyses of yeast and human high affinity copper transporters suggest a conserved mechanism for copper uptake. *The Journal of biological chemistry* **277**, 26021-26030

14. De Feo, C. J., Aller, S. G., Siluvai, G. S., Blackburn, N. J., and Unger, V. M. (2009) Three-dimensional structure of the human copper transporter hCTR1. *Proceedings of the National Academy of Sciences of the United States of America* **106**, 4237-4242

15. Nose, Y., Kim, B. E., and Thiele, D. J. (2006) Ctr1 drives intestinal copper absorption and is essential for growth, iron metabolism, and neonatal cardiac function. *Cell metabolism* **4**, 235-244

16. Aller, S. G., and Unger, V. M. (2006) Projection structure of the human copper transporter CTR1 at 6-A resolution reveals a compact trimer with a novel channel-like architecture. *Proceedings of the National Academy of Sciences of the United States of America* **103**, 3627-3632

17. Lee, J., Pena, M. M., Nose, Y., and Thiele, D. J. (2002) Biochemical characterization of the human copper transporter Ctr1. *The Journal of biological chemistry* **277**, 4380-4387

18. Knutson, M. D. (2007) Steap proteins: implications for iron and copper metabolism. *Nutrition reviews* **65**, 335-340

19. Ohgami, R. S., Campagna, D. R., McDonald, A., and Fleming, M. D. (2006) The Steap proteins are metalloreductases. *Blood* **108**, 1388-1394

20. McKie, A. T., Barrow, D., Latunde-Dada, G. O., Rolfs, A., Sager, G., Mudaly, E., Mudaly, M., Richardson, C., Barlow, D., Bomford, A., Peters, T. J., Raja, K. B., Shirali, S., Hediger, M. A., Farzaneh, F., and Simpson, R. J. (2001) An iron-regulated ferric reductase associated with the absorption of dietary iron. *Science* **291**, 1755-1759

21. Kuo, Y. M., Zhou, B., Cosco, D., and Gitschier, J. (2001) The copper transporter CTR1 provides an essential function in mammalian embryonic development. *Proceedings of the National Academy of Sciences of the United States of America* **98**, 6836-6841

22. Lee, J., Petris, M. J., and Thiele, D. J. (2002) Characterization of mouse embryonic cells deficient in the ctr1 high affinity copper transporter. Identification of a Ctr1-independent copper transport system. *The Journal of biological chemistry* **277**, 40253-40259

23. Nose, Y., Wood, L. K., Kim, B. E., Prohaska, J. R., Fry, R. S., Spears, J. W., and Thiele, D. J. (2010) Ctr1 is an apical copper transporter in mammalian intestinal epithelial cells in vivo that is controlled at the level of protein stability. *The Journal of biological chemistry* **285**, 32385-32392

24. Guo, Y., Smith, K., Lee, J., Thiele, D. J., and Petris, M. J. (2004) Identification of methionine-rich clusters that regulate copper-stimulated endocytosis of the human Ctr1 copper transporter. *The Journal of biological chemistry* **279**, 17428-17433

25. Petris, M. J., Smith, K., Lee, J., and Thiele, D. J. (2003) Copper-stimulated endocytosis and degradation of the human copper transporter, hCtr1. *The Journal of biological chemistry* **278**, 9639-9646

26. Ohrvik, H., Nose, Y., Wood, L. K., Kim, B. E., Gleber, S. C., Ralle, M., and Thiele, D. J. (2013) Ctr2 regulates biogenesis of a cleaved form of mammalian Ctr1 metal transporter lacking the copper- and cisplatin-binding ecto-domain. *Proceedings of the National Academy of Sciences of the United States of America* **110**, E4279-4288

27. van den Berghe, P. V., Folmer, D. E., Malingre, H. E., van Beurden, E., Klomp, A. E., van de Sluis, B., Merkx, M., Berger, R., and Klomp, L. W. (2007) Human copper transporter 2 is localized in late endosomes and

lysosomes and facilitates cellular copper uptake. *The Biochemical journal* **407**, 49-59

28. Ohrvik, H., Logeman, B., Turk, B., Reinheckel, T., and Thiele, D. J. (2016) Cathepsin Protease Controls Copper and Cisplatin Accumulation via Cleavage of the Ctr1 Metal-binding Ectodomain. *The Journal of biological chemistry* **291**, 13905-13916

29. Fleming, M. D., Romano, M. A., Su, M. A., Garrick, L. M., Garrick, M. D., and Andrews, N. C. (1998) Nramp2 is mutated in the anemic Belgrade (b) rat: evidence of a role for Nramp2 in endosomal iron transport. *Proceedings of the National Academy of Sciences of the United States of America* **95**, 1148-1153

30. Zimnicka, A. M., Ivy, K., and Kaplan, J. H. (2011) Acquisition of dietary copper: a role for anion transporters in intestinal apical copper uptake. *American journal of physiology. Cell physiology* **300**, C588-599

31. Shawki, A., Anthony, S. R., Nose, Y., Engevik, M. A., Niespodzany, E. J., Barrientos, T., Ohrvik, H., Worrell, R. T., Thiele, D. J., and Mackenzie, B. (2015) Intestinal DMT1 is critical for iron absorption in the mouse but is not required for the absorption of copper or manganese. *American journal of physiology. Gastrointestinal and liver physiology* **309**, G635-647

32. Prohaska, J. R., Broderius, M., and Brokate, B. (2003) Metallochaperone for Cu,Zn-superoxide dismutase (CCS) protein but not mRNA is higher in organs from copper-deficient mice and rats. *Archives of biochemistry and biophysics* **417**, 227-234

33. Bertinato, J., and L'Abbe, M. R. (2003) Copper modulates the degradation of copper chaperone for Cu,Zn superoxide dismutase by the 26 S proteosome. *The Journal of biological chemistry* **278**, 35071-35078

34. Caruano-Yzermans, A. L., Bartnikas, T. B., and Gitlin, J. D. (2006) Mechanisms of the copper-dependent turnover of the copper chaperone for superoxide dismutase. *The Journal of biological chemistry* **281**, 13581-13587

35. Brady, G. F., Galban, S., Liu, X., Basrur, V., Gitlin, J. D., Elenitoba-Johnson, K. S., Wilson, T. E., and Duckett, C. S. (2010) Regulation of the copper chaperone CCS by XIAP-mediated ubiquitination. *Molecular and cellular biology* **30**, 1923-1936

36. Wong, P. C., Waggoner, D., Subramaniam, J. R., Tessarollo, L., Bartnikas, T. B., Culotta, V. C., Price, D. L., Rothstein, J., and Gitlin, J. D. (2000) Copper chaperone for superoxide dismutase is essential to activate mammalian Cu/Zn superoxide dismutase. *Proceedings of the National Academy of Sciences of the United States of America* **97**, 2886-2891

37. Prohaska, J. R., Geissler, J., Brokate, B., and Broderius, M. (2003) Copper, zinc-superoxide dismutase protein but not mRNA is lower in copper-deficient mice and mice lacking the copper chaperone for superoxide dismutase. *Experimental biology and medicine* **228**, 959-966

38. Hamza, I., Faisst, A., Prohaska, J., Chen, J., Gruss, P., and Gitlin, J. D. (2001) The metallochaperone Atox1 plays a critical role in perinatal copper homeostasis. *Proceedings of the National Academy of Sciences of the United States of America* **98**, 6848-6852

39. Itoh, S., Ozumi, K., Kim, H. W., Nakagawa, O., McKinney, R. D., Folz, R. J., Zelko, I. N., Ushio-Fukai, M., and Fukai, T. (2009) Novel mechanism for regulation of extracellular SOD transcription and activity by copper: role of antioxidant-1. *Free radical biology & medicine* **46**, 95-104

40. Heuchel, R., Radtke, F., Georgiev, O., Stark, G., Aguet, M., and Schaffner, W. (1994) The transcription factor MTF-1 is essential for basal and heavy metal-induced metallothionein gene expression. *The EMBO journal* **13**, 2870-2875

41. Park, J. D., Liu, Y., and Klaassen, C. D. (2001) Protective effect of metallothionein against the toxicity of cadmium and other metals(1). *Toxicology* **163**, 93-100

42. Suzuki, K. T., Someya, A., Komada, Y., and Ogra, Y. (2002) Roles of metallothionein in copper homeostasis: responses to Cu-deficient diets in mice. *Journal of inorganic biochemistry* **88**, 173-182

43. Ogra, Y., Aoyama, M., and Suzuki, K. T. (2006) Protective role of metallothionein against copper depletion. *Archives of biochemistry and biophysics* **451**, 112-118

44. Ogra, Y., Miyayama, T., and Anan, Y. (2010) Effect of glutathione depletion on removal of copper from LEC rat livers by tetrathiomolybdate. *Journal of inorganic biochemistry* **104**, 858-862

45. Singleton, W. C., McInnes, K. T., Cater, M. A., Winnall, W. R., McKirdy, R., Yu, Y., Taylor, P. E., Ke, B. X., Richardson, D. R., Mercer, J. F., and La Fontaine, S. (2010) Role of glutaredoxin1 and glutathione in regulating the

activity of the copper-transporting P-type ATPases, ATP7A and ATP7B. *The Journal of biological chemistry* **285**, 27111-27121

46. Soto, I. C., Fontanesi, F., Liu, J., and Barrientos, A. (2012) Biogenesis and assembly of eukaryotic cytochrome c oxidase catalytic core. *Biochimica et biophysica acta* **1817**, 883-897

47. Tsukihara, T., Aoyama, H., Yamashita, E., Tomizaki, T., Yamaguchi, H., Shinzawa-Itoh, K., Nakashima, R., Yaono, R., and Yoshikawa, S. (1996) The whole structure of the 13-subunit oxidized cytochrome c oxidase at 2.8 A. *Science* **272**, 1136-1144

48. Herrmann, J. M., and Funes, S. (2005) Biogenesis of cytochrome oxidase-sophisticated assembly lines in the mitochondrial inner membrane. *Gene* **354**, 43-52

49. Pacheu-Grau, D., Bareth, B., Dudek, J., Juris, L., Vogtle, F. N., Wissel, M., Leary, S. C., Dennerlein, S., Rehling, P., and Deckers, M. (2015) Cooperation between COA6 and SCO2 in COX2 maturation during cytochrome c oxidase assembly links two mitochondrial cardiomyopathies. *Cell metabolism* **21**, 823-833

50. La Fontaine, S., and Mercer, J. F. (2007) Trafficking of the copper-ATPases, ATP7A and ATP7B: role in copper homeostasis. *Archives of biochemistry and biophysics* **463**, 149-167

51. Petris, M. J., Camakaris, J., Greenough, M., LaFontaine, S., and Mercer, J. F. (1998) A C-terminal di-leucine is required for localization of the Menkes protein in the trans-Golgi network. *Human molecular genetics* **7**, 2063-2071

52. Petris, M. J., and Mercer, J. F. (1999) The Menkes protein (ATP7A; MNK) cycles via the plasma membrane both in basal and elevated extracellular copper using a C-terminal di-leucine endocytic signal. *Human molecular genetics* **8**, 2107-2115

53. Greenough, M., Pase, L., Voskoboinik, I., Petris, M. J., O'Brien, A. W., and Camakaris, J. (2004) Signals regulating trafficking of Menkes (MNK; ATP7A) copper-translocating P-type ATPase in polarized MDCK cells. *American journal of physiology. Cell physiology* **287**, C1463-1471

54. Guo, Y., Nyasae, L., Braiterman, L. T., and Hubbard, A. L. (2005) NH2-terminal signals in ATP7B Cu-ATPase mediate its Cu-dependent anterograde traffic in polarized hepatic cells. *American journal of physiology. Gastrointestinal and liver physiology* **289**, G904-916

55. Banci, L., Bertini, I., Cantini, F., and Ciofi-Baffoni, S. (2010) Cellular copper distribution: a mechanistic systems biology approach. *Cellular and molecular life sciences : CMLS* **67**, 2563-2589

56. Kaler, S. G. (2011) ATP7A-related copper transport diseases-emerging concepts and future trends. *Nature reviews. Neurology* **7**, 15-29

57. Ohrvik, H., and Thiele, D. J. (2014) How copper traverses cellular membranes through the mammalian copper transporter 1, Ctr1. *Annals of the New York Academy of Sciences* **1314**, 32-41

58. Kuo, Y. M., Gybina, A. A., Pyatskowit, J. W., Gitschier, J., and Prohaska, J. R. (2006) Copper transport protein (Ctr1) levels in mice are tissue specific and dependent on copper status. *The Journal of nutrition* **136**, 21-26

59. Ralle, M., Huster, D., Vogt, S., Schirrmeister, W., Burkhead, J. L., Capps, T. R., Gray, L., Lai, B., Maryon, E., and Lutsenko, S. (2010) Wilson disease at a single cell level: intracellular copper trafficking activates compartment-specific responses in hepatocytes. *The Journal of biological chemistry* **285**, 30875-30883

60. Kim, H., Son, H. Y., Bailey, S. M., and Lee, J. (2009) Deletion of hepatic Ctr1 reveals its function in copper acquisition and compensatory mechanisms for copper homeostasis. *American journal of physiology. Gastrointestinal and liver physiology* **296**, G356-364

61. Kim, B. E., Turski, M. L., Nose, Y., Casad, M., Rockman, H. A., and Thiele, D. J. (2010) Cardiac copper deficiency activates a systemic signaling mechanism that communicates with the copper acquisition and storage organs. *Cell metabolism* **11**, 353-363

62. Harris, Z. L., Durley, A. P., Man, T. K., and Gitlin, J. D. (1999) Targeted gene disruption reveals an essential role for ceruloplasmin in cellular iron efflux. *Proceedings of the National Academy of Sciences of the United States of America* **96**, 10812-10817

63. Meyer, L. A., Durley, A. P., Prohaska, J. R., and Harris, Z. L. (2001) Copper transport and metabolism are normal in aceruloplasminemic mice. *The Journal of biological chemistry* **276**, 36857-36861

64. Roberts, E. A., Schilsky, M. L., and American Association for Study of Liver, D. (2008) Diagnosis and treatment of Wilson disease: an update. *Hepatology* **47**, 2089-2111

65. Jiang, Y., Reynolds, C., Xiao, C., Feng, W., Zhou, Z., Rodriguez, W., Tyagi, S. C., Eaton, J. W., Saari, J. T., and Kang, Y. J. (2007) Dietary copper supplementation reverses hypertrophic cardiomyopathy induced by chronic pressure overload in mice. *The Journal of experimental medicine* **204**, 657-666

66. Leitch, J. M., Yick, P. J., and Culotta, V. C. (2009) The right to choose: multiple pathways for activating copper,zinc superoxide dismutase. *The Journal of biological chemistry* **284**, 24679-24683

67. Keller, G., Bird, A., and Winge, D. R. (2005) Independent metalloregulation of Ace1 and Mac1 in Saccharomyces cerevisiae. *Eukaryotic cell* **4**, 1863-1871

68. Rutherford, J. C., and Bird, A. J. (2004) Metal-responsive transcription factors that regulate iron, zinc, and copper homeostasis in eukaryotic cells. *Eukaryotic cell* **3**, 1-13

69. Martins, L. J., Jensen, L. T., Simon, J. R., Keller, G. L., and Winge, D. R. (1998) Metalloregulation of FRE1 and FRE2 homologs in Saccharomyces cerevisiae. *The Journal of biological chemistry* **273**, 23716-23721

70. Norgate, M., Southon, A., Zou, S., Zhan, M., Sun, Y., Batterham, P., and Camakaris, J. (2007) Copper homeostasis gene discovery in Drosophila melanogaster. *Biometals : an international journal on the role of metal ions in biology, biochemistry, and medicine* **20**, 683-697

71. Chen, X., Hua, H., Balamurugan, K., Kong, X., Zhang, L., George, G. N., Georgiev, O., Schaffner, W., and Giedroc, D. P. (2008) Copper sensing

function of Drosophila metal-responsive transcription factor-1 is mediated by a tetranuclear Cu(I) cluster. *Nucleic acids research* **36**, 3128-3138

72. Atanesyan, L., Gunther, V., Celniker, S. E., Georgiev, O., and Schaffner, W. (2011) Characterization of MtnE, the fifth metallothionein member in Drosophila. *Journal of biological inorganic chemistry : JBIC : a publication of the Society of Biological Inorganic Chemistry* **16**, 1047-1056

73. Anderson, C. P., and Leibold, E. A. (2014) Mechanisms of iron metabolism in Caenorhabditis elegans. *Frontiers in pharmacology* **5**, 113

74. Roh, H. C., Collier, S., Guthrie, J., Robertson, J. D., and Kornfeld, K. (2012) Lysosome-related organelles in intestinal cells are a zinc storage site in C. elegans. *Cell metabolism* **15**, 88-99

75. Severance, S., and Hamza, I. (2009) Trafficking of heme and porphyrins in metazoa. *Chemical reviews* **109**, 4596-4616

76. Maduro, M. F., and Rothman, J. H. (2002) Making worm guts: the gene regulatory network of the Caenorhabditis elegans endoderm. *Developmental biology* **246**, 68-85

77. Simon, T. C., and Gordon, J. I. (1995) Intestinal epithelial cell differentiation: new insights from mice, flies and nematodes. *Current opinion in genetics & development* **5**, 577-586

78. Meredith, D., and Boyd, C. A. (2000) Structure and function of eukaryotic peptide transporters. *Cellular and molecular life sciences : CMLS* **57**, 754-778

79. Davis, D. E., Roh, H. C., Deshmukh, K., Bruinsma, J. J., Schneider, D. L., Guthrie, J., Robertson, J. D., and Kornfeld, K. (2009) The cation diffusion

facilitator gene cdf-2 mediates zinc metabolism in Caenorhabditis elegans. *Genetics* **182**, 1015-1033

80. Romney, S. J., Newman, B. S., Thacker, C., and Leibold, E. A. (2011) HIF-1 regulates iron homeostasis in Caenorhabditis elegans by activation and inhibition of genes involved in iron uptake and storage. *PLoS genetics* **7**, e1002394

81. Rao, A. U., Carta, L. K., Lesuisse, E., and Hamza, I. (2005) Lack of heme synthesis in a free-living eukaryote. *Proceedings of the National Academy of Sciences of the United States of America* **102**, 4270-4275

82. Korolnek, T., Zhang, J., Beardsley, S., Scheffer, G. L., and Hamza, I. (2014) Control of metazoan heme homeostasis by a conserved multidrug resistance protein. *Cell metabolism* **19**, 1008-1019

83. Chen, C., Samuel, T. K., Sinclair, J., Dailey, H. A., and Hamza, I. (2011) An intercellular heme-trafficking protein delivers maternal heme to the embryo during development in C. elegans. *Cell* **145**, 720-731

84. Bargmann, C. I. (2006) Chemosensation in C. elegans. *WormBook : the online review of C. elegans biology*, 1-29

85. Wakabayashi, T., Nakamura, N., Sambongi, Y., Wada, Y., Oka, T., and Futai, M. (1998) Identification of the copper chaperone, CUC-1, in Caenorhabditis elegans: tissue specific co-expression with the copper transporting ATPase, CUA-1. *FEBS letters* **440**, 141-146

86. Sambongi, Y., Wakabayashi, T., Yoshimizu, T., Omote, H., Oka, T., and Futai, M. (1997) Caenorhabditis elegans cDNA for a Menkes/Wilson disease

gene homologue and its function in a yeast CCC2 gene deletion mutant. *Journal of biochemistry* **121**, 1169-1175

87. Consortium, C. e. D. M. (2012) large-scale screening for targeted knockouts in the Caenorhabditis elegans genome. *G3* **2**, 1415-1425

88. Carroll, M. C., Girouard, J. B., Ulloa, J. L., Subramaniam, J. R., Wong, P. C., Valentine, J. S., and Culotta, V. C. (2004) Mechanisms for activating Cu- and Zn-containing superoxide dismutase in the absence of the CCS Cu chaperone. *Proceedings of the National Academy of Sciences of the United States of America* **101**, 5964-5969

89. Leitch, J. M., Jensen, L. T., Bouldin, S. D., Outten, C. E., Hart, P. J., and Culotta, V. C. (2009) Activation of Cu,Zn-superoxide dismutase in the absence of oxygen and the copper chaperone CCS. *The Journal of biological chemistry* **284**, 21863-21871

90. Livak, K. J., and Schmittgen, T. D. (2001) Analysis of relative gene expression data using real-time quantitative PCR and the 2(-Delta Delta C(T)) Method. *Methods* **25**, 402-408

91. Kamath, R. S., Fraser, A. G., Dong, Y., Poulin, G., Durbin, R., Gotta, M., Kanapin, A., Le Bot, N., Moreno, S., Sohrmann, M., Welchman, D. P., Zipperlen, P., and Ahringer, J. (2003) Systematic functional analysis of the Caenorhabditis elegans genome using RNAi. *Nature* **421**, 231-237

92. Rual, J. F., Ceron, J., Koreth, J., Hao, T., Nicot, A. S., Hirozane-Kishikawa, T., Vandenhaute, J., Orkin, S. H., Hill, D. E., van den Heuvel, S., and Vidal,

M. (2004) Toward improving Caenorhabditis elegans phenome mapping with an ORFeome-based RNAi library. *Genome research* **14**, 2162-2168

93. Dodani, S. C., Firl, A., Chan, J., Nam, C. I., Aron, A. T., Onak, C. S., Ramos-Torres, K. M., Paek, J., Webster, C. M., Feller, M. B., and Chang, C. J. (2014) Copper is an endogenous modulator of neural circuit spontaneous activity. *Proceedings of the National Academy of Sciences of the United States of America* **111**, 16280-16285

94. Cotruvo, J. A., Jr., Aron, A. T., Ramos-Torres, K. M., and Chang, C. J. (2015) Synthetic fluorescent probes for studying copper in biological systems. *Chemical Society reviews* **44**, 4400-4414

95. Ouji, Y., Yoshikawa, M., Moriya, K., Nishiofuku, M., Ouji-Sageshima, N., Matsuda, R., Nishimura, F., and Ishizaka, S. (2010) Isolation and characterization of murine hepatocytes following collagenase infusion into left ventricle of heart. *Journal of bioscience and bioengineering* **110**, 487-490

96. Chen, H., Su, T., Attieh, Z. K., Fox, T. C., McKie, A. T., Anderson, G. J., and Vulpe, C. D. (2003) Systemic regulation of Hephaestin and Ireg1 revealed in studies of genetic and nutritional iron deficiency. *Blood* **102**, 1893-1899

97. Lee, J., Prohaska, J. R., and Thiele, D. J. (2001) Essential role for mammalian copper transporter Ctr1 in copper homeostasis and embryonic development. *Proceedings of the National Academy of Sciences of the United States of America* **98**, 6842-6847

98. McWilliam, H., Li, W., Uludag, M., Squizzato, S., Park, Y. M., Buso, N., Cowley, A. P., and Lopez, R. (2013) Analysis Tool Web Services from the EMBL-EBI. *Nucleic acids research* **41**, W597-600

99. Krogh, A., Larsson, B., von Heijne, G., and Sonnhammer, E. L. (2001) Predicting transmembrane protein topology with a hidden Markov model: application to complete genomes. *Journal of molecular biology* **305**, 567-580

100. Madsen, E., and Gitlin, J. D. (2007) Copper and iron disorders of the brain. *Annual review of neuroscience* **30**, 317-337

101. Nyasae, L., Bustos, R., Braiterman, L., Eipper, B., and Hubbard, A. (2007) Dynamics of endogenous ATP7A (Menkes protein) in intestinal epithelial cells: copper-dependent redistribution between two intracellular sites. *American journal of physiology. Gastrointestinal and liver physiology* **292**, G1181-1194

102. Monty, J. F., Llanos, R. M., Mercer, J. F., and Kramer, D. R. (2005) Copper exposure induces trafficking of the menkes protein in intestinal epithelium of ATP7A transgenic mice. *The Journal of nutrition* **135**, 2762-2766

103. Southon, A., Burke, R., Norgate, M., Batterham, P., and Camakaris, J. (2004) Copper homoeostasis in Drosophila melanogaster S2 cells. *The Biochemical journal* **383**, 303-309

104. Syracuse Research Corporation., United States. Department of Health and Human Services., United States. Agency for Toxic Substances and Disease Registry., and United States. Public Health Service. Toxicological profile for copper. Agency for Toxic Substances and Disease Registry, Atlanta, GA.

105. Edgley, M. L., Baillie, D. L., Riddle, D. L., and Rose, A. M. (2006) Genetic balancers. *WormBook : the online review of C. elegans biology*, 1-32

106. Wang, Y., Zhu, S., Weisman, G. A., Gitlin, J. D., and Petris, M. J. (2012) Conditional knockout of the Menkes disease copper transporter demonstrates its critical role in embryogenesis. *PloS one* **7**, e43039

107. Qadota, H., Inoue, M., Hikita, T., Koppen, M., Hardin, J. D., Amano, M., Moerman, D. G., and Kaibuchi, K. (2007) Establishment of a tissue-specific RNAi system in C. elegans. *Gene* **400**, 166-173

108. Oka, T., Toyomura, T., Honjo, K., Wada, Y., and Futai, M. (2001) Four subunit a isoforms of Caenorhabditis elegans vacuolar H+-ATPase. Cell-specific expression during development. *The Journal of biological chemistry* **276**, 33079-33085

109. Chen, B., Jiang, Y., Zeng, S., Yan, J., Li, X., Zhang, Y., Zou, W., and Wang, X. (2010) Endocytic sorting and recycling require membrane phosphatidylserine asymmetry maintained by TAT-1/CHAT-1. *PLoS genetics* **6**, e1001235

110. Hong-Hermesdorf, A., Miethke, M., Gallaher, S. D., Kropat, J., Dodani, S. C., Chan, J., Barupala, D., Domaille, D. W., Shirasaki, D. I., Loo, J. A., Weber, P. K., Pett-Ridge, J., Stemmler, T. L., Chang, C. J., and Merchant, S. S. (2014) Subcellular metal imaging identifies dynamic sites of Cu accumulation in Chlamydomonas. *Nature chemical biology* **10**, 1034-1042

111. Dodani, S. C., Leary, S. C., Cobine, P. A., Winge, D. R., and Chang, C. J. (2011) A targetable fluorescent sensor reveals that copper-deficient SCO1 and

SCO2 patient cells prioritize mitochondrial copper homeostasis. *Journal of the American Chemical Society* **133**, 8606-8616

112. Aron, A. T., Ramos-Torres, K. M., Cotruvo, J. A., Jr., and Chang, C. J. (2015) Recognition- and reactivity-based fluorescent probes for studying transition metal signaling in living systems. *Accounts of chemical research* **48**, 2434-2442

113. Gilleard, J. S., Barry, J. D., and Johnstone, I. L. (1997) cis regulatory requirements for hypodermal cell-specific expression of the Caenorhabditis elegans cuticle collagen gene dpy-7. *Molecular and cellular biology* **17**, 2301-2311

114. Hermann, G. J., Schroeder, L. K., Hieb, C. A., Kershner, A. M., Rabbitts, B. M., Fonarev, P., Grant, B. D., and Priess, J. R. (2005) Genetic analysis of lysosomal trafficking in Caenorhabditis elegans. *Molecular biology of the cell* **16**, 3273-3288

115. Kostich, M., Fire, A., and Fambrough, D. M. (2000) Identification and molecular-genetic characterization of a LAMP/CD68-like protein from Caenorhabditis elegans. *Journal of cell science* **113 (Pt 14)**, 2595-2606

116. Schroeder, L. K., Kremer, S., Kramer, M. J., Currie, E., Kwan, E., Watts, J. L., Lawrenson, A. L., and Hermann, G. J. (2007) Function of the Caenorhabditis elegans ABC transporter PGP-2 in the biogenesis of a lysosome-related fat storage organelle. *Molecular biology of the cell* **18**, 995-1008

117. McGhee, J. D. (2007) The C. elegans intestine. *WormBook : the online review of C. elegans biology*, 1-36

118. Hermann, G. J., Scavarda, E., Weis, A. M., Saxton, D. S., Thomas, L. L., Salesky, R., Somhegyi, H., Curtin, T. P., Barrett, A., Foster, O. K., Vine, A., Erlich, K., Kwan, E., Rabbitts, B. M., and Warren, K. (2012) C. elegans BLOC-1 functions in trafficking to lysosome-related gut granules. *PloS one* **7**, e43043

119. Cheli, V. T., Daniels, R. W., Godoy, R., Hoyle, D. J., Kandachar, V., Starcevic, M., Martinez-Agosto, J. A., Poole, S., DiAntonio, A., Lloyd, V. K., Chang, H. C., Krantz, D. E., and Dell'Angelica, E. C. (2010) Genetic modifiers of abnormal organelle biogenesis in a Drosophila model of BLOC-1 deficiency. *Human molecular genetics* **19**, 861-878

120. Cheli, V. T., and Dell'Angelica, E. C. (2010) Early origin of genes encoding subunits of biogenesis of lysosome-related organelles complex-1, -2 and -3. *Traffic* **11**, 579-586

121. Setty, S. R., Tenza, D., Sviderskaya, E. V., Bennett, D. C., Raposo, G., and Marks, M. S. (2008) Cell-specific ATP7A transport sustains copper-dependent tyrosinase activity in melanosomes. *Nature* **454**, 1142-1146

122. Roh, H. C., Dimitrov, I., Deshmukh, K., Zhao, G., Warnhoff, K., Cabrera, D., Tsai, W., and Kornfeld, K. (2015) A modular system of DNA enhancer elements mediates tissue-specific activation of transcription by high dietary zinc in C. elegans. *Nucleic acids research* **43**, 803-816

123. Taubert, S., Hansen, M., Van Gilst, M. R., Cooper, S. B., and Yamamoto, K. R. (2008) The Mediator subunit MDT-15 confers metabolic adaptation to ingested material. *PLoS genetics* **4**, e1000021

124. Radtke, F., Heuchel, R., Georgiev, O., Hergersberg, M., Gariglio, M., Dembic, Z., and Schaffner, W. (1993) Cloned transcription factor MTF-1 activates the mouse metallothionein I promoter. *The EMBO journal* **12**, 1355-1362

125. Brugnera, E., Georgiev, O., Radtke, F., Heuchel, R., Baker, E., Sutherland, G. R., and Schaffner, W. (1994) Cloning, chromosomal mapping and characterization of the human metal-regulatory transcription factor MTF-1. *Nucleic acids research* **22**, 3167-3173

126. Zhang, B., Egli, D., Georgiev, O., and Schaffner, W. (2001) The Drosophila homolog of mammalian zinc finger factor MTF-1 activates transcription in response to heavy metals. *Molecular and cellular biology* **21**, 4505-4514

127. Bahadorani, S., Bahadorani, P., Marcon, E., Walker, D. W., and Hilliker, A. J. (2010) A Drosophila model of Menkes disease reveals a role for DmATP7 in copper absorption and neurodevelopment. *Disease models & mechanisms* **3**, 84-91

128. Mak, H. Y. (2012) Lipid droplets as fat storage organelles in Caenorhabditis elegans: Thematic Review Series: Lipid Droplet Synthesis and Metabolism: from Yeast to Man. *Journal of lipid research* **53**, 28-33

129. Palgunow, D., Klapper, M., and Doring, F. (2012) Dietary restriction during development enlarges intestinal and hypodermal lipid droplets in Caenorhabditis elegans. *PloS one* **7**, e46198

130. Muckenthaler, M. U. (2008) Fine tuning of hepcidin expression by positive and negative regulators. *Cell metabolism* **8**, 1-3

131. Noble, T., Stieglitz, J., and Srinivasan, S. (2013) An integrated serotonin and octopamine neuronal circuit directs the release of an endocrine signal to control C. elegans body fat. *Cell metabolism* **18**, 672-684

132. Hung, W. L., Wang, Y., Chitturi, J., and Zhen, M. (2014) A Caenorhabditis elegans developmental decision requires insulin signaling-mediated neuron-intestine communication. *Development* **141**, 1767-1779

133. Chew, Y. L., Gotz, J., and Nicholas, H. R. (2015) Neuronal protein with tau-like repeats (PTL-1) regulates intestinal SKN-1 nuclear accumulation in response to oxidative stress. *Aging cell* **14**, 148-151

134. Linz, R., and Lutsenko, S. (2007) Copper-transporting ATPases ATP7A and ATP7B: cousins, not twins. *Journal of bioenergetics and biomembranes* **39**, 403-407

135. Kim, B. E., Smith, K., and Petris, M. J. (2003) A copper treatable Menkes disease mutation associated with defective trafficking of a functional Menkes copper ATPase. *Journal of medical genetics* **40**, 290-295

136. Menkes, J. H., Alter, M., Steigleder, G. K., Weakley, D. R., and Sung, J. H. (1962) A sex-linked recessive disorder with retardation of growth, peculiar hair, and focal cerebral and cerebellar degeneration. *Pediatrics* **29**, 764-779

137. Petris, M. J., Mercer, J. F., Culvenor, J. G., Lockhart, P., Gleeson, P. A., and Camakaris, J. (1996) Ligand-regulated transport of the Menkes copper P-type ATPase efflux pump from the Golgi apparatus to the plasma membrane: a novel mechanism of regulated trafficking. *The EMBO journal* **15**, 6084-6095

138. Petris, M. J., Strausak, D., and Mercer, J. F. (2000) The Menkes copper transporter is required for the activation of tyrosinase. *Human molecular genetics* **9**, 2845-2851

139. Tchaparian, E. H., Uriu-Adams, J. Y., Keen, C. L., Mitchell, A. E., and Rucker, R. B. (2000) Lysyl oxidase and P-ATPase-7A expression during embryonic development in the rat. *Archives of biochemistry and biophysics* **379**, 71-77

140. Xie, L., and Collins, J. F. (2013) Copper stabilizes the Menkes copper-transporting ATPase (Atp7a) protein expressed in rat intestinal epithelial cells. *American journal of physiology. Cell physiology* **304**, C257-262

141. (1999) Proceedings of a satellite meeting of the European Human Genetic Society on Copper Transport and Its Disorders: Molecular and Cellular Aspects. Sestri Levante, Italy, May 21-25, 1997. *Advances in experimental medicine and biology* **448**, 1-269

142. Pyatskowit, J. W., and Prohaska, J. R. (2008) Copper deficient rats and mice both develop anemia but only rats have lower plasma and brain iron levels. *Comparative biochemistry and physiology. Toxicology & pharmacology : CBP* **147**, 316-323

143. Allen, K. J., Buck, N. E., Cheah, D. M., Gazeas, S., Bhathal, P., and Mercer, J. F. (2006) Chronological changes in tissue copper, zinc and iron in the toxic milk mouse and effects of copper loading. *Biometals : an international journal on the role of metal ions in biology, biochemistry, and medicine* **19**, 555-564

144. Lenartowicz, M., Wieczerzak, K., Krzeptowski, W., Dobosz, P., Grzmil, P., Starzynski, R., and Lipinski, P. (2010) Developmental changes in the expression of the Atp7a gene in the liver of mice during the postnatal period. *Journal of experimental zoology. Part A, Ecological genetics and physiology* **313**, 209-217

145. Pase, L., Voskoboinik, I., Greenough, M., and Camakaris, J. (2004) Copper stimulates trafficking of a distinct pool of the Menkes copper ATPase (ATP7A) to the plasma membrane and diverts it into a rapid recycling pool. *The Biochemical journal* **378**, 1031-1037

146. Holloway, Z. G., Grabski, R., Szul, T., Styers, M. L., Coventry, J. A., Monaco, A. P., and Sztul, E. (2007) Activation of ADP-ribosylation factor regulates biogenesis of the ATP7A-containing trans-Golgi network compartment and its Cu-induced trafficking. *American journal of physiology. Cell physiology* **293**, C1753-1767

147. Abada, P. B., Larson, C. A., Manorek, G., Adams, P., and Howell, S. B. (2012) Sec61beta controls sensitivity to platinum-containing chemotherapeutic agents through modulation of the copper-transporting ATPase ATP7A. *Molecular pharmacology* **82**, 510-520

148. Wake, S. A., and Mercer, J. F. (1985) Induction of metallothionein mRNA in rat liver and kidney after copper chloride injection. *The Biochemical journal* **228**, 425-432

149. Polishchuk, E. V., Concilli, M., Iacobacci, S., Chesi, G., Pastore, N., Piccolo, P., Paladino, S., Baldantoni, D., van, I. S. C., Chan, J., Chang, C. J., Amoresano, A., Pane, F., Pucci, P., Tarallo, A., Parenti, G., Brunetti-Pierri, N., Settembre, C., Ballabio, A., and Polishchuk, R. S. (2014) Wilson disease protein ATP7B utilizes lysosomal exocytosis to maintain copper homeostasis. *Developmental cell* **29**, 686-700

150. Chen, H., Huang, G., Su, T., Gao, H., Attieh, Z. K., McKie, A. T., Anderson, G. J., and Vulpe, C. D. (2006) Decreased hephaestin activity in the intestine of copper-deficient mice causes systemic iron deficiency. *The Journal of nutrition* **136**, 1236-1241

151. Lutsenko, S., Barnes, N. L., Bartee, M. Y., and Dmitriev, O. Y. (2007) Function and regulation of human copper-transporting ATPases. *Physiological reviews* **87**, 1011-1046

152. Nittis, T., and Gitlin, J. D. (2004) Role of copper in the proteosome-mediated degradation of the multicopper oxidase hephaestin. *The Journal of biological chemistry* **279**, 25696-25702

153. Tao, T. Y., and Gitlin, J. D. (2003) Hepatic copper metabolism: insights from genetic disease. *Hepatology* **37**, 1241-1247

154. Balklava, Z., Pant, S., Fares, H., and Grant, B. D. (2007) Genome-wide analysis identifies a general requirement for polarity proteins in endocytic traffic. *Nature cell biology* **9**, 1066-1073

155. Holloway, Z. G., Velayos-Baeza, A., Howell, G. J., Levecque, C., Ponnambalam, S., Sztul, E., and Monaco, A. P. (2013) Trafficking of the Menkes copper transporter ATP7A is regulated by clathrin-, AP-2-, AP-1-, and Rab22-dependent steps. *Molecular biology of the cell* **24**, 1735-1748, S1731-1738

156. Yi, L., and Kaler, S. G. (2015) Direct interactions of adaptor protein complexes 1 and 2 with the copper transporter ATP7A mediate its anterograde and retrograde trafficking. *Human molecular genetics* **24**, 2411-2425

157. Pascale, M. C., Franceschelli, S., Moltedo, O., Belleudi, F., Torrisi, M. R., Bucci, C., La Fontaine, S., Mercer, J. F., and Leone, A. (2003) Endosomal trafficking of the Menkes copper ATPase ATP7A is mediated by vesicles containing the Rab7 and Rab5 GTPase proteins. *Experimental cell research* **291**, 377-385

158. Xu, W., Barrientos, T., Mao, L., Rockman, H. A., Sauve, A. A., and Andrews, N. C. (2015) Lethal Cardiomyopathy in Mice Lacking Transferrin Receptor in the Heart. *Cell reports* **13**, 533-545